Implementation of a Dynamic Geodetic Datum in Papua New Guinea

A case study

Richard F. Stanaway

A thesis submitted for the degree of Master of Philosophy
of The Australian National University

February 2004

Declaration

I declare that the work described in this thesis was carried out while I was a student at the Research School of Earth Sciences, The Australian National University, between August 2001 and February 2004. Except where mentioned in the text, all research described within this thesis is my own work. No part of this thesis has been submitted to another university or institution.

Richard Frank Stanaway
26th February 2004

Acknowledgements

Firstly, I want to thank my supervisor, Paul Tregoning, for his generous and selfless encouragement, support, and guidance right from the outset. Special thanks go to my advisers, Kurt Lambeck, Herb McQueen and Bob Curley, not just for making this whole study possible, but for their sage advice, albeit from widely differing perspectives and backgrounds. Herb, for his unflinching assistance at the drop of a hat, and for keeping all systems alive (even at strange hours of the evening, whatever the time-zone). Bob, for his selfless, professional yet acerbic advice, often delivered in true Mancunian fashion, acquired from many years toil and dedication in the world of "real" surveying. I have a lot to thank Bob for, for it was his suggestion that I contact Kurt and Paul, that started the whole thing off back in 2000.

There are many people in Papua New Guinea, too many to name here, that have assisted in some positive way. Firstly, a big thanks to all the staff and students in the survey department at Unitech. The department made all their resources and equipment available, and this generosity was very much appreciated. Special thanks go to Suvenia Hasiata, Sylvester Tiki and Zaccheus for their technical support and interest in the project, in sometimes trying conditions. To all the students who were involved in the GPS fieldwork and levelling, especially Jagath Wijewardene, and Nicholas Ruku. To Robert Rosa, Wesley Loratung, John Kwasi and Peter Pako at NMB in Moresby, for their assistance, and for making available the extensive archive of data there. To Melchior, and a whole raft of people in PNG who have eagerly assisted with advice, help and cheerful hospitality.

Laura Wallace, John Manning, Hugh Davies, Steve Saunders, and Geoff Patterson all freely provided invaluable comments and suggestions from diverse fields of specialisation. Their investment of time has been very much appreciated. I am also indebted to Murray Harris, Kevin Jones, and John Cook from the Queensland University of Technology for providing me with much of the background knowledge during my Surveying degree, necessary to complete this study.

There's more to life than dynamic datums, and my friends and colleagues at RSES have all made the two years here in Canberra a very enjoyable one. I offer a special thanks to Nick for his friendship, and his sensational curries. I know few people who are so immune to sub-zero pain. To Eric, Louise, Fred, Dave, Derek, Stewart, Jim, Anya, Malcolm, Emma-Kate, and Jean and many other transitory characters, for their friendship, lunchtime discussions and pleasant evenings (and mornings) at the Wig and Phoenix. To Messrs. Squire and Cooper, for their refreshing perspectives and sparkling charisma, despite the odd dark moment. To Tony, raconteur and roommate, for his good company, advice, expansive knowledge of almost everything important (and unimportant), and tolerance of our chaotic office.

All of this wouldn't have been possible without the love and support of Mum, Dad, David and Anne, back in Allenstraβe and McAllen. To Sandra, for your love, support and friendship, especially during such a very difficult personal time. Thank you too, for your extensive use of the red pen at various critical stages of the write-up. I don't know how to thank you for all you've done! I hope you feel 110% better in 2004. I'm really looking forward to spend some relaxing time with you all, now that this is finished!

Finally, a big thanks to all those people indirectly involved with this project, who often work behind the scenes to make things happen, but never seem to get a mention.

Abstract

National geodetic datums that span tectonic plate boundaries and deforming zones are subject to distortion increasing in magnitude with time. Relative velocities between adjoining rigid plates and zones of anelastic deformation are often highly linear, however distortion near plate margins and deforming zones is often non-linear as a result of co-seismic and post-seismic displacement. Different realisations of the International Terrestrial Reference Frame (ITRF) have provided geophysicists with a dynamic geodetic reference frame. However, few countries in tectonically complex areas have established workable national geodetic datums which include dynamic elements to allow for the temporal displacement of the datum. Papua New Guinea, located between the Australian and Pacific Plates and including several smaller microplates, is an ideal case study to demonstrate the application of the algorithm for dynamic datum computations.

Motion of datum monuments with respect to ITRF can exceed 1 metre every decade. Localised deformation can result in baseline changes of up to 10 parts per million (ppm) per year, exceeding many cadastral and engineering tolerances. Inappropriate use of positioning technology can lead to inconsistent local distortions and realisations of a national datum, if the reference datum monuments and relative positions are dynamic with respect to each other. In the long-term this discrepancy will have an adverse effect on the spatial infrastructure where relative precision is an important consideration.

A strategy is presented whereby national geodetic datums and survey networks in tectonically active regions can include a geodetic velocity field, strain dislocation model and other non-secular offset data in order to maintain the integrity of the datum. A least-squares adjustment algorithm, including dynamic elements, is described and tested. This adjustment reduces geodetic measurements made in dynamic local networks to a reference epoch and results in significant improvements in accuracy.

Contents

List of Figures

List of Tables

Acronyms

ACLMP	Australian Contribution to the Land Mobilisation Project (PNG)
AGD66	Australian Geodetic Datum 1966
ANU	The Australian National University
APRGP	Asia and the Pacific Regional Geodetic Project
ARP	Antenna Reference Point
A-S	Anti-Spoofing
AUSLIG	Australian Surveying and Land Information Group
BSSL	Bismarck Sea Seismic Lineation
C/A	Coarse Acquisition
CPD	Continuing Professional Development
CEP	Celestial Ephemeris Pole
CGPS	Continuous GPS
CRS	Continuous Reference Station
DCA	Department of Civil Aviation (PNG)
DCDB	Digital Cadastral Database
DGPS	Differential GPS
DoD	Department of Defense (United States of America)
DORIS	Doppler Orbitography by Radiopositioning Integrated by Satellite
ECEF	Earth-Centred Earth-Fixed
EDM	Electronic Distance Meter
EGM96	Earth Geopotential Model 1996
EOP	Earth Orientation (Rotation) Parameters
EPCT	East Papuan Composite Terrane
ESA	European Space Agency
ftp	file transfer protocol
GA	Geoscience Australia
GDA94	Geocentric Datum of Australia 1994
GIS	Geographical Information System
GNSS	Global Navigation Satellite System
GPS	Global Positioning System
GRS80	Geodetic Reference System 1980
GUI	Graphical User Interface
HFTB	Highlands Fold and Thrust Belt
HTDP	Horizontal Time Dependent Positioning Software

ICRF	International Celestial Reference Frame
ICRS	International Celestial Reference System
ICSM	Intergovernmental Committee for Surveying and Mapping
IDS	International DORIS Service
IERS	International Earth Rotation and Reference System Service
IGS	International GPS Service
IGNS	Institute of Geological and Nuclear Sciences, New Zealand
InSAR	Interferometric Synthetic Aperture Radar
ISO	International Standards Organisation
ITRF	International Terrestrial Reference Frame
ITRF2000	International Terrestrial Reference Frame 2000
ITRF92	International Terrestrial Reference Frame 1992
ITRS	International Terrestrial Reference System
JPL	Jet Propulsion Laboratory (NASA)
LAAS	Local Area Augmentation System
LBS	Location Based Services
LC	Linear Combination in GPS (also referred to as L3)
LINZ	Land Information New Zealand
LLR	Lunar Laser Ranging
LOD	Length of Day
Ma	Million years ago
MIT	Massachusetts Institute of Technology
MRS	Multiple Reference Station (network)
My	Million years (duration)
NAD83	North American Datum 1983
NASA	National Aeronautics and Space Administration (USA)
NBT	New Britain Trench
NGH	New Guinea Highlands (Plate)
NMB	National Mapping Bureau (PNG)
NMD	National Mapping Division, Geoscience Australia
NNR	no-net-rotation
NTF	National Tidal Facility
NZGD2000	New Zealand Geodetic Datum 2000
NZGD49	New Zealand Geodetic Datum 1949
OJP	Ontong Java Plateau
OOST	Out-of-Sequence Thrust

OSFZ	Owen-Stanley Fault Zone
PCGIAP	Permanent Committee on GIS Infrastructure for Asia and the Pacific
PNG	Papua New Guinea (Independent State of)
PNG94	Papua New Guinea Geodetic Datum 1994
ppb	parts per billion
ppm	parts per million
PRN	Pseudo-Random Noise
PUB	Papuan Ultramafic Belt
RINEX	Receiver Independent Exchange Format
RMF	Ramu-Markham Fault
RMFZ	Ramu-Markham Fault Zone
RPL	Reverse Polish Lisp
RSES	Research School of Earth Sciences (ANU)
RTK	Real-time Kinematic (GPS)
RVO	Rabaul Volcanological Observatory
SBIS	South Bismarck Plate
SCDB	Survey Control Database
SIO	Scripps Institution of Oceanography
SLR	Satellite Laser Ranging
SPSLCMP	South Pacific Sea Level and Climate Monitoring Project
UNITECH	Papua New Guinea University of Technology
UNSW	University of New South Wales
UCSC	University of California, Santa Cruz
UT	Universal Time
UT1	Universal Time (reduced to Conventional Terrestrial Pole)
VCV	Variance-Covariance (Matrix)
VLBI	Very Long Baseline Interferometry
VRS	Virtual Reference Station
WADGPS	Wide-Area Differential GPS
WBSC	Woodlark Basin Spreading Centre
WGS	World Geodetic System
WGS-72	World Geodetic System 1972
WGS-84	World Geodetic System 1984
WL	Wide-lane Observable

Chapter 1

Introduction

1.1 Geodetic Datums in the 21st Century

Since 1990, positioning technology has undergone a dramatic improvement in terms of accuracy and accessibility. Prior to 1990, national geodetic datums were considered to be static, with fixed coordinates assigned to the datum origin by convention. Datum coordinates were dynamic only as a consequence of re-observation and re-adjustment, or localised disturbance. This strategy has been suitable for terrestrial surveys within stable continental areas. In recent years, however, space-based geodetic methods have enabled relative measurements over thousands of kilometres to be estimated with a precision of a few millimetres. Crustal deformation surveys using space-based geodetic methods are now commonplace. The accessibility of centimetre-accurate point positions is now widespread with the provision of free online processing facilities by various geodetic agencies. Wide area real-time differential services are on the increase and it is conceivable that absolute point positioning with inexpensive satellite positioning receivers will be possible to an accuracy of better than half a metre sometime within the next twenty years.

Such ready accessibility to a global datum has serious implications for the interaction of this technology with static geocentric datums. The Geocentric Datum of Australia 1994 (GDA94), for example, is now offset by approximately half a metre from the World Geodetic System 1984 Datum (WGS-84) version G873 and the International Terrestrial Reference Frame 2000 (ITRF2000) due to the inexorable tectonic movement of the Australian continent since the datum's realisation in 1994. By 2010 the offset will be over a metre. Similarly, the North American Datum 1983 (NAD83) is now offset from ITRF2000 by about 1.5 m (Snay, 1999). Unless local geocentric datums are kept in step with global terrestrial reference frames, discrepancies between the two will increase in magnitude over time and will become discernable, even using point positioning methods. Users of high accuracy point positioning technology in the future may

be unaware of this datum offset and incorrectly assume a coordinated datum monument is in error if there is found to be a disagreement greater than the level of accuracy of the positioning technique.

The situation in tectonically active regions is even more complex. Countries that straddle or include active plate boundaries and deforming zones must develop strategies to deal with internal deformation of their national geodetic networks.

Crustal deformation rates in localised areas are often significant enough to exceed many geographic referencing, cadastral and engineering tolerances within short time periods, even using conventional terrestrial surveying methods. Surveyors using long-range differential satellite positioning techniques to extend or densify control across tectonic plate boundaries and deforming zones may notice that their baseline observations do not agree with previous measurements within the specified precision of the measurement, or positional accuracy specifications.

The effects of crustal deformation can only be mitigated by the implementation of a dynamic datum which can accommodate time variation of the coordinates that realise the datum. Alternatively, a semi-dynamic datum approach can be implemented (Grant, 1998; Blick *et al*., 2003). A semi-dynamic datum uses dynamic coordinates for computation and network adjustment purposes, however, the adjusted coordinates are regressed back to a fixed reference epoch using a deformation model. Countries, such as New Zealand, which has a well-developed geodetic and spatial infrastructure, have already implemented a semi-dynamic datum (Pearse, 2000; Blick *et al.* 2003) to deal with this problem. The challenge remains for developing countries in tectonically active and resource rich regions, such as Papua New Guinea (PNG), to develop a geodetic datum that is not only homogeneous, but straightforward to implement and maintain. Implementation of a dynamic geodetic datum in such regions would ensure that the geodetic infrastructure is not compromised by inappropriate use of positioning technology and ignorance of systematic biases in geodetic networks resulting from tectonic distortion.

1.2 The requirement for a dynamic geodetic datum in PNG

The existing geodetic datum gazetted in PNG is the Papua New Guinea Geodetic Datum 1994 (PNG94), a geocentric datum implemented in 1996 to supersede the Australian Geodetic Datum 1966 (AGD66). PNG94 is a realisation of the International Terrestrial Reference Frame 1992 (ITRF92) at epoch 1994.0. Unfortunately, at the time the datum was realised, the geodetic velocity field for PNG had not yet been clearly defined. As a consequence, little provision was made for tectonic motion in the datum realisation (Morgan *et al*., 1996; Allman, 1996). PNG is located in one of the most tectonically complex and active regions in the world, straddling the Australian and Pacific plates and including several smaller microplates, tectonic blocks and extensive zones undergoing very rapid deformation. Co-seismic displacements up to several metres in magnitude occur frequently. Geodetic networks that include first order PNG94 stations located on different tectonic plates are becoming increasingly distorted. At present there is no strategy in place within the geodetic community in PNG to deal with both tectonic and co-seismic displacement of geodetic stations, monuments and their coordinates within a defined reference frame.

In recent years, surveyors in PNG have been rapidly adopting differential Global Positioning System (GPS) techniques for high precision positioning over large distances (Curley, 1999). In many instances the reference and remote stations have been located on different tectonic units within PNG. For example, the continuous GPS station at MORE may be used to establish PNG94 control in a remote part of New Britain which is on a different tectonic plate. Consequently, subsequent surveys using the same reference station or other first order stations located on different plates may produce coordinates inconsistent with earlier local realisations of PNG94. If tectonic deformation is unaccounted for in network adjustments, inappropriate application of this technology has the potential to substantially weaken PNG's geodetic infrastructure. Digital Cadastral Databases (DCDBs), Geographical Information Systems (GIS), Location Based Services (LBS), large-scale mapping, engineering and mining projects will be adversely affected by inaccurate geodetic base information. The use of post-processed point positioning services such as AUSPOS (Dawson *et al.*, 2001) and global real-time differential services, such as OMNISTAR (http://www.omnistar.com), can produce coordinates inconsistent with PNG94

if they are not correctly transformed into the local reference system using velocity and strain models to account for tectonic distortion of the datum.

Furthermore, inadequate monitoring of geological hazards poses risks for densely populated areas and locations of mining infrastructure. An effective geodetic monitoring network is an essential component of any geological hazard disaster management plan. Provincial survey networks in PNG are also not immune to distortion problems, especially in rapidly deforming zones such as the Gazelle Peninsula in East New Britain (Tregoning *et al*., 2000). Deformation surveys are a common task for surveyors, but the deformation is usually monitored from a stable network. To what extent can deformation of a "stable" network be tolerated? What are the implications for hazard assessment and stability monitoring of major engineering and mining works? What effect does deformation have on local grids, the coordinated cadastre and the GIS? If the monitoring network is itself deforming, is there a constraint or adjustment strategy which can discriminate between deformation of the reference network and that of the free network? These important questions are raised if a network assumed to be stable is deforming internally at significant levels.

What effect does the constraining of static PNG94 coordinates have on national and local geodetic surveys and the spatial data infrastructure in PNG? Will PNG benefit from implementation of a dynamic datum? What will the benefits be specifically? There is a requirement to analyse and assess to what extent the static geodetic datum in PNG is distorting, and to discuss the implications of this datum distortion holistically in the PNG context. What are the practical issues involved with the requirements of geodetic datums in PNG in the 21st Century? New Zealand has examined in great detail the feasibility of a dynamic geodetic datum before final implementation (Grant, 1998) and forms a good reference for this study.

1.3 Thesis aims and outline

The aims of this thesis are to:

- Provide an overview of geodetic reference systems, datums, modern positioning techniques, and the accuracy requirements of geodetic datums for a wide variety of positioning applications.

- Discuss the effects of tectonic motion and localised deformation on a geodetic datum, and the implications of these effects for users of the datum.

- Discuss the considerations and requirements for a dynamic geodetic datum in PNG.

- Compute a geodetic velocity and strain field for PNG.

- Examine the effects of tectonic distortion on a static geodetic datum in PNG (PNG94).

- Examine in detail, case studies in areas of economic significance within PNG where localised tectonic deformation is significant.

- Develop an algorithm for the computation and adjustment of geodetic networks which includes both linear and non-linear motion of stations.

- Review different strategies for implementing a dynamic datum in PNG to mitigate against tectonic distortion.

Chapter Two provides an overview of geodetic reference systems and their role in providing a framework for modern geodetic datums together with an overview of the different space geodetic techniques used in datum definition. The requirements and applications of geodetic datums in the era of space geodetic positioning are discussed with relevance to PNG, in particular, the

implications of various scales of tectonic deformation on positioning accuracy there.

Chapter Three summarises the development of geodetic datums and crustal deformation surveys in PNG. Considerations for further datum development are discussed. Chapter Four provides an overview of the tectonic history and current tectonic setting in the country. The major tectonic plates and boundary zones in PNG are outlined.

Chapter Five describes the approach and methodology adopted to re-analyse the tectonic deformation in PNG using all known geodetic data, specifically GPS. The effects of tectonic deformation on both national and local geodetic datums are described quantitatively with an evaluation of the existing datum in PNG. An algorithm is developed which mitigates the effects of tectonic distortion of the geodetic datum when performing network adjustments using geodetic measurements.

Chapter Six reviews different strategies for implementation of a geodetic datum in PNG which make allowance for tectonically induced distortion and co-seismic displacement of geodetic stations. The appendices list in detail the datum definitions, results and algorithms used in this thesis.

Chapter 2

Requirements of Geodetic Datums in the 21st Century

2.1 Geodetic Reference Systems – A review

A geodetic reference system provides a homogeneous framework to enable positions in space and time, gravity, as well as derived inverse quantities such as distances, azimuths and velocities, to be described uniquely relative to the origin and orientation of the system in inertial, or terrestrial space.

Traditionally, geodesy has strived to provide positions uniquely referenced to the Earth's surface, primarily for the purposes of sea and land navigation, and charting. Until the advent of artificial satellites and astrometric interferometry, absolute positioning was only achievable at charting scale (20-400m) using direct astrometric methods. Relative positioning requirements for the purposes of urban and rural planning, engineering works and land definition were somewhat arbitrary and localised due to the great expense and difficulty bringing a local datum into a global frame with absolute accuracy. We have inherited from this era of terrestrial geodesy and geodetic astronomy a multitude of disparate local and regional datums. The relationships and transformation parameters between these datums were poorly defined until the application of modern space geodesy made this possible.

Geodetic datums have evolved with positioning technology. As the precision of position determination has improved, so too has the definition with which geodetic datums have been realised. The accuracy of datum definition should be at least as high as the measurements made by users of the datum. Improvements in positioning and information technology have often resulted in revolutions in the manner in which geographical information has been used. Since the 1980s these improvements have driven rapidly increasing demands for homogeneously referenced spatial data to suit a very wide range of positioning applications.

2.2 Hierarchy of Reference Systems, datums and positioning methods

The most fundamental reference system is one whose origin, orientation and scale is fixed and considered invariant in time, in other words an inertial reference system. A hierarchy of geodetic reference systems and their physical realisation exists between space-fixed and local terrestrial reference systems. A reference system is defined conventionally by three orthogonal axes in space and is the basis for uniquely describing positions within the system by coordinates. A reference frame or datum, on the other hand, defines the location of the origin and axes of reference system/s indirectly by the use of coordinates and velocities of a monumented network. In other words, the exact location of the origin and axes of the reference system are inferred. A datum is accessible in that it is a network of physical stations that materialise the reference system. Table 2.1 shows a comparison of the different geodetic reference systems and the primary positioning technique used to define the frame or datum. These are discussed in more depth below.

2.2.1 A Conventional Inertial Celestial Reference System

A space-fixed inertial reference system is required to describe the motion of the Earth, artificial satellites and other celestial bodies with respect to it. To people on the Earth, the Earth itself had been considered an inert reference for most of the human era, the heavens apparently moving in relation to an earth-centred, earth-fixed (ECEF) reference system. It has only become evident in relatively recent times that the earth is itself a rotating body, orbiting larger bodies in the universe, and that the "sky" or celestial sphere appears to be fixed (Copernicus, Galileo, Kepler) resulting in the development of the International Celestial Reference System (ICRS). A number of very distant, extra-galactic radio sources, quasars, whose relative angular motions are very small, realise the ICRS with the International Celestial Reference Frame (ICRF) (Ma *et al.*, 1998).

Concept	System	Frame/Datum (System realisation) *connections in italics	Principal Positioning Method *connections in italics
Conventional Inertial Celestial Reference System	International Celestial Reference System (ICRS)	International Celestial Reference Frame (ICRF) Precession and nutation	Very Long Baseline Interferomery (VLBI)
↓	↓	*Earth Orientation Parameters (EOP)*	*Collocated VLBI/SLR/GPS*
Conventional Terrestrial Reference System (Dynamic)	International Terrestrial Reference System (ITRS)	International Terrestrial Reference Frame (ITRF)	GPS and Satellite Laser Ranging (SLR), also DORIS
↓		*14 parameter transformation*	*Collocated SLR/GPS*
Continental Reference System (Static)		e.g. Geodetic Datum of Australia (GDA94) & Papua New Guinea Datum (PNG94)	Permanent Global Positioning System (GPS)
↓		*7 parameter transformation or projective transformation*	*Multiple Reference Station (MRS) or Virtual Reference Station (VRS)*
Local Plane Grid System		e.g. Lae City Datum, Project datums	Kinematic GPS & Conventional Terrestrial methods

Table 2.1 Hierarchy of Reference Systems, Datums and Positioning methods. The arrows indicate the flow of the hierarchy from an Inertial Celestial System to a local Earth system. The defining positioning techniques and linkages between the systems and their realisation are also indicated.

2.2.2 Very Long Baseline Interferometry (VLBI)

A network of Very Long Baseline Interferometry (VLBI) tracking stations precisely measures the motion of the network with respect to the ICRF. The spatial relationship between VLBI stations on Earth has been well estimated (to within a few mm), forming a global polyhedron of sites, which in turn define the

orientation of the Terrestrial reference frame in relation to the celestial system and its temporal variation.

2.2.3 Satellite Laser Ranging (SLR)

A constellation of small artificial Earth satellites (LAGEOS and ETALON) equipped with retro-reflectors enables laser ranging measurement precision to less than a centimetre. Reflectors have also been placed on the lunar surface. A network of Satellite Laser Ranging (SLR) and Lunar Laser Ranging (LLR) stations provide high resolution monitoring of the Earth's gravity field, centre of mass (geocentre) and solid Earth tides.

2.2.4 A Conventional Terrestrial Reference System

An ECEF reference system is required to describe motions of the Earth and its gravity field. The Earth's surface is tectonically active and some "fixed" Earth system is required to relate motion of the lithosphere to a more stable mantle coupled to the Earth's rotation. Geological and geomagnetic Earth models have initially provided a basis to relate these two motions to form a *no-net-rotation* (NNR) Earth where this condition is satisfied (DeMets *et al.*, 1990; Argus and Gordon, 1991; DeMets *et al.*, 1994).

VLBI, SLR, and GPS are the primary geodetic techniques used to define a global reference system, the International Terrestrial Reference System (ITRS). The ITRF is the physical realisation of the ITRS.

2.2.5 Earth Orientation Parameters (EOP)

The EOP relate the ICRS, precession, and nutation to the ITRS at a given epoch. The VLBI network precisely measures the rate of rotation and orientation of the Earth in space. VLBI monitors reduced Universal Time (UT1) and the location of the Earth's axis of rotation (the International Earth Rotation and Reference System Service (IERS) Reference Pole or IRP) with respect to the ICRS reference pole, the Celestial Ephemeris Pole (CEP) and its temporal variation (nutation and

precession). These are collectively referred to as the Earth Orientation Parameters (EOP) (Altamimi *et al*., 2002).

2.2.6 Global Navigation Satellite Systems (GNSS)

Various satellite navigation and positioning systems have been developed during the last forty years. These are collectively referred to as Global Navigation Satellite Systems (GNSS) and include; the Global Positioning System (GPS) developed by the US Department of Defense, the Russian Global Navigation Satellite System (GLONASS), the French Doppler Orbitography by Radiopositioning Integrated by Satellite (DORIS) and, in the near future, the European Space Agency's GALILEO. It is envisaged that receiver hardware and processing software will evolve to allow for integration of the different systems in the future, however only the GPS system has been used in this study.

2.2.7 The Global Positioning System

GPS has become the dominant system for geodetic surveying and geodynamics studies, due to its accessibility, low cost of hardware and relative accuracy. GPS is essentially a radio-navigation system used to determine positions on the earth by simultaneous ranging from roving antenna/receiver combinations (the user segment) to a constellation of ~28 satellites (the space segment). The positions and orbits of the GPS satellites are estimated accurately by measurements from a fixed ground control network (the control segment). The GPS satellites orbit the earth in six orbital planes at an inclination angle of 55° to the equatorial plane at a range of *c.* 20,200 km with a period of *c.* 12 sidereal hours (Hoffman-Wellenhof *et al.*, 2001).

The basic positioning principle is similar to that of classical trilateration. A minimum of three ranges from GPS satellites, whose positions are known, to a GPS antenna at an unknown location are required to estimate the position of the antenna. A range measurement to a fourth satellite is required to synchronise the receiver clock to the GPS system. The apparent range from the antenna to the GPS satellite, which includes the range offset resulting from the clock bias in the

receiver, is referred to as the pseudorange. The true range is computed once the receiver clock bias has been estimated. GPS satellites transmit ranging code and time on two L-band frequencies;

- L1 at 1575.42 MHz, λ 190 mm, and
- L2 at 1227.60 MHz. λ 244 mm

Three pseudo-random noise (PRN) ranging codes are used. The Coarse/Acquisition (C/A) code has a 1.023 MHz chip rate, a sequence period of one millisecond (ms) and a wavelength of *c.* 300 m. The precision (P) code has a 10.23 MHz chip rate, a sequence period of seven days and is the principal navigation ranging code. The P code has a wavelength of 30 m. The Y-code is used in place of the P-code whenever the anti-spoofing (A-S) mode of operation is activated by the US DoD (Hoffman-Wellenhof *et al.*, 2001).

The C/A code is modulated upon the L1 frequency and the P-code is modulated upon both L1 and L2 frequencies. The GPS satellites all transmit on the same frequencies, L1 and L2, with individual pseudo-random codes (PRNs) to enable distinction between the different satellites. Each satellite also transmits a navigation message containing the GPS system orbital elements (the broadcast ephemeris), clock correction coefficients, GPS system time, ionospheric models and other status messages. Improvements to the GPS system have been planned, including; broadcast of C/A code on the L2, from 2003, and implementation of a third frequency, the L5 at 1176.45 MHz from 2005 (Hoffman-Wellenhof *et al.*, 2001).

Absolute and differential point positioning using the pseudorange is only accurate to 2-30m, suitable only for navigation purposes and small scale mapping. Geodetic and geodynamics applications require measurements at the centimetre and millimetre level. To attain this accuracy, the GPS carrier phase needs to be observed. Phase resolution at 0.1% of the wavelength can provide a theoretical precision of *c.* 0.2 mm

The carrier beat phase of the L1 and L2 carrier waves can be reconstructed by differencing the phase of the carrier wave of the signal received from the GPS satellite and the phase of the clock signal generated by the receiver. While the

fractional phase can be measured directly, the whole or integer number of phase cycles is not known. This number is referred to as the phase integer ambiguity and must be estimated before a full range measurement is known.

GPS measurements and analysis are affected by a number of errors and modellable biases, including;

- Satellite and receiver clock errors (biases)
- Ionospheric delay
- Orbit errors
- Tropospheric delay
- Antenna phase centre variations
- Multipath
- Antenna height measurement
- Antenna mis-centering
- Monument and antenna instability
- Solid earth tides
- Pole tide
- Ocean tide loading
- Atmospheric pressure loading

If the contribution of the error sources in the GPS measurements are collectively significantly less than the cycle wavelength, the integer values of the biases can be computed unambiguously. If these errors are too great, then the integer values may be incorrectly estimated. The process of determining the correct number of integers is called ambiguity resolution or fixing. Where ambiguities are not resolved, this is referred to as a float solution. Many software packages scale the Variance-Covariance matrix (VCV) of the float solution. A more detailed description of the GPS system and its application to geodesy can be found in Hoffman-Wellenhof *et al*., 2001.

2.2.8 The International Terrestrial Reference Frame (ITRF)

An increasingly dense network of continuous GPS tracking stations has formed the basis of the International GPS Service (IGS). Collocation of many of these stations with other GNSS, VLBI and SLR, and improvements in the precision of measurement of the vectors between these tracking stations and their variation with time have resulted in a sequence of increasingly accurate realisations of the ITRF (Figure 2.1). The current realisation is ITRF2000 (Altamimi *et al.*, 2002).

In essence, the ITRF is a global geodetic datum in an "absolute" sense. The datum is dynamic in that velocities of the stations are integral to the realisation. The coordinates of the ITRF datum stations vary with time due to tectonic displacement and can be considered "absolute" due to the fact that they represent the closest estimation of their relationship to a no-net-rotation condition geocentric reference system at a given epoch in time. The different space geodetic methods are used to define and cross-validate the ITRF by means of precisely surveyed site ties between the reference points of each techniques' instrumentation at collocated sites (Altamimi *et al.*, 2002). Many of the geodetically stable stations have been operational sufficiently long for their site velocity to be estimated with an accuracy of less than 1 mm/yr (Altamimi *et al.*, 2002).

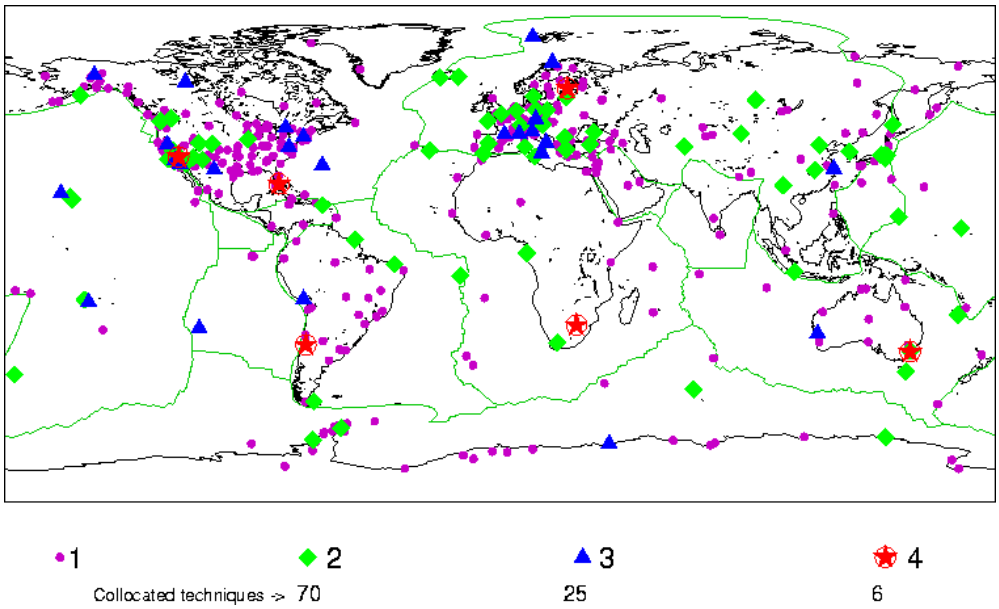

Figure 2.1 ITRF network in 2003. Diamonds, triangles and stars indicate sites collocated with different techniques (http://lareg.ensg.ign.fr/ITRF/network.html)

2.2.9 Continental Reference Systems

Larger tectonic plates have been found to be internally rigid on decadal timescales (Beavan *et al*. 2002; Sella *et al.*, 2002), moving regularly about a well-defined pole of rotation, referred to as an Euler pole. Instantaneous site velocities on rigid plates have been found to be highly linear for the duration of contemporary geodetic observation histories, with insignificant baseline changes between different stations located on the rigid plate. The plate reference frame rotates with respect to the terrestrial frame and the dynamic transformation parameters between the two reference systems can be derived.

A continental reference system is essentially a continent-fixed, earth-centered system where tectonic motion of a rigid continental plate is removed, i.e., coordinates in the system are described relative to a stable continental plate, with zero site velocities in the plate reference frame. Before the space geodetic era, national geodetic datums were defined by origins located on the surface of the Earth by astronomical means. The accuracy of position estimation of a primary datum origin was typically *c.* 30 m with respect to a mean earth reference spheroid* that best fitted the global geoid. A spheroidal surface was chosen to best fit the national geoid for national geodetic purposes in order to minimise geoid-spheroid separation and deflection of the vertical (astro-geodetic deflection). The astro-geodetic deflection is the local difference between the geoidal vertical and the spheroidal normal. The geoidal vertical is a curved line due to the non-parallel nature of surfaces of equal gravitational potential. At the datum origin, the deviation of the vertical and geoid-spheroid separation were usually assumed to be zero, or a value which minimised the deviations within the region encompassed by the datum. By virtue of such a definition, the origin, orientation and scale of a best fitting spheroid were not coincident with a geocentric spheroid, but a best fit to the local region.

* The terms ellipsoid and spheroid have been used somewhat interchangeably in geodetic literature. In the case of the Earth, the ellipsoid is the shape formed by the rotation of an ellipse around the Earth's minor axis which best fits the geoid. A spheroid is defined as any shape resembling a sphere, including an ellipsoid, but the definition can also include other mathematically defined shapes. The ellipsoid is the defined mathematical reference surface for ellipsoidal coordinates related to the ITRS.

The geodetic datum was established using the highest precision terrestrial surveying equipment available at the time. Initially triangulation techniques, constrained by high precision baselines and astronomically derived azimuths, were used to extend the horizontal geodetic datum. Geometric levelling from tide gauges, trigonometric heighting, differential barometric heighting and gravimetry have been the main techniques used to extend height datums and develop geoidal models. The advent of electronic distance measuring equipment (EDM) in the 1950s enabled positions to be derived to a higher degree of accuracy using trilateration techniques.

Continental scale geodetic networks were usually heterogeneous by virtue of the impossibility of extending terrestrial measurements across the oceans. The almost complete reliance on terrestrial measurements, and geodetic astronomy meant that it was not feasible to connect these different national datums until the advent of long-range trilateration and satellite positioning made this possible. Geophysical studies were the driving force for datum integration using gravimetric and lunar observations (Bomford, 1980; Torge, 2001). Continental scale reference systems can be related to ITRF either by forward/reverse computation using the relative Euler pole between the systems, or by a 14-parameter similarity transformation which includes the rate of change of the conformal seven parameters.

2.2.10 Local Reference Systems

In areas of limited extent, such as smaller urban areas and engineering projects, variations in scale-factor and arc-to-chord corrections to geodetic measurements are often small in magnitude and generally consistent enough to be insignificant at the level of precision required. A common practice for land surveyors and engineers has been to establish a local reference system, usually a horizontal plane grid whose datum stations may either coincide with national geodetic datum stations, or be completely arbitrary. Where stations are common to both local and geodetic datums, the transformation parameters between them are easily derived when required.

National geodetic datums evolve over time, resulting in a change of coordinates for the monuments that realise the national datum. Should a local reference system remain fixed, recomputation of the transformation parameters between national and local datum is required. This is a very practical approach for a number of reasons;

(i) The arbitrary coordinate system for local cadastral and engineering surveys does not need to change, thus avoiding confusion as to which geodetic datum is prevalent at the time.

(ii) No projection scale factor and arc-to-chord corrections are required to be applied to surveying measurements. This suits many cadastral, engineering and construction surveyors who are often unfamiliar with these. The only corrections required to be made to measurements are for reduction of slope to horizontal, deviation of the vertical, and atmospheric corrections for higher precision measurements.

(iii) A stable local network is all that is required to accomplish locally referenced positioning tasks to a satisfactory accuracy. Many cadastral surveyors prefer to avoid coordinate systems altogether, since datum independent internal angles and distances define cadastral boundaries and their relationship to reference marks. The only standard required is that of length scale.

The distinction between a local horizontal plane grid and a map grid should be made clear. A map grid such as UTM (Universal Tranverse Mercator) is a projection of the reference ellipsoid realised by a geodetic datum. Necessarily, scale factors for elevation above the reference ellipsoid and grid projection scale factor have to be applied to transform local plane distances in a local plane grid system to a map grid. A common practice is to adopt the UTM coordinates of a local plane datum origin and apply a scale factor of 1 to all other measurements made to extend the local datum. This is a potentially confusing practice unless the distinction between UTM or Plane coordinates is made clear, and should be avoided, due to the similarity in magnitude of the coordinates.

The increasing adoption of real-time kinematic (RTK) GPS methods for cadastral surveys, engineering surveys and other LBS poses some problems when used in conjunction with local plane datums. Geocentric Cartesian coordinates and derived inverse quantities are usually projected from a reference ellipsoid onto a surface not usually coincident with the local ground surface or a local datum plane. Transformation parameters from WGS-84 and other satellite datums to the local datum are required to be computed and entered into the GNSS processing software, either in real-time or during post-processing in order for the GNSS measurements to be relevant and useful. If the local transformation parameters have not been preset into the software, then some skill and geodetic knowledge is required by the user to set up a user-defined local reference system, or transform the coordinates by some other process. Most of the commonly used geodetic datums' transformation parameters from the satellite datum have been setup in the GNSS software, however, many users will use "default" settings if they lack sufficient understanding of the consequences of datum shifts.

2.2.11 Positional and Local Uncertainty

Subsidiary networks allow for degradation of "absolute" accuracy, as long as relative accuracy requirements are met. This datum concept has been acceptable while positioning precision was achievable only at local level, and while the hierarchy of survey networks "order" was understood. By definition "order" is a measure of how close a local network's coordinates are to the parent network, whereas "class" is a measure of the precision of the survey network, regardless of its goodness of fit to the parent network. In other words, a survey network of high class may have a very low order.

Such concepts, although still important in the distinction between national and local surveys, have the potential for confusion when considering the absolute precision capabilities of positioning technologies today. The advent of centimetre accurate absolute positioning will soon make the distinction between surveys of different order difficult, unless the datum origin is included in metadata. It is now already feasible for surveyors using elementary space geodetic methods to assign the highest classical geodetic order to local networks.

The concept of *Positional Uncertainty* is a better description of the accuracy of absolute positions. It provides a comparison of coordinate accuracy derived by different means and reference stations with respect to the parent datum (ICSM, 2002).

For localised surveys, a related concept of *Local Uncertainty* provides a comparison of coordinate accuracy derived by different means and reference stations with respect to a local reference system or local ties (ICSM, 2002). A measure of local uncertainty has more relevance to cadastral and engineering surveys. While absolute coordinates of varying degrees of accuracy are important for global mapping and navigation purposes, their greatest accuracy is specifically of interest to geodynamic studies and the development of geodetic datums.

2.3 Applications and accuracy requirements of a Geodetic Datum

A geodetic datum provides the positional framework for an increasingly wide variety of applications, including;

- Navigation – Air / Land / Sea
- GIS / Digital Cadastral database (DCDB)
- Control of imagery (space, aerial photogrammetry, Interferometric Synthetic Aperture Radar (InSAR))
- Land boundary definition
- Environmental mapping and monitoring
- Geological and natural resource mapping, exploration
- Urban Planning / Census mapping
- Civil Engineering (Urban infrastructure, services, utilities, roads, powerlines, dams, water reticulation)
- Location Based Services (LBS)
- Mining Engineering (mine workings, haul and access roads, pipelines, tailings dams)

- Geophysical Hazard Monitoring (Volcano monitoring, fault movement, strain monitoring, slope stability and subsidence)
- Sea level monitoring
- Asset management
- Rescue operations

Land Development is increasingly becoming dependent upon spatial information technology to provide homogeneous geographic referencing. Hard copy spatial information (e.g. charts, maps, survey plans, coordinate lists) are not suited to time varying coordinate information if the variations are noticeable at plottable scale during the lifetime of the document. In fact, many digital GIS or remote sensing packages that are in widespread use today have no provision for temporal variation of the base coordinate system.

Accuracy specifications are widely documented in many standards documents (e.g. ISO 4463-1:1989 Measurement methods for building - Setting-out and measurement - Part 1: Planning and organization, measuring procedures, acceptance criteria; ISO 19111:2003 Spatial Referencing by Coordinates), survey coordination regulations and engineering specifications.

2.3.1 Accuracy requirements for mapping, GIS and LBS

One of the primary functions of a geodetic datum is to provide a control framework for mapping, navigation, GIS and LBS. The accuracy requirements for paper-based mapping have been dictated by the plotting accuracy at map scale. A plotting accuracy of 0.2mm with respect to the map graticule is represented on the ground at different plot scales in the table 2.2 below. Minimum survey tolerances should be one third of the required accuracy, using a widely accepted "rule of thumb" related to statistical confidence ($3\sigma \approx 99\%$ confidence level) and the need to provide a safety margin to allow for network misfits resulting from error propagation.

Map Scale	Application	0.2mm plot accuracy on the ground	minimum survey tolerance
1:1,000,000	International maps	200m	~70m
1:250,000	Aeronautical charts	50m	~20m
1:100,000	small scale topographical maps	20m	~5m
1:50,000	cadastral index maps	10m	~3m
1:10,000	town maps	2m	~0.5m
1: 2,500	urban service maps	0.5m	~0.1m
1:1,000	urban cadastral maps	0.2m	~0.05m
1: 500	construction site plans	0.1m	~0.1m

Table 2.2 Mapping plot accuracies and survey tolerances

Digital maps and GIS remove the limitations of plotting accuracy, so that the accuracy of the georeferencing is directly related to the accuracy of the data acquisition. Coordinates of object nodes in a GIS layer may have a snap precision of millimetres, yet have a true accuracy of kilometres. Metadata containing spatial data accuracy information is absolutely essential in any GIS, and is an aspect that is often overlooked by users of GIS and analysts of geographical data. Cadastral boundaries digitised off a 1:10,000 cadastral index map may be 2m or more in error from their surveyed positions with respect to the local survey system, and yet have positions quoted to millimetre accuracy in the database. DCDBs can be either survey accurate, or plot accurate depending on whether the database is constructed from survey plan dimensions, actual measurements or simply digitised off a plan.

2.3.2 Accuracy requirements for Cadastral surveying in PNG

The accuracy of cadastral boundary marking is dictated largely by the real or perceived value of the land enclosed. The value of the land is influenced by potential economic yield, its suitability for food production, or its spiritual or aesthetic value. In general, the larger the parcel of land the greater the tolerance with which boundaries need to be demarcated. It is unnecessary and uneconomical for land-holders of large estates to have their boundaries surveyed to millimetre precision. An error of one metre in the location of a corner of a

large property of say 10,000 Ha does not impact as significantly on the computation of the enclosed area as it would for a property of 100 m^2!

Traditionally, in PNG, land boundaries have been defined by natural or artificial "general" boundaries, rather than by surveyed dimensions. In the absence of surveying measurements, well-marked general boundaries have stood the test of time. The exact location of these boundaries in a spatial sense has often been of little interest to the landholder. As long as the boundary monumentation has been durable and witnessed by impartial authorities, boundary disputes have been rare. Table 2.3 outlines the cadastral surveying accuracies in PNG.

The underlying principle of cadastral surveying is that monuments have precedence over measurements in defining the boundary. As surveying technology has improved, so too has the accuracy of the measured or apparent dimensions of boundaries, assuming that the boundary monuments have been stable relative to each other. Surveyors aware of the lack of precision of their measurements have adopted a wise practice of including excess into their measurements to prevent disputes over perceived shortages at some later date. An important exception to this principle is where natural boundaries move with time, for example riparian boundaries such as centrelines of watercourses (*ad medium filium aquae*) and shorelines resulting from processes of accretion and avulsion. Co-seismic offsets could be accommodated in a similar way. It is impractical to hold boundary coordinates fixed in these instances.

Approximately 97% of PNG is unsurveyed customary land (Done, 1984), where ownership is vested in a community, clan group or family. The remaining 3% is either freehold or leasehold land vested in the PNG state.

There are several classes of cadastral surveying standards in PNG (Papua New Guinea, 1990; G. Patterson, *pers. comm*. 2002);

- **Urban Class 1**; Urban residential, commercial

- **Rural Class 1**; Land used for resource extraction (e.g. exploration and

mining leases, plantations), utilities and utility corridors (e.g. power stations, power lines, gas/oil pipelines). Survey costs are a small proportion of the development cost.

- **Rural Class 2**; Land used by small holders, settlement blocks etc.., Land which has a low economic yield, yet where survey costs have to be minimised.

- **Rural Class 3**; Land less than 75 hectares and not bundled up with other surveys of similarly poor quality. Intended for customary land registration for individuals or family groups.

- **Rural Class 4**; intended for clan boundary definition in excess of 200 hectares.

- **Unsurveyed land**; Customary land general boundaries – defined by customary law.

Classification	Derived Positional Tolerances	Closure	Prop. Closure (ppm)	Angular Misclosure*	Linear misclosure*
Urban Class 1	0.03 m (at 200m)	1:5,000	200	30″	0.01m + 100 ppm
Rural Class 1	0.5 m (at 5 km)	1:4,000	250	30″	0.01m + 100 ppm
Rural Class 2 (A)	2 m (at 10 km)	1:2,000	500	30″	0.02m + 200 ppm
Rural Class 2 (B)	10 m (at 10 km)	1: 200	5000	30″	0.02m + 200 ppm
Rural Class 3	10 m (at 15km)	1:200	5000	1′	0.1m + 1000 ppm
Rural Class 4	25 m (off map)	not specified	not specified	not specified	not specified

Table 2.3 PNG Cadastral surveying accuracy requirements (Papua New Guinea, 1990), *for a typical four-sided block of land

2.3.3 Positioning tolerances in engineering and construction

Physical tolerances and gradients dictate the positioning accuracy requirements for engineering and construction. Horizontal and vertical datums for projects should be rigorous in a relative sense. Errors in heighting impact significantly on drainage, hydraulic flow and head calculations. The need for a stable vertical datum related to the local gravity field is of paramount importance.

Many regions of PNG have geoidal gradients approaching 0.25m/km (0.025%) with respect to the Geodetic Reference System Ellipsoid 1980 (GRS80) (Kearsley and Ahmad, 1996). Use of satellite positioning methods for height determination in engineering projects require high resolution relative geoid models in order to compute orthometric heights. This prevents errors in hydraulic grade calculations should ellipsoidal heights be used, due to the effects of geoidal undulation.

The following engineering and construction relative positioning tolerances are typical;

- Surface preparation (clearing, grading etc..); 0.3 m
- Earthwork setout subject to accuracy requirements; 0.1 m
- Road surfacing, kerb and guttering; 10 mm horizontal 5 mm vertical
- General Construction; 1:5000 (<10 mm relative to a 50 m site)
- Bridge setout, in-situ concrete structures; 5 mm horizontal, 2 mm vertical
- Pre-fitted slab construction, pre-cast structure setout; 2 mm
- Airport runways, taxiways and apron; 5 mm Horizontal, 2 mm Vertical
- Geological sample locations; (3 m relative to exploration datum)
- Geological and Geotechnical Drill hole locations; (0.4 m relative to exploration datum)

2.4 Geophysical Hazard Monitoring

Geological hazards pose a very serious threat to the population and economy of PNG. The destruction of most of the city of Rabaul by the twin volcanic eruptions in 1994 (Davies, 1995) and the tsunami disaster near Aitape in July 1998 (Davies, 1998) resulting in the deaths of ~2,500 people attest to this. Seismic hazards are more dangerous in their tsunami and landslide potential in PNG than the risk of building collapse, due to a larger proportion of the population living along the coast in smaller, lightly constructed houses. Geodetic monitoring in seismically active areas is of critical importance if these areas are close to highly populated coastal areas and major wharves. While earthquake prediction using geodetic measurements is still inexact, measurement of inter-seismic strain, co-seismic displacement and post-seismic relaxation allows for better forecasting and hazard assessment in these areas. The USA (Southern California), Japan and New Zealand are some of the seismically active countries and regions where extensive geodetic monitoring networks have been established for this purpose.

Steep submarine walls located along oceanic trenches and seamounts close to the shore can initiate tsunamis when they subside or collapse. Monitoring of slope stability on land is related to seismic hazard, since earthquakes have a tendency to destabilise unconsolidated slopes in mountainous areas, particularly where there is high rainfall. Many deaths in PNG have resulted from landslides overwhelming villages and gardens.

Slope and uplift monitoring of active or potentially active volcanoes allows volcano observers to better predict when a full-scale eruption is imminent. Many coastal volcanoes also have unstable cones and caldera walls, undercut by wave and tide action. Collapse of these can generate localised tsunamis of very large magnitude. The 780m high cone of Ritter Island off the west coast of New Britain collapsed in 1888, generating a 12-15m tsunami which resulted in the deaths of thousands of people on nearby coasts (Cooke, 1981).

Many low-lying coastal regions and islands in PNG are not only threatened by potential tsunami but are potentially subject to an increase in sea level as a result of climate change. The risk is magnified if tectonic subsidence is also occurring. The South Pacific Sea Level and Climate Monitoring Project (SPSLCMP)

(http://www.pacificsealevel.org/index.htm) has recently become operational, whereby continuous GPS measurements are made in close proximity to SEAFRAME tide gauges operated by the National Tidal Facility (NTF). Comparison of the vertical displacement of the tide-gauge with the actual tide data removes the systematic bias resulting from tectonic uplift or subsidence at the monitoring site from the estimation of absolute sea-level change in the region.

Volcano slope monitoring by geodetic methods can be achieved by accurate measurements from a nearby stable network; however inter-seismic strain which often occurs over broad areas can really only be effectively monitored from a geophysically stable network such as ITRF. A network of four Continuous GPS (CGPS) stations has been established around the Rabual Caldera by the Rabaul Volcanological Observatory (RVO) to monitor any volcanically related deformation, particularly uplift resulting from magma movement close to the surface (S. Saunders, *pers. comm.,* 2003).

Regional monitoring of vertical deformation resulting from widespread magma diapirism along the active volcanic arc zones in PNG will be useful for long-term hazard prediction, and to provide some control for localised deformation in close proximity to potentially active volcanoes (S. Saunders, *pers. comm.,* 2003). Connection of the Rabaul, Ulawin and Pago GPS networks to ITRF or a dynamic PNG datum will enable differentiation between regional and localised deformation that the existing networks cannot provide.

2.5 Tectonic stability of Geodetic Datums

2.5.1 Deformation of Geodetic Datums

A widespread misconception persists with many practitioners within the surveying and spatial information professions that geodetic datums are static and do not move with time. Coordinates of first order stations have been considered to be error free, or at least of very small uncertainties, only changing when more precise measurements in the primary network are made and datum

coordinates subsequently readjusted. Baseline measurement precision is now achievable at the 1 ppb level with high accuracy space geodetic techniques and computation methods, and, less than 0.5 ppm with proprietary methods, making direct measurement of tectonic deformation possible. The assumption that geodetic networks are stable in locations where the signal of tectonic deformation is greater than the precision of the measurement technique is clearly wrong. The strategy of adjusting very precise geodetic baseline observations to fit a distorted primary network by constraining more than one datum station can result in misfits (heterogeneities) between sections of the densified network. If measurement of datum deformation is possible, then the datum should accommodate a velocity or deformation model to mitigate resulting distortion. This is particularly important where the distortion exceeds tolerances for surveying and positioning applications.

2.5.2 Datum stability

A static geodetic datum is considered stable if the coordinates of the primary stations do not change significantly between different adjustments. In other words, both the monuments and coordinates are stable with respect to each other and their spatial relationship is known better than the limits of measurement capability. The current Australian Geodetic Datum (GDA94) is a very good example of a stable datum. No deformation is detectable across the continent at significant levels (> 1 mm/yr) (Tregoning, 2003) and, despite the Australian continent's drift of between 55 and 70 mm per year in a north-northeasterly direction, few baseline changes are evident internally with the exception of occasional intra-plate earthquakes that may result in localised deformation. The Australian Datum is stable relative to the Australian continent.

2.5.3 Datum instability

The former New Zealand Geodetic Datum is a good example of an unstable datum. Before 2000, New Zealand had adopted the New Zealand Geodetic Datum 1949 (NZGD49) as realised by a national re-adjustment in 1949 (Lee, 1978). NZGD49 served New Zealand well for medium scale mapping (1:10,000 or

smaller scale), navigation and surveys of limited extent. The relative displacement (baseline change) between Auckland and Dunedin as a result of the convergence of the Pacific and Australian plates at *c.* 50 mm/yr had no impact on local surveyors in either of those two cities. These local surveyors were able to fully constrain local geodetic surveys to local first order NZGD49 stations with good agreement.

The problem in New Zealand arose in the rapidly deforming zones along the Pacific / Australian Plate boundary. After fifty years, relative deformation across the boundary had amounted to *c.* 2-3 m and it had become impossible to fully constrain geodetic networks to the 1949 adjustment straddling the plate boundary without applying very loose *a priori* constraints to the measurements. In essence, good measurements were made to fit a distorted network. By the 1990s widespread use of long range differential GPS services was beginning to identify major distortions in the NZGD49 network (Grant and Pearse, 1995).

An intensive GPS campaign during the 1990s resulted in the development of a high resolution velocity field and deformation model for New Zealand relative to the Australian Plate (Figure 2.2) and, by 2000, a "semi-dynamic" geodetic datum had been implemented (Pearse, 2000; Beavan and Haines, 2001).

In PNG, the tectonic deformation also propagates directly into geodetic networks which span internal plate boundaries (Tregoning and Jackson, 1999). Distortion of geodetic networks is observable at both national and localised scales when the magnitude of the distortion increases beyond the level of precision of geodetic observations. National and larger scale survey networks are subject to distortion if they include baselines which straddle plate boundaries and deforming zones.

Transition zones of strain partitioning occur within plate boundary zones, where relative plate motion between adjoining plates is transferred from one plate to the other through a diffuse deforming zone. The breadth of the deforming zone is largely related to the strength of the underlying lithosphere (e.g. Turcotte and Schubert, 2001). Oceanic lithosphere is generally stronger or "stiffer" than continental lithosphere. As a consequence, deforming zones tend to be broader across continental collision margins than oceanic margins. The extensive

deforming zone resulting from the collision of the Indian and Eurasian plates is one good example (Turcotte and Schubert, 2001).

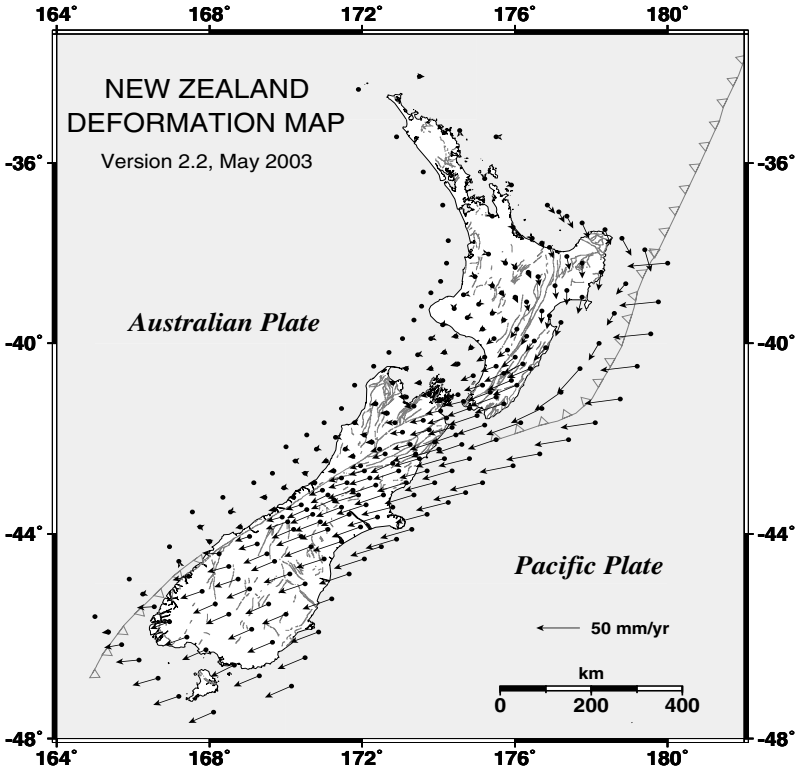

Figure 2.2 The New Zealand Deformation map (Beavan and Haines, 2001; Blick *et al*., 2003)

2.5.4 Localised datum instability

The assumption that smaller cadastral and engineering control surveys are immune from distortion is incorrect if the networks are located within rapidly deforming zones. These localised survey networks are often subject to distortion resulting from diffuse inter-seismic strain accumulation, co-seismic displacements, post-seismic relaxation and other secular movements. Many locations of economic significance in PNG, such as major towns (e.g. Lae, Wewak and Rabaul), ports, mines and plantations, are located within deforming zones near tectonic plate boundaries. By virtue of their intensive land use,

homogeneous survey networks are required to provide primary control for the purposes of positioning and management of spatial data. Distortion of these networks outside acceptable limits undermines the integrity of the entire spatial data infrastructure.

RTK and rapid static GPS are becoming increasingly popular for localised surveys as these methods satisfy precision and accuracy specifications for most surveys using shorter (i.e. < 10 km) baselines. Continuous or virtual reference stations (CRS and VRS) are also becoming popular for providing control for these local surveys, as they connect different surveys to a homogeneous local reference frame. Before the GPS era, cadastral and engineering surveys were strongly constrained by local reference marks by virtue of the limitations of the positioning technology, in particular intervisibility and range. Any discrepancy observed between different hierarchies of local survey networks was not critical as long as internal closure was achieved. Tectonic distortion over a 50 m baseline is only likely to be detected if the line crosses a seismically active fault. The same cannot be said for a 10 km line in a rapidly deforming zone where inter-seismic distortion can exceed the capability of the precision of the survey technique. This mitigates against the use of VRS and CRS systems in these areas.

2.5.5 Co-seismic and post-seismic deformation

Due to the elastic nature of the crustal lithosphere, strain accumulates across locked faults or asperities during the inter-seismic period. Inter-seismic strain has been shown to be highly linear for the majority of geodetic sites located in actively deforming zones undergoing strain accumulation (Feigl *et al.*, 1993; Tregoning *et al.*, 2000).

Once the strain exceeds the elastic limit or locking strength of the asperity, a release of strain occurs resulting in an earthquake and co-seismic deformation. If the material structure of a tectonic block subjected to stress is highly elastic, then strain may accumulate over a considerable period of time before failure. Alternatively, the block may deform aseismically or anelastically if the block material is relatively unconsolidated (alluvium etc.) or the frictional coefficient is very small along the fault, (e.g. Turcotte and Schubert, 2001). Localised surface

deformation resulting from earthquakes can be predicted using dislocation models (e.g. Okada, 1985). Sun *et al*.(1996) have developed a model for larger scale dislocations which includes corrections for the sphericity of the Earth for dislocations across major asperities.

An anelastic post-seismic relaxation phase is often evident where movement across the asperity stabilises after an episode of major co-seismic displacement. The time series for Rabaul in PNG before and after the Mw 8.0 New Ireland earthquake on 16th November 2000 was analysed as part of this study. The time series clearly shows the three stages of the earthquake cycle, (Figure 2.3): linear inter-seismic motion up until the time of rupture, an abrupt co-seismic offset followed by an exponential post-seismic relaxation phase as the velocity stabilises to inter-seismic levels.

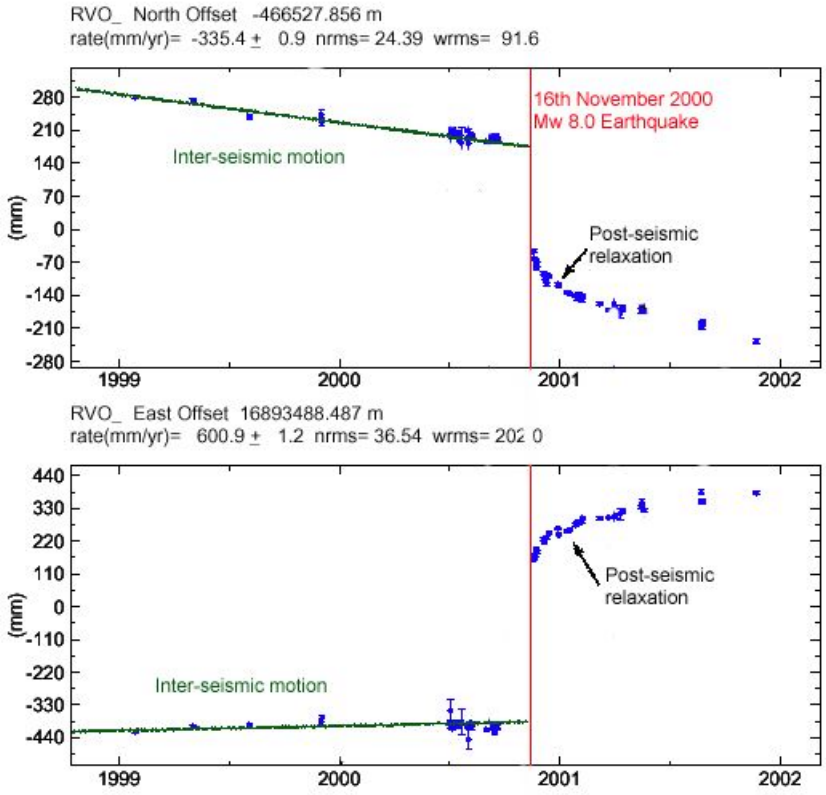

Figure 2.3 Time series from this analysis for RVO_ (Rabaul Volcanological Observatory, PNG) site showing co-seismic offset (~0.21m N and ~0.55m E) and post-seismic relaxation as a result of the 16th November 2000 Mw 8.0 earthquake near New Ireland. The earthquake epicentre was *c.* 33 km from the site.

2.5.6 Surface creep

Geodetic monuments located on unconsolidated ground are very susceptible to creep. Unconsolidated ground can "flow" over underlying bedrock (Anhert, 1967; Braun *et al*., 2001). The rate of movement is governed by the slope of the ground and the frictional character of the ground with respect to the underlying bedrock. In areas of high rainfall, permeation of the unconsolidated material by water decreases the frictional coefficient substantially. Location of monuments in such areas makes it very difficult to distinguish whether movement of the monument actually reflects movement of the underlying geological structure, or simply surface creep. Consequently, geodetic control sites, especially geodynamic monitoring sites, should be established in stable locations where creep is unlikely to occur, unless the creep itself is the subject of the monitoring.

Local site ties located between a few hundred metres and a few kilometres from the monument can be used to verify the stability of the monument location. These ties can be measured to a precision of a few mm in a relative network. Monitoring of this network provides some level of confidence for the stability of the monument with respect to local geological structures and to ascertain whether the site is affected by localised deformation or creep.

Likewise, stability of geodetic monuments in the ground can only be verified by a recovery network within a radius of about 10 metres. Re-measurement of this network by terrestrial, datum-free methods gives some indication of whether the monument is stable in its location at the millimetre level, otherwise monument instability may be incorrectly interpreted as movement of the underlying geology or creep. A recovery network also enables monument disturbance to be measured and applied as an offset to the monument's coordinates (Beavan *et al.*, 2002).

2.5.7 Monument Noise

Seasonal variations (red spectrum noise) (Langbein and Johnson, 1997; Zhang et al., 1997; Mao et al., 1999; Williams, 2003) and random motions (random-walk) in monument stability with the respect to the surrounding crust are also known

to occur, particularly where large variations in hydrology and seasonal temperature are evident. The random-walk noise can exceed 0.33mm^2/yr (Johnson and Agnew, 2000) and seasonal variations can be as much as 3 mm, though usually less than 0.5 mm for stable sites (Langbein and Johnson, 1997). Monument noise should be considered for the highest accuracy geodetic measurements.

2.6 Tolerance limits for tectonic deformation on survey networks.

The magnitude of tectonic distortion on a geodetic datum needs to be put into perspective. A geodetic datum is primarily used for utilitarian purposes. Although millimetre-accurate absolute coordinates and site velocities with respect to a geodetic reference system are important for geophysical studies, the relative accuracy and precision requirements for non-scientific purposes need to be considered. At what stage does the deformation of a datum exceed these accuracy requirements? To what extent, or over what time period can local networks be extended or used in rapidly deforming zones before deformation becomes significant? Surveying accuracy is an expensive commodity, and, ultimately, the cost of acquiring this accuracy is related to economic or engineering tolerance imperatives. Where tectonic deformation rates exceed the tolerances for surveying and positioning the effect of this deformation should be mitigated. Table 2.4 shows time periods for typical absolute positioning applications where the effects of plate motion become significant. This is particularly important for point positioning, online GPS processing in ITRF, or wide-area differential GPS (WADGPS) applications using WGS-84. For example, a user of a high precision WADGPS (0.2m) using WGS-84 to position a site on the Australian Continent will notice significant differences in positions for a monument within four years of a static realisation of an Australian datum. Table 2.5 shows time periods for typical surveys in a range of deformation scenarios where resulting network distortion becomes significant.

	Absolute (ITRF) site velocity in mm/yr				
Absolute positioning tolerances & applications	**5**	**10**	**20**	**50**	**100**
1 mm Highest precision geodynamics studies	0.2	0.1	0.05	0.02	0.01
2 mm High precision geodynamics studies	0.4	0.2	0.1	0.04	0.02
5 mm ITRF horizontal coordinates	1	0.5	0.25	0.1	0.05
10 mm National fiducial geodetic network	**2**	**1**	**0.5**	**0.2**	**0.1**
20 mm National primary geodetic network	**4**	**2**	**1**	**0.4**	**0.2**
50 mm Provincial geodetic network	**10**	**5**	**2.5**	**1**	**0.5**
100 mm Local geodetic network	20	**10**	**5**	**2**	**1**
200 mm High precision WADGPS (RTK)	40	20	**10**	**4**	**2**
500 mm GIS, higher accuracy mapping	100	50	25	**10**	**5**
1000 mm (1 m) Asset mapping, LBS	200	100	50	20	**10**
2000 mm (2 m) DGPS Navigation	400	200	100	40	20
5000 mm (5 m) Lower accuracy mapping	1000	500	250	100	50
10000 mm (10 m) Navigation point positioning	2000	1000	500	200	100

Table 2.4 A calculation of the number of years in which tectonic motion of different magnitudes would become significant for typical point positioning applications in different tectonic scenarios. Shaded areas highlight periods of ten years or less for static datums. Ten years is an arbitrary period based upon the life expectancy of a typical geodetic datum.

	Tectonic deformation rate in ppm per year				
Relative positioning tolerances	**0.5**	**1**	**2**	**5**	**10**
Equivalent deformation (mm) in 1 year at a range of 10km	*5*	*10*	*20*	*50*	*100*
1 ppm Local geodynamic monitoring	2	1	0.5	0.2	0.1
2 ppm Deformation surveys	**4**	**2**	**1**	**0.4**	**0.2**
5 ppm High precision Engineering surveys	**10**	**5**	**2.5**	**1**	**0.5**
10 ppm Engineering Surveys	20	**10**	**5**	**2**	**1**
20 ppm Urban Cadastral Surveys	40	20	**10**	**4**	**2**
50 ppm Urban Cadastral Surveys (lower grade)	100	50	25	**10**	**5**
100 ppm DCDB Surveys	200	100	50	20	**10**
200 ppm Rural Cadastral Surveys	400	200	100	40	20
500 ppm GIS / Asset Mapping	1000	500	250	100	50

Table 2.5 A calculation of the number of years in which tectonic deformation of different magnitudes would become significant for typical relative positioning applications in different deformation scenarios. Deformation rates are assumed to be linear and do not account for episodic co-seismic displacements which may be of much larger magnitude.

2.6.1 The need for modelling of tectonic distortion

Internal distortion of the PNG94 network will increase in magnitude with time if coordinates are fixed at ITRF1992 epoch 1994.0. If surveyors do not connect independent PNG94 local networks, constrain their survey networks using coordinates of local PNG94 reference stations, and do not observe baselines across plate boundaries or in deforming zones, tectonic motion and deformation will be largely mitigated. However, in areas where the greatest deformation is evident (*i.e.* the greatest rate of baseline change) the discrepancy has already become observable and may exceed many positional tolerances, for example across active boundary zones such as the Ramu-Markham Fault. The distortion also impacts in the long term on engineering project datums and other local plane datums which span or include rapidly deforming zones.

A strategy is required in PNG and in active localised deforming zones to enable tectonic deformation to be modelled during geodetic computations and network adjustments to mitigate against distortion of the geodetic network and derived infrastructure. This is particularly important where the difference in time between the reference epoch and measurement epochs is large enough for the accumulated distortion to be significant to impact on the users of the datum. A convention is also required whereby coordinates are either regressed to a reference epoch in a quasi-dynamic sense using a deformation model, or presented as dynamic coordinates with time tagging of the data with the epoch of estimation.

Chapter 3

Geodesy in Papua New Guinea

3.1 The development of Geodetic Datums in PNG

Until the 1950s, geodetic surveys in Papua and New Guinea were largely unconnected and usually of limited extent. Due to the extremely rugged and hostile terrain and lack of infrastructure, local datum origins were usually determined by astronomical observations. The first large scale surveys in New Guinea were conducted between 1954 and 1957 using ship-to-shore triangulation by the US Corps of Engineers (Project Xylon in New Britain) and the Australian Survey Corps (Project Cutlass in New Ireland) (Done, 1984). In 1962 the first extensive land based geodetic survey in the territories was commenced by the PNG Department of Lands, National Mapping and the Australian Survey Corps. Land based sections of the network were measured with newly available tellurometers deployed by helicopter, and coastal sections were observed in conjunction with the United States Air Force HIRAN trilateration survey which connected the Marshall Islands with Cape York in Australia (USAF, 1959). HIRAN, an electromagnetic ranging system, had been developed during the Second World War to position combat aircraft. The PNG HIRAN net was computed on the Mercury 165 Ellipsoid and subsequently adjusted to AGD66 (Done, 1984). The extension of geodetic control across PNG was a considerable technical and logistic accomplishment for the time.

The weaker AGD66 HIRAN connection between PNG and Australia has resulted in a variation of up to 10 metres between PNG AGD66 and Australian continental AGD66. The PNG origin of AGD66 was gazetted as Bevan Rapids and AGD66 coordinates in PNG are generally internally consistent at the 4 m level (Allman, 1996).

Between 1974 and 1979, the Royal Australian Survey Corps (RASvy) established a widespread network of stations using the TRANSIT Doppler satellite positioning system to provide control for the "Skai-Piksa" aerial photography

and 1:100,000 series topographic mapping program. The analysis of these observations was computed in a geocentric datum based upon the Naval Weapons Laboratory Spheroid (NWL-9D or NSWC-9Z-2). Coordinates were then transformed to World Geodetic System 1972 (WGS-72) Datum and spheroid (Done, 1984).

Transformation parameters for PNG between WGS-72 and AGD66 were derived from stations observed common to the two datums. The transformation did not result in an adjustment of the AGD66 network in PNG. Offshore islands, not connected to AGD66, retained WGS-72 coordinates (Done, 1984; Allman, 1996).

3.2 GNSS and the Realisation of PNG94

GNSS positioning techniques, such as the GPS, are particularly suited for control surveying and geodynamic monitoring in PNG, due to the inaccessibility and lack of intervisibility of much of the terrain, factors which preclude the use of terrestrial surveying techniques. Satellite positioning methods require only a clear view of the sky. A wide-spread network of airstrips and helipads provide ideal station locations for GNSS observations due to their ease of access, ground stability, drainage and good satellite visibility.

The increasing use of satellite positioning techniques required development of compatible geocentric datums to alleviate the difficulty of transforming positions to other non-geocentric datums. Furthermore, the heterogeneous nature of local datums in PNG would make application of this new technology impractical unless transformation parameters from WGS to the local datum were computed. The development of geocentric datums in Australia and New Zealand during the 1990s provided an opportunity for regional ties to be made between the two datums and, between 1992 and 1994, a number of stations in PNG were observed concurrently with fiducial sites in Australia (Figure 3.1). These observations formed the basis for the realisation of a geocentric datum in PNG, PNG94. The realisation of the PNG94 primary network was undertaken in conjunction with that of the Australian Fiducial Network (Morgan *et al.*, 1996).

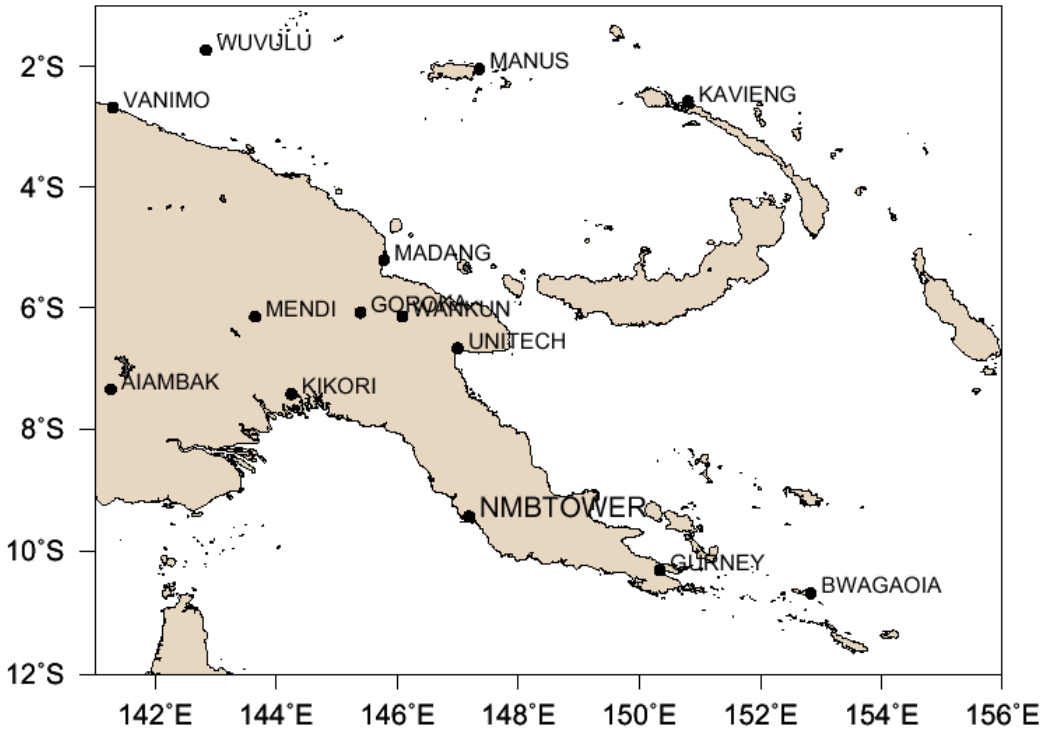

Figure 3. 1 PNG94 geodetic datum stations (Allman, 1996)

3.3 Geodetic monitoring of crustal deformation in PNG

PNG has been the subject of a number of crustal deformation surveys. In the 1970s, two trilateration networks were established by the Australian National Mapping Division (Sloane and Steed; 1976a, 1976b) to measure tectonic movement in two areas in PNG suspected to be undergoing rapid deformation. The first network was established across the Markham Valley near Kaiapit, west of Lae and the second across the St. Georges Channel between the Gazelle Peninsula and southern New Ireland. The results from these initial surveys were inconclusive, due largely to the short observation span of the surveys.

In 1981, a network of stations around PNG was surveyed using the Transit Doppler satellite navigation system (Morgan, 1981; Angus Leppan *et al*., 1983). Data from the 1981 survey were reprocessed to achieve a relative accuracy of *c.* 0.3m in the monitoring network (McClusky *et al.,* 1994). This network was resurveyed in 1990 by a team from the University of New South Wales (UNSW) funded in part by the Research School of Earth Sciences at the Australian National University (RSES, ANU) using GPS. There were difficulties re-

processing the earlier Doppler data in order to achieve the desired accuracy in order to determine baseline changes at a significant level, however, the first geodetic measurements of the rapid convergence across the New Britain Trench were made with this study (McClusky *et al.,* 1994). The network was extended and resurveyed in 1991 and 1992 by UNSW and RSES (McClusky *et al.,* 1994; Mobbs, 1997).

From 1993 onwards, research groups from the University of California, Santa Cruz (UCSC) (Stevens *et al.*, 1998; Wallace, 2002) and the Research School of Earth Sciences, Australian National University have undertaken extensive GPS monitoring campaigns in PNG in collaboration with local institutions. These surveys were designed to observe and densify the geodetic monitoring network, in order to define the large-scale tectonic framework and to investigate deformation in plate boundary zones in PNG. Local institutions involved in these campaigns have included the PNG National Mapping Bureau (NMB), Department of Surveying and Land Studies, Papua New Guinea University of Technology (Unitech) and RVO.

Since 1996, eight permanent geodetic tracking stations have been established by different geodetic agencies in PNG (Table 3.1). The four GPS stations in the Rabaul Network provide real time monitoring of the main active caldera. The Manus SPSLCMP site was installed by the National Mapping Division of Geoscience Australia in 2002 to monitor vertical motion of the NTF SEAFRAME tide gauge site on Manus. The SPSLCMP is an AusAID project.

A substantial archive has been formed of GPS dual-frequency observations since 1990 from an extensive network of sites around PNG (Figure 3.2). This archive is ideal for the geodetic estimation of the PNG velocity field and the computation of a new geodetic datum. The data quality and quantity vary significantly but approximately 110 sites in PNG have sufficient quality data to define their ITRF position with an accuracy of < 20mm.

SITE	Network	Method	Installed	Location	Responsible Agencies
LAE1	IGS	GPS	1996	Sandover Building, Papua New Guinea University of Technology, Lae	RSES, ANU UNITECH, PNG
MORE	WING Western Pacific Integrated Network	GPS	1993	NMB Tower at Waigani, Port Moresby	ERI (Earthquake Research Institute), University of Tokyo NMB
MORB	DORIS	DORIS	2002	NMB, Waigani, Port Moresby	Institut Geographique National, France NMB
RVO_	Rabaul Caldera Network	GPS	1998	Rabaul Volcanological Observatory	PNG Department of Minerals & Energy
SPT_	Rabaul Caldera Network	GPS	1998	Sulphur Point, Rabaul	PNG Department of Minerals & Energy
SDA_	Rabaul Caldera Network	GPS	1998	Matupit SDA Church, Rabaul	PNG Department of Minerals & Energy
VIS_	Rabaul Caldera Network	GPS	1998	Vulcan Island, Rabaul	PNG Department of Minerals & Energy
PNGM	SPSLCMP South Pacific Sea Level and Climate Monitoring Project	GPS	2002	Lombrum Naval Base, Manus	AusAID NMD, GA

Table 3.1 Continuous GPS/DORIS sites in PNG in 2003

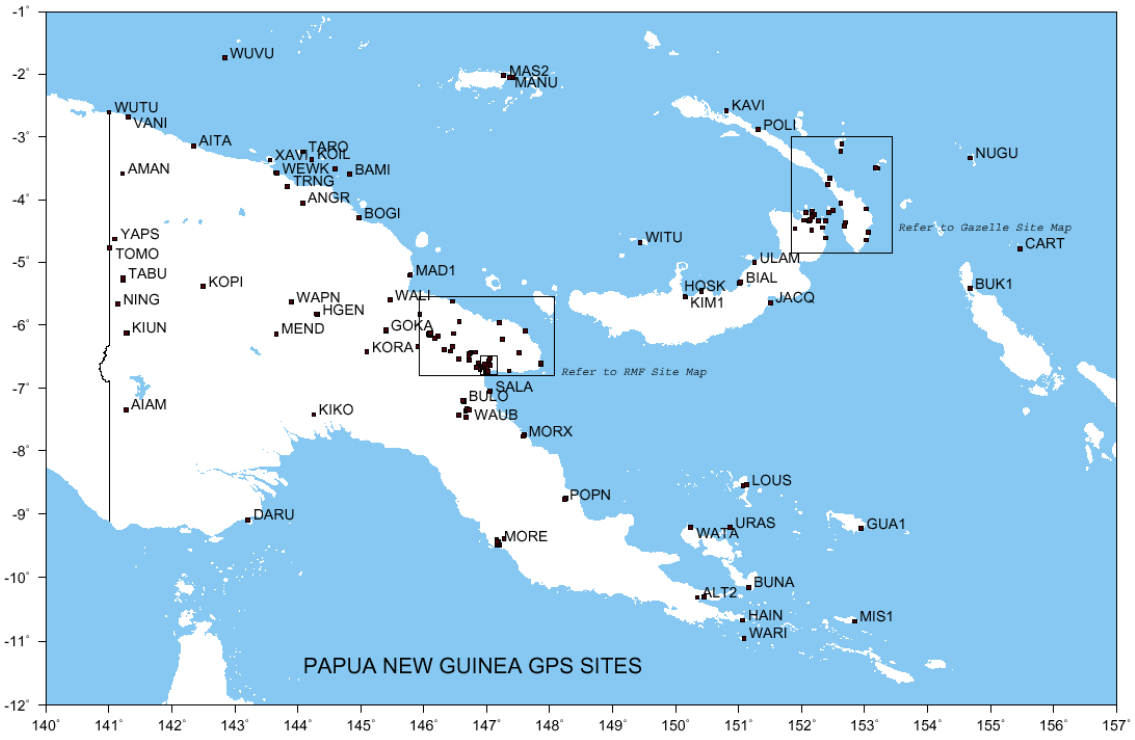

a) GPS Site locations in Papua New Guinea

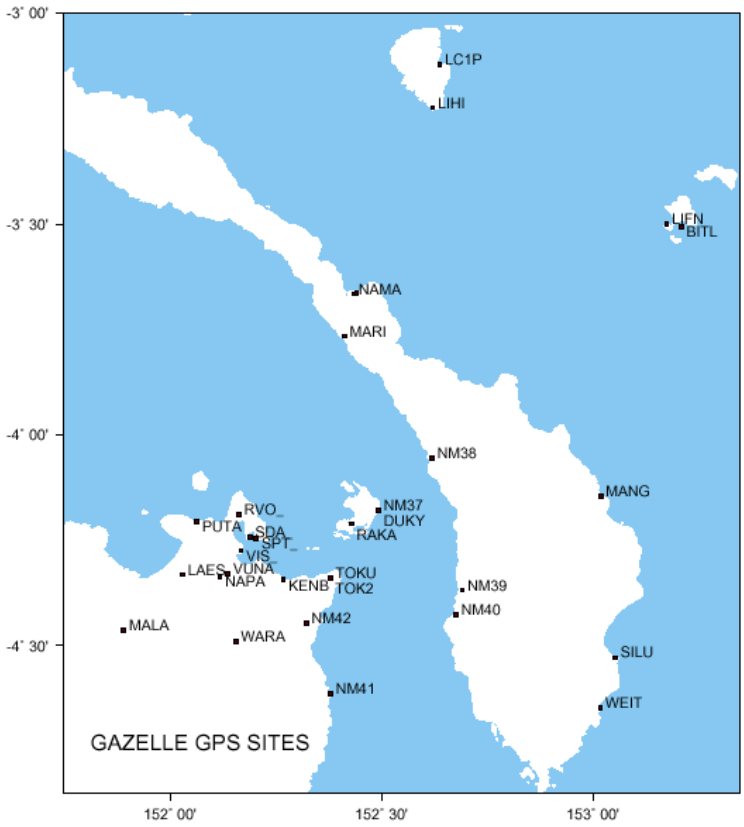

b) GPS Site locations on the Gazelle Peninsula, East New Britain & Southern New Ireland

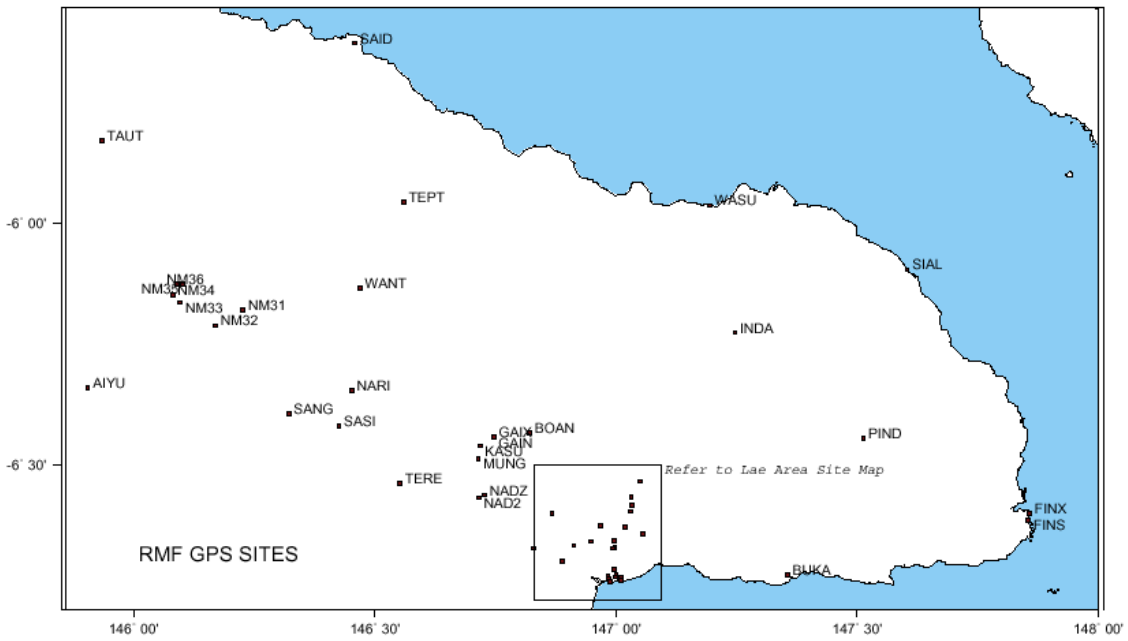

c) GPS Sites along the Ramu-Markham Fault and the Huon Peninsula

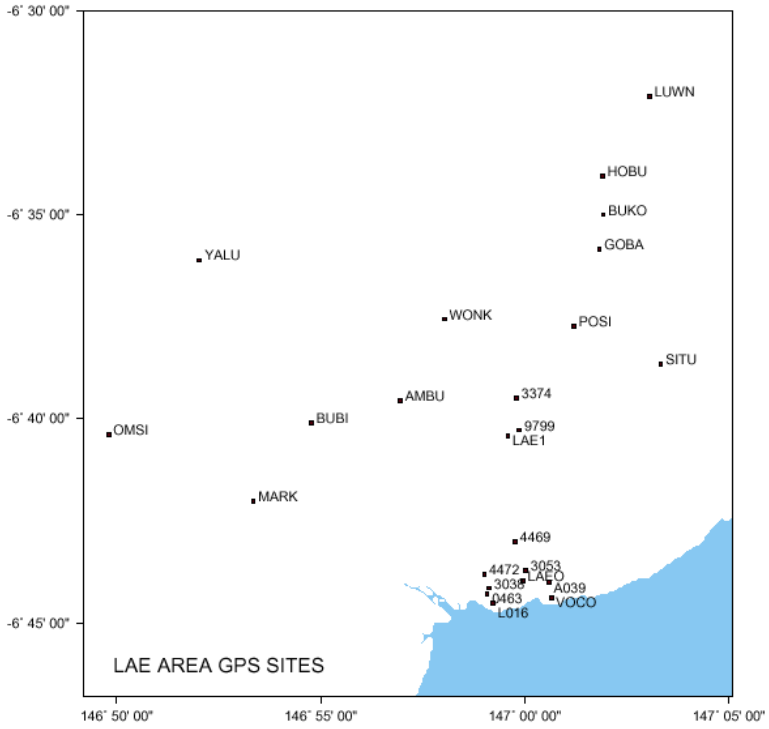

d) GPS Sites in the Lae Urban area

Figure 3.2 Locations of GPS stations in Papua New Guinea

GPS has been used extensively in PNG for geodynamics studies and regional geodetic datum development. The aim of the earlier GPS campaigns was to obtain the first geodetic measurements across the larger plate boundaries in PNG, between the South Bismarck, Woodlark, Pacific and Australian Plates and also to realise the PNG94 Datum. Subsequent campaigns have increasingly focused on identifying smaller microplates, rigid blocks and measuring strain rates in deforming zones near plate boundaries. The campaigns have necessarily been collaborative in nature, due to the logistical difficulties operating in PNG and the mutual interests of many of the participating institutions. Many of the GPS data collected by campaigns conducted by NMB for mapping and land development purposes have also been useful for geodynamics studies.

The following is a summary of major GPS campaigns completed to date in PNG;

- **PNG National Mapping Bureau**
  1992 (ARN92), 1993 (PNG93), 1994 (AUS94), 1994 and 1995 (Gazelle crustal deformation), 1996-2002 (DCDB, mapping and Gazelle Restoration surveys), 1997-1998 (DCA Aerodrome Survey), APRGP; campaigns 1997, 1998, 2000

- **University of New South Wales (funded by RSES)**
  1990, 1991 and 1992 crustal motion surveys in Eastern PNG

- **Research School of Earth Sciences, Australian National University**
  1991, 1992 (with UNSW), 1996, 1997 (with UCSC), 1998 and 2000 campaigns, 2002 Lae area survey

- **University of California, Santa Cruz**
  Ramu Markham Fault (RMF) and Huon Peninsula crustal motion surveys 1993, 1994, 1997 (with RSES), 1998, 1999, 2000, 2001 and 2002 (2002 fieldwork conducted by RSES).

- **PNG University of Technology**
  1997-2002 student projects in the Lae area,

- **PNG University of Technology (funded by RSES)**
  1999 North Bismarck Plate survey, Weitin fault survey, 2000-2001 Weitin Fault post earthquake monitoring, 2002 Wewak post-earthquake survey

- **Rabaul Volcanological Observatory**
  1998-2003 Rabaul Caldera monitoring, 2000-2003 Gazelle network monitoring (funded by ANU)

In addition to these major survey campaigns a significant amount of GPS data have also been obtained from private survey firms, exploration and mining companies operating in PNG.

These studies, together with other seismological and geological studies, have collectively formed the basis for the current understanding of plate kinematics and crustal deformation in PNG (Tregoning *et al*., 1998; Wallace, 2002). Continued re-observation and densification of the monitoring network is underway to improve the resolution of the velocity field and strain estimates.

3.4 Drivers for future datum development in PNG

The main driver for further development of the geodetic datum in PNG is whether the country will benefit from it, or, if maintaining the existing static geodetic datum is considered to pose a risk to population, infrastructure and economy.

3.4.1 A risk assessment of maintaining a static PNG94

In PNG, volcanic and earthquake hazards pose significant risk to the population and the economic infrastructure of the country. Presently, monitoring of these hazards is carried out within localised networks, or spasmodically in ITRF by research organisations. The PNG94 datum as it stands is not an integral part of any geophysical hazard monitoring in PNG. PNG94 as a static geodetic datum is not suitable for hazard monitoring, nor does it currently benefit from repeated

high precision geodetic measurements which are made for this purpose. Furthermore, there is no proposal in place to integrate the datum with the monitoring network as has been successfully developed in Japan and New Zealand with their GeoNet and PositionNZ networks (http://mekira.gsi.go.jp/ENGLISH/index.html; http://www.geonet.org.nz). In these cases, the same network that provides Multiple Reference stations for positioning requirements, also monitors geological hazards. Implementation of a dynamic datum in PNG would enable localised geodetic surveys and monitoring networks to be connected to ITRF with centimetre level absolute accuracy via such a datum, thus removing some of the defects of a localised reference system caused by regional deformation.

Risk to human life and safety is also particularly borne out in PNG by the extensive use of air transport in difficult flying conditions due to prevalent cloud and rugged topography. Aircraft navigation equipment is required to be in sympathy with ground based guidance and landing systems and aeronautical charts to ensure safe navigation. Although the prime consideration here is the large offset between earlier datums such as AGD66 and WGS-84, navigation at the sub 10 metre level requires a high level of absolute precision or active use of a Local Area Augmentation GPS System (LAAS). Accurate navigation of sea-going vessels through reefs and shoals similarly requires a high degree of absolute accuracy. Positioning errors during the construction of major engineering projects, such as earthworks and dams, can result in the loss of structural integrity leading to potentially catastrophic failure resulting in environmental and property damage, as well as risk to human safety. Positioning tolerances are shown in Table 2.5.

The cadastral system forms the basis for any economic development in PNG dependent upon land use. PNG has inherited a cadastral survey system from the colonial era which is perhaps not best suited to PNG's long term development when considering the importance of customary land tenure in Melanesian society. Survey specifications do not make any allowance for creep of boundary monuments resulting from tectonic motion or co-seismic displacement. The attrition rate of survey monumentation is extraordinarily high in PNG due to the high rainfall, rapid vegetation regrowth rate, land instability and frequent anthropogenic disturbances, often deliberate. Boundary marks reinstated from a

locally deforming network assumed to be static will not be placed in the same location as the original mark. This will increasingly become the source of disputes and doubts about the integrity of the survey system as positioning technology becomes more accessible and accurate.

Chapter Two discussed the principle of cadastral positioning where boundary monuments have precedence over measurements as a legal definition of land boundary definition. The purpose of cadastral surveys has been to measure the relative positions of boundary monuments, mark boundaries and place recovery (or reference) marks relative to the boundary to enable later reinstatement should ever boundary monuments or marks be destroyed or disturbed. The physical realisation of localised cadastral reference systems, such as plane grids, is independent of any overlying geodetic datum and coordinate system.

The recent trend towards a coordinated cadastral system in many countries has been driven by the need to integrate the cadastre with other geographical information in a homogeneous spatial database to support cadastral and mapping automation. The strength of a coordinated cadastre lies in the integrity and spatial stability of its defining reference frame. Legal validity of cadastral coordinates could be flawed if the coordinates of the defining reference frame are changing as a result of tectonic motion, or if the site is moving relative to the frame, unless some time dependent parameter such an epoch, or velocity is also applied to the coordinate data.

Misalignment of spatial data layers in a GIS resulting from offsets in the source datum presents serious difficulties for managers of spatial data. Planning, construction and maintenance of engineering works is hampered if there is uncertainty as to the relative accuracy of survey information derived from a heterogeneous spatial database. Valuable assets may be incorrectly assigned to the wrong landholder resulting in legal complications and compensation payments.

3.5 Requirements of a new datum in PNG

PNG94 as it stands is only suitable for small scale mapping applications, and as an origin for local control. Should PNG decide to update PNG94 in the future, the question arises as to what type of datum should be implemented and how any subsequent updates will be accommodated and maintained. Should the datum remain static, fully dynamic like the ITRF, or be a practical compromise between the two? New Zealand has recently implemented a semi-dynamic datum, New Zealand Geodetic Datum 2000 (NZGD2000) to supersede the static NZGD49 datum (Pearse, 2000) to model the distortion of the New Zealand datum resulting from the convergence of the Pacific and Australian plates. The New Zealand model of implementation could be applied to PNG with some modification.

3.5.1 Requirements and benefits of datum development

Various discussion papers on datum development in the Australasian region region (e.g. ICSM, 2000) highlight the need for a rigorous, accurate and accessible datum to support the needs of the providers, managers and users of spatial data into the future. The UN sponsored Permanent Committee on GIS Infrastructure for Asia and the Pacific (PCGIAP) has proposed the idea of adopting a realisation of ITRF to support GIS. Several geodetic campaigns have been completed as part of the Asia and Pacific Regional Geodetic Project (APRGP) in order to densify the geodetic network in the Asia-Pacific region and develop a higher resolution velocity field. Only four stations in PNG have been observed in the APRGP campaign. Because of the extremely complex tectonic setting in PNG, the APRGP would benefit greatly from integration of the existing crustal motion survey dataset and analysis. The spatial resolution of the existing PNG APRGP sites is insufficient to define a PNG velocity field to support geodetic datum development in its own right.

Any new datum for PNG should be tied to the ITRF at some nominated epoch of realisation. This ensures compatibility with other regional datums and satellite positioning technology. The GRS80 ellipsoid should be retained as this already forms the reference ellipsoid for ITRF and PNG94 in accordance with the

guidelines of IAG resolutions. A new datum in PNG should include a velocity or deformation model, similar to what has been established in New Zealand (Blick *et al*., 2003), to enable tectonic deformation and other offsets to be accommodated in network adjustments and geographical information.

3.6 Issues with vertical datums in PNG

This study focusses upon the effects of the horizontal component of tectonic deformation on the PNG geodetic datum. The datum definitions in Appendix A are intrinsically 3D due to their derivation from space geodetic techniques. Vertical (UP) deformation rates, however, have not been tabulated. In most instances vertical deformation rates are too small to be significant, or have too greater uncertainties assigned to them, unless co-seismic displacement has occurred. Volcano and tide-gauge monitoring require high precision measurement of vertical deformation as an important exception. The application of the existing geoid model (Kearsley and Ahmad, 1996) to estimate the geoid-ellipsoid separation 'N' value should be sufficient for most heighting purposes (e.g., mapping and GIS), though relative geoidal profiling is important in areas where there is significant geoidal undulation and heighting tolerances are tight. In many parts of PNG, especially in Highland areas, the origin of the local realisation of the height datum may be up to several metres different from the orthometric height derived from the geoid model. The main consideration is consistency, and in the short term it makes sense to apply a local offset to the 'N' value derived from the geoid model in order to maintain sympathy with existing local height datums.

Chapter 4

The tectonic setting in Papua New Guinea

PNG is located in a very complex tectonic region, where the Pacific and Australian plates collide obliquely. The mainland of New Guinea forms the northern margin of the Australian continental plate. Several smaller microplates are also involved in this collision process (Figure 4.1). A detailed understanding of the tectonic setting is required for the development of a geodetic velocity model, particularly in locating rigid blocks and deforming zones. Densification of monitoring sites is required in the boundary zones in order to obtain more geodetic data to better model the deformation and strain field and to enable dynamic geodetic coordinates of other sites to be inferred using velocity and strain models for any given epoch. The magnitude and complexity of the tectonic deformation in PNG has a dramatic effect on the geodetic datum.

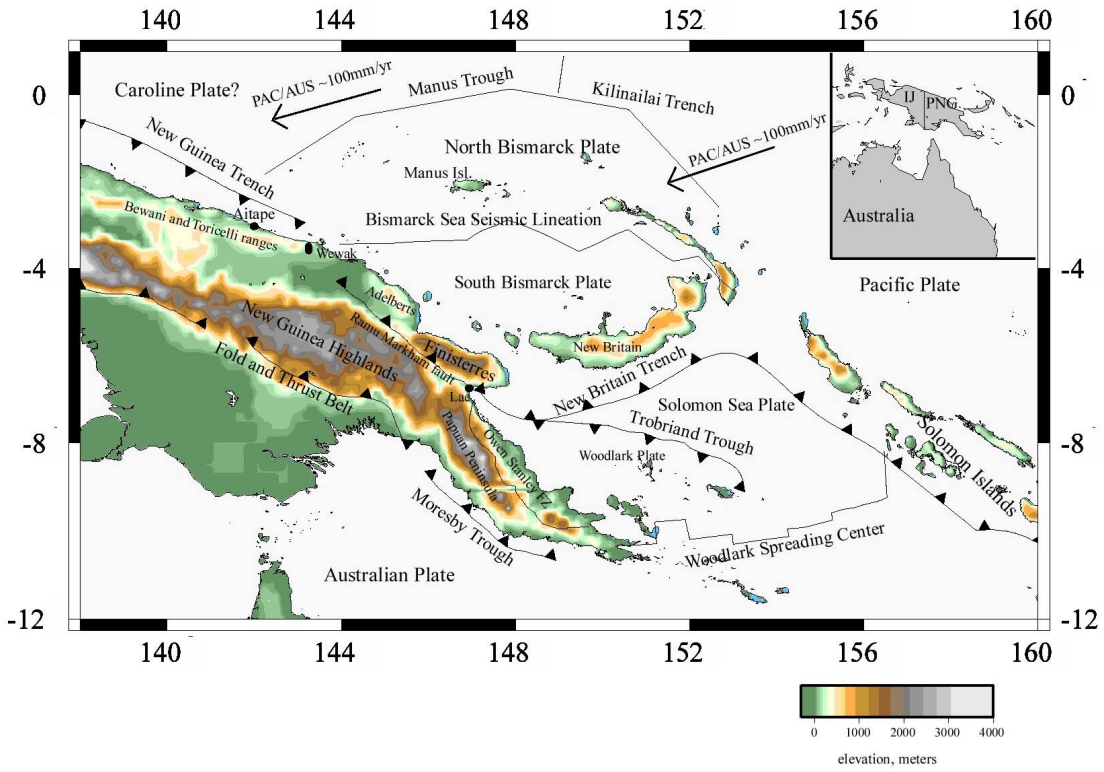

Figure 4.1 Present day tectonic setting of PNG (from Wallace, 2002).

4.1 Tectonic history of Papua New Guinea

A brief tectonic history of PNG is presented to provide a framework for understanding the contemporary tectonic setting of the country. Many ancient tectonic processes still influence present day geodetic interpretation and kinematic models. The geological time scale used in this discussion is from Young and Laurie, 1996.

4.1.1 Late Cretaceous (98-65 Ma)

The Australian continent began to slowly rift north from Antarctica *c.* 95 Ma as part of the break up of Gondwana (Williamson *et al.* 1990). Rifting of the NE margin of the Australian plate ensued at *c.* 80 Ma as a prelude the formation of the Coral Sea basin and another basin, now closed, further to the north (Davies *et al.*, 1984). Outboard of the NE margin lay previously rifted continental fragments (Pigram and Panggabean, 1984) and ocean plateaux which were later to amalgamate to form the Sepik Terrane and East Papuan Composite Terrane (EPCT) (Pigram and Davies, 1987).

4.1.2 Paleocene (65-55 Ma)

Extension of the Australian northeastern margin continued during the Paleocene with the Coral Sea basin and other marginal basins to the north opening between 62 and *c.* 52 Ma (Weissel and Watts, 1979; Pigram and Davies, 1987). Salients of the rifted Australian continental northeastern margin, the Eastern, Papuan and Louisaide oceanic plateaux, separated the Coral Sea basin from seas to the north. During this time, oceanic lithosphere was emplaced over one of these salients (forming the Owen Stanley metamorphics) to constitute the Papuan Ultramafic Belt ophiolite (Lus *et al.*, 1998).

4.1.3 Early Eocene (55-48 Ma)

Spreading of the Coral Sea basin ceased *c.* 52 Ma as a consequence of a newly initiated oblique convergence of Pacific and Australian plates. Müller *et al.* (2000) attribute this change to the collision of the Indian and Eurasian plates.

4.1.4 Middle and Late Eocene (48-34 Ma)

Subduction related volcanism north of the Australian margin formed the basement rocks of the Outer Melanesian island arcs comprising the Toricelli, Adelbert, Finisterre, New Britain, New Ireland and Solomon island arcs (Crowhurst *et al.* 1996). Volcanism was active in these arcs between 30 – 20 Ma (Jaques and Robinson, 1977).

Northward motion of the Australian plate increased rapidly from 8 mm/yr at 44 Ma to 30 mm/yr by 40 Ma.(Veevers, 2000). This was coincident with a major change in the Pacific plate rotation, and fusion of the Indian and Australian plates as a result of the collision of the Indian craton with Eurasia (Veevers, 2000). This period was also associated with opening of the Solomon Sea basin (39-28 Ma) (Honza *et al.*, 1987) and counter clockwise rotation of New Britain (Davies *et al.*, 1984).

4.1.5 Early Oligocene (34-29 Ma)

Between 30 and 25 Ma, the Australian craton collided obliquely with the Sepik terrane, a mixture of volcanic arc and Gondwanan continental fragments (Pigram and Davies, 1987). Uplift, resulting from the collision, formed what are now the Central, Hunstein and Burger Ranges between the Highlands and Sepik River. These terranes are referred to collectively as the New Guinea Mobile Belt.

4.1.6 Late Oligocene (29-24 Ma)

By *c.* 27 Ma the Menyamya, Kutu and Port Moresby terranes, remnants of the former marginal Australian ocean basin, accreted onto the EPCT (Pigram and Davies, 1987). This agglomeration now forms the coastal ranges along the southern side of the Owen Stanley Ranges.

Northward subduction of the westernmost Solomon Sea plate ceased abruptly at 25 Ma following the collision of the Australian continent with the Sepik terrane (Pigram and Davies, 1987).

4.1.7 Early Miocene (24-17 Ma)

Approximately 22 Ma, the Ontong Java Plateau (OJP), an extensive oceanic flood basalt on the Pacific Plate, entered the North Solomons Trench. This reactivated southwesterly subduction of the Solomon Sea plate along the New Guinea trench and Trobriand troughs and resulted in the formation of the Maramuni and Trobriand volcanic arcs along the northern New Guinea margin. This southwesterly subduction also hastened the migration of the Outer Melanesian island arcs towards the New Guinea margin. Refer to Figure 4.2 (Hill and Raza, 1999)

4.1.8 Mid Miocene (17-11 Ma)

The westward motion of the Pacific Plate initiated left-lateral shearing of the northern Australian margin by 18 Ma (Hill and Raza, 1999). The Jimi and Bena Bena terranes were displaced up to 300km west along the Bismarck fault zone between *c.* 14-12 Ma (Pigram and Davies, 1987).

Between 14 Ma and 11 Ma the EPCT docked with the Australian Craton. This collison propagated from the northwest to the southeast and formed the Ekuti and Owen Stanley Ranges and uplift of the Papuan Ultramafic belt (Pigram and Davies, 1987).

From 12 Ma, the Western Outer Melanesian island arcs started to collide obliquely with the northern margin of the Australian plate. Consequently, southward subduction of the Solomon Sea plate along the Trobriand trough began to wane and the trough began to close from the west. Subduction along the Solomon Arc reversed with northeasterly directed subduction of the Solomon Sea plate reactivating along the New Britain Trench.

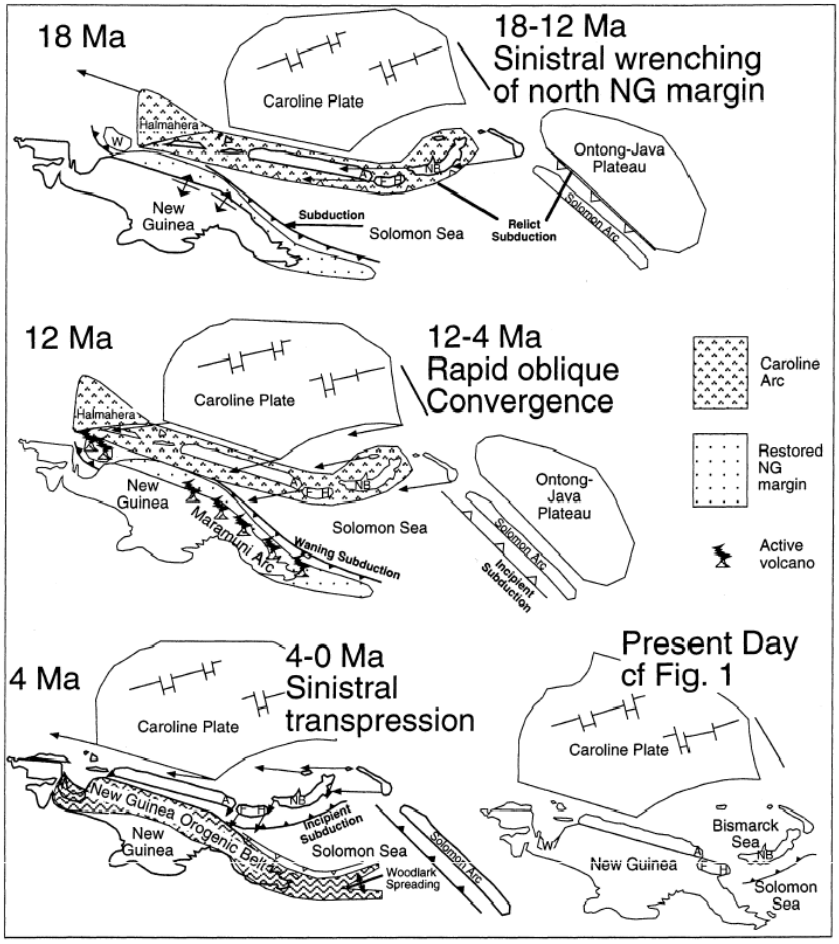

Figure 4.2 Tectonic reconstruction of New Guinea 18 Ma – present day (from Hill and Raza, 1999)
A – Adelbert Range, F – Finisterre Range, H – Huon Peninsula, NB – New Britain

4.1.9 Late Miocene (11-5 Ma)

By 10 Ma, the western Outer Melanesian arc terranes had docked with the Australian margin to form the Bewani, Torricelli and Prince Alexander Ranges in the Sandaun and East Sepik provinces. The Jimi, Bena Bena and Schrader terranes had assumed their present location with respect to the Australian craton

by this time forming the present day Bismarck and Kratke Ranges in the Eastern Highlands. The east trending docking of these island arc terranes with northern New Guinea eventually closed the Trobriand trough west of the existing Ramu and Markham valleys. By *c.* 7 Ma, the Adelbert terrane had also docked (Cooper and Taylor, 1987)

Between 8–5 Ma continued convergence caused the development of the New Guinea fold and thrust in the Southern Highlands region (Hill and Raza, 1999).

The OJP finally jammed the North Solomons Trench 6 Ma with the collision intensifying between 4-2 Ma (Wessel and Kroenke, 2000; Coleman, 1997). This resulted in subduction of the Solomon Sea Plate along the New Britain Trench (Kroenke, 1984), which in turn initiated northwesterly spreading of the Woodlark Basin Spreading Centre (WBSC) (Milsom, 1970; Taylor *et al.* 1995). The Plio-Quaternary volcanoes of Bougainville developed due to northeasterly subduction of the Solomon Sea Plate (SSP) (Johnson, 1979; Davies *et al.* 1984).

4.1.10 Pliocene (5-1.8 Ma)

Exhumation of the Highlands fold and thrust belt was accelerated between 5 Ma and 3 Ma with 50-90 km of shortening occurring across the belt during this time (Jenkins, 1974; Abers and McCaffrey, 1988). Frontal thrust sheets were uplifted to elevations in excess of 4000 m. By 3.7 Ma the Finisterre terrane collision had commenced (Abbott *et al.*, 1994), coincident with opening of the Manus Basin, incipient clockwise rotation of the New Britain arc and subduction of the Solomon Sea plate along the New Britain Trench (Jaques and Robertson, 1977; Davies *et al.* 1984). The rotational convergence of the collision of the Finisterre terrane resulted in rapid uplift of the terrane (Veeh and Chappell, 1970). Volcanism was active in the Highlands as a relic of southward subduction of the Solomon Sea along the now closed Trobriand trough (Johnson, 1979).

4.2 The present day (Holocene) tectonic setting in PNG.

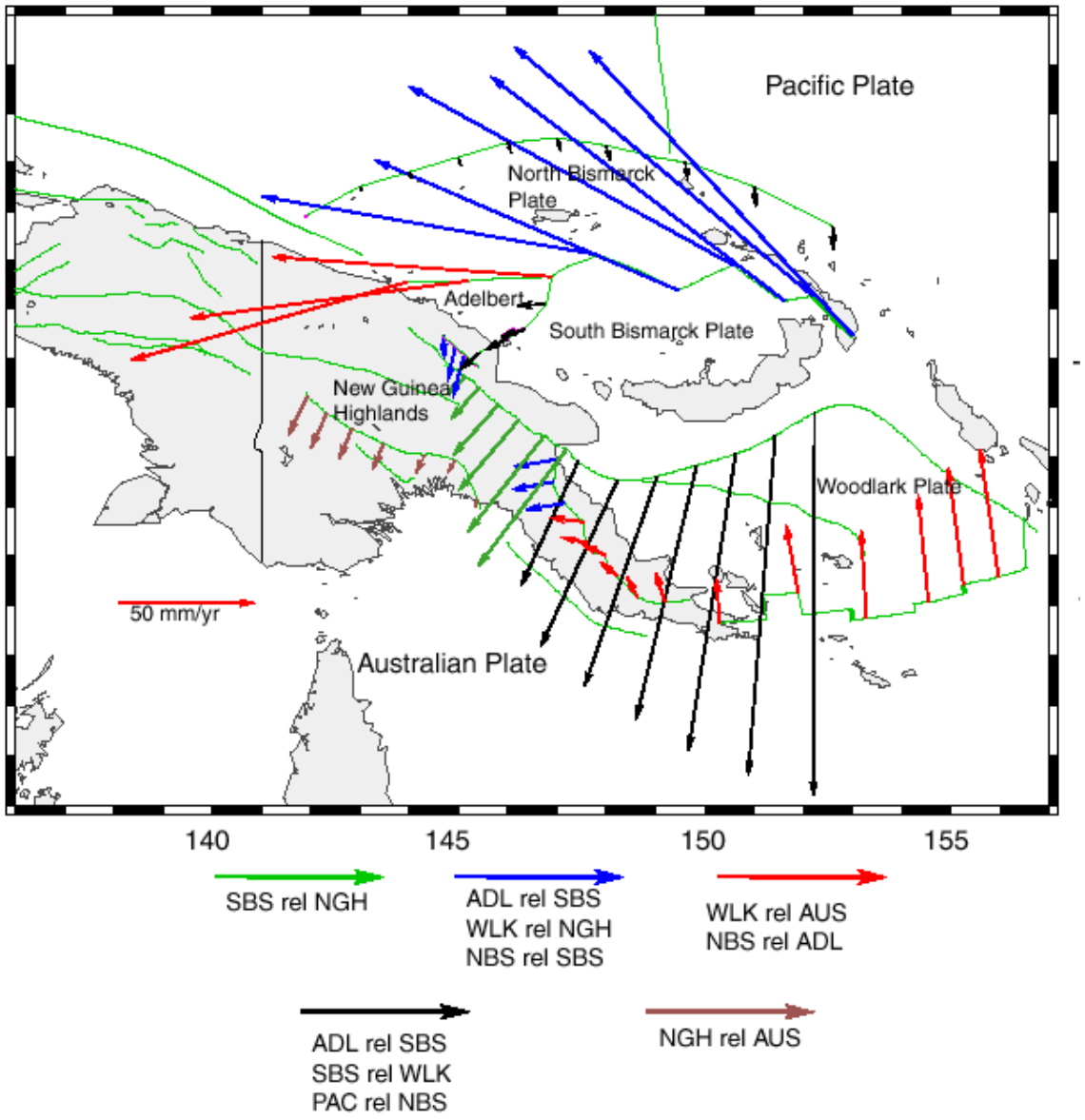

Figure 4.3 First-order tectonic model of Papua New Guinea (from Wallace *et al.*, 2004). **WLK**: Woodlark Plate; **SBS**: South Bismarck Plate; **NGH**: New Guinea Highlands; **NBS** North Bismarck Plate; **ADL**: Adelbert Block. Vectors show relative predicted motions across plate boundaries located within PNG.

Integration of recent geodetic, geological, geomorphological and seismological analyses has provided an increasingly detailed neotectonic picture of the current kinematic regime (Figure 4.3) in PNG (Tregoning *et al.*, 1998; Stevens *et al.*, 1998; Wallace, 2002). Major improvements in positioning technology, space imagery

and the definition of the ITRF have enabled geodetic measurements to validate tectonic models derived by other methods. Before sufficiently accurate regional geodetic measurements were possible, a number of models of the present day tectonic regime in PNG were developed from geological and geophysical observations (Johnson and Molnar, 1972; Curtis, 1973; Taylor, 1979; Johnson, 1979; Hamilton, 1979; Davies *et al.*, 1984).

4.2.1 The Tectonic Framework in PNG

The following summary of the tectonic setting in PNG is sourced from a large number of references; (Johnson and Molnar, 1972; Curtis, 1973; Taylor, 1979; Johnson, 1979; Hamilton, 1979; Davies *et al.*, 1984; Tregoning et al., 1998; Wallace, 2002).

The Australian plate is moving in a north-northeasterly direction, colliding with the New Guinea Highlands (NGH) along the Highlands Fold and Thrust Belt. Here, the NGH are actively overthrusting the Australian plate. The North Bismarck Plate, whose motion is similar to the Pacific Plate, is being subducted obliquely beneath the NGH along the New Guinea Trench. Further to the east, the NGH is colliding with the Adelbert block and South Bismarck Plate along the Ramu-Markham Fault Zone (RMFZ). Here, the western part of the South Bismarck Plate (SBIS) is currently overthrusting the NGH. The collision is propagating towards the east-southeast along the RMFZ as the SBIS rotates clockwise, opening up the Manus Basin with spreading and strike-slip along the Bismarck Sea Sesimic Lineation (BSSL) to the north, and northwesterly subduction of the Solomon Sea Plate along the New Britain Trench (NBT) to the south. Southward subduction of the Solomon Sea Plate beneath the Woodlark Plate along the Trobriand trough is believed to be inactive, or very slow, and the two plates can be considered to be a single entity. The Woodlark Plate is rifting anti-clockwise away from the Australian Plate along the WBSC with continental rifting occurring at the eastern end of the Papuan Peninsula. To the northeast, the Woodlark Plate is subducting northeasterly beneath the Pacific plate along the NBT and San Cristobal Trench south of the Solomon Island arc. To the west, the Woodlark Plate is moving northwest relative to the Australian Plate through strike-slip along the Owen Stanley Fault Zone (OFSZ), becoming transpressional

closer to the RMFZ. The Pacific Plate is moving west-northwestwards across the northern margin of PNG, with a major left-lateral strike slip boundary with the SBIS along the Weitin Fault, and slow oblique subduction beneath the North Bismarck Plate along the Kilinailau and Manus Trenches.

All types of plate boundary are represented in PNG, with relative motions between distinct microplates some of the most rapid anywhere on the Earth. Each of these boundary zones is described in detail below.

4.2.2 The Highlands Fold and Thrust Belt (HFTB)

The HFTB in PNG extends from the Star Mountains in the west passing through the Southern Highlands by Lake Kutubu, before trending southward to the east of Kerema. New Guinea, south of the central cordillera, forms the northern margin of the advancing Australian Plate. It is thought that the forearc HFTB is migrating southwards across the Papuan foreland and probably accommodates much of the convergence between the northeasterly directed motion of the Australian plate and other plates to the northeast (Abers and McCaffrey, 1988; Hill and Raza, 1999). Shortening across the HFTB is estimated to be 15 mm/yr east of 142°E decreasing to 6 mm/yr at 145°E (Wallace, 2002), although no direct geodetic measurements of shortening across the HFTB have been made to date. It is assumed that sites south of the HFTB have velocities close to that predicted for the rigid Australian Plate, although there are no geodetic measurements to verify this. The HFTB is seismically active with recently active faulting (Abers and McCaffrey, 1988; Ripper and McCue, 1983) and is clearly visible on topographic maps and space imagery as a narrow band of rugged, linear, predominantly limestone karst topography.

Wallace (2002) suggests that the assemblage of accreted terranes and mobile belts north and east of the HFTB, comprising the bulk of the New Guinea Highlands, and possibly the Sepik Block, form a New Guinea Highlands Plate (NGH). The NGH could also be a region of diffuse and partitioned deformation between the Australian and North/South Bismarck Plates. Densification of the velocity field in the Highlands/Sepik region should provide a better understanding of the nature of the distribution of convergence between the Australian Plate and NBIS

and verify the existence of smaller microplates or rigid blocks. A small amount of convergence, manifest as diffuse deformation, is predicted along structures between Goroka, Mt. Hagen and the southern part of HFTB (Wallace, 2002).

The Moresby Trough may accommodate 2-3mm/yr convergence between the Australian Plate and the NGH (Wallace, 2002), though there is little seismic evidence to support this. The geodetic site at Port Moresby (MORE) indicates 4mm/yr relative motion north-northwest with respect to predicted Australian rigid plate velocity (Tregoning, 2003). However, as the MORE site is located on a steel frame tower situated on reclaimed swamp, this velocity should be verified by a geologically stable, local monitoring network in order to model any deformation arising from potential localised creep or instability before this assumption is made.

4.2.3 New Guinea Trench (NGT)

The North Bismarck Plate (NBIS) is subducting obliquely beneath the NGH along the New Guinea Trench. The NGT accommodates most of the convergence between the NBIS and Australian plates (Abers and McCaffrey, 1988). The convergent component normal to the trench is estimated to be *c.* 67 mm/yr and the left-lateral strike slip component, 78 mm/yr (Tregoning *et al.,* 2000). The exact location of the triple junction between the SBIS, NBIS and Australian Plate is still unclear, however the relative motion near Wewak is predicted to be *c.* 115mm/yr left-lateral and *c.* 50mm north/south convergent using the geodetic models of Tregoning *et al.* (1998) and Wallace *et al*. (2004). The BSSL continues through the Torricelli Ranges as a series of east/west anastomising faults (Cooper and Taylor, 1987).

4.2.4 Ramu-Markham Fault Zone (RMFZ)

The Finisterre arc terrane, which constitutes most of the Huon Peninsula, is currently being emplaced onto the New Guinea Highlands along the RMFZ, located along the Ramu and Markham Valleys in northern PNG (Jaques and Robinson, 1977; Abbott *et al*., 1997). The Ramu-Markham Fault (RMF) is a

shallow (15°) north-northeasterly dipping mid-crustal detachment ramp connecting to a steeply dipping ramp at *c.* 20km depth beneath the Markham River (Kulig *et al.*, 1993; Abbott *et al.*, 1994; Stevens *et al.*, 1998). Intermittent locking of the main RMF has resulted in uplift and some convergence being accommodated along "out-of-sequence" thrust faults (OOSTs) along the southern face of the Finisterre ranges to the north of the RMF (Abbott *et al.*, 1994). New Britain, the Finisterre Terrane and the Southern Bismarck sea constitute a stable tectonic microplate, the South Bismarck Plate (SBIS) (Tregoning *et al.*, 1998, 1999; Weiler and Coe, 2000). The northeast convergence of the SBIS with the NGH along the RMFZ results in a rotation of the SBIS by 8°/My, clockwise about an Euler pole near the western extremity of the Finisterre terrane on the RMFZ (Tregoning *et al.*, 1998). The collision appears to be driving the plate rotation due to the resistance of the buoyant continental lithosphere of the New Guinea Highlands to underthrusting (Wallace, 2002).

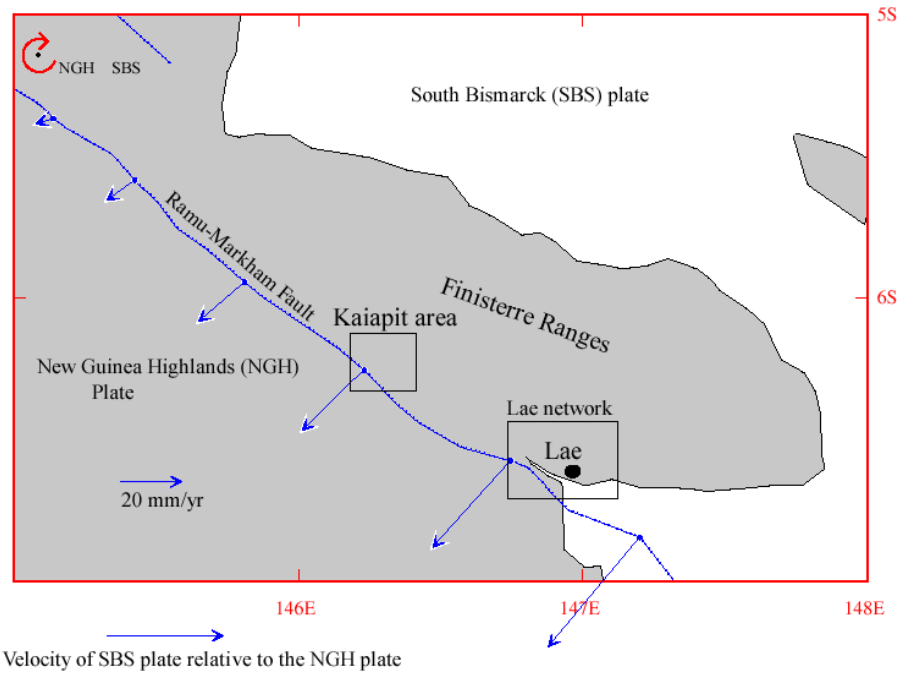

Figure 4.4 Predicted rigid plate motion between the South Bismarck Plate and the New Guinea Highlands along the Ramu-Markham Fault (from Wallace, 2002)

Over the last 4 My this rotational convergence has resulted in propagation of the SBIS/Australian Plate collision from the northwest to the southeast along the RMFZ (Cooper and Taylor, 1987; Silver *et al.*, 1991; Abers and McCaffrey, 1994; Weiler and Coe, 1999). Convergence rates vary from zero at the SBIS/NGH

relative Euler Pole at 144.75°E, *c.* 100km northwest of Usino in the Ramu Valley (Wallace, 2002), to *c.* 50 mm/yr in the Lae area, *c.* 80 mm/yr at the 149°E Embayment and up to *c.* 150mm/yr at 152.5°E (Figure 4.4). The collision has progressively uplifted the Finisterre terrane. Uplift rates are estimated to be 2 – 5 mm/yr along the northern coast, as indicated by raised coral terraces (Chappell *et al.*, 1996), 0.8 – 2.1 mm/yr along the southern flanks of the Finisterre Range as indicated by uplifted fluvial terraces; and increasing to *c.* 7mm/yr in the Lae area (Abbott *et al.*, 1997; Crook, 1989). Uplift rates increase towards the southeast commensurate with the rate of horizontal convergence.

In the Lae region the SBIS is overthrusting the NGH and convergence is accommodated along a major narrow north-dipping frontal thrust system which forms part of the RMFZ (Abbott, 1997) (Figure 4.5). Two out-of-sequence (OOSTs) thrust faults, the Wongat and Gain thrusts, or more numerous smaller OOSTs and zones of anelastic deformation could accommodate most of the convergence.

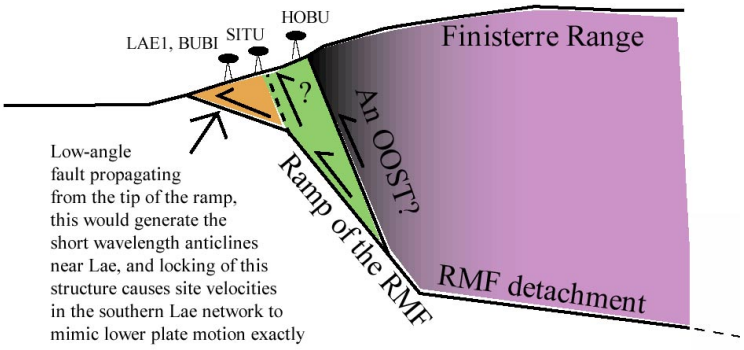

Figure 4.5 Ramp detachment geometry across the RMFZ near Lae (from, Wallace, 2002); The Lae commercial area, wharf and residential areas are located around the LAE1 site, above the low-angle fault. The Finisterre Range is on the SBIS overriding the NGH/Australia Plate along the ramp of the RMF.

From GPS measurements, approximately 40% of the convergence of the NGH and SBIS plates appears to be accommodated in the vicinity of Bukaua, a site to the east of Lae (Wallace, 2002). This suggests that OOSTs may be extensive to the

east of Lae. It is possible that smaller, less active faults, as yet unidentified, exist further to the north of the Hobu, as indicated by slight retardation of those sites with respect to predicted rigid South Bismarck Plate velocity (Wallace, 2002) although it is also possible that the retardation is due to aseismic, anelastic creep.

The Lae urban area appears to be located on the hanging wall of the South Bismarck Plate, and the RMF projects to the south of Lae (Kulig *et al.*,1993; Wallace, 2002). This hypothesis is supported by strain dislocation modelling using realistic local fault geometries that show a slip deficit in the Lae area (Wallace, 2002). Anticlines in the vicinity of Lae, such as the Atzera range and hills near Situm, appear to indicate that the RMF changes dip close to the surface from a steep ramp to a shallow fault, breaching the surface south of Lae. If the RMF is a steep ramp between 20km and 1 km depth and a shallow detachment to the surface, the velocities in the Lae block and the rapid uplift between Situm and Hobu can be reproduced provided the Lae block is locked to the RMF. It is still unclear, however on which side of the Lae block the faults are still active and the exact location of the RMF near Lae is uncertain.

Site velocities north of the Markham valley, up to the foothills of the Sarawaged Range, are consistently different from predicted Australian Plate by *c.* 12mm/yr west-southwest. Sites south of the valley show greater correlation with predicted Australian Plate velocities. This suggests that the region incorporating the Lae urban area, Unitech and the ribbon development along the Highlands Highway to Nadzab airport is internally contiguous. Baselines measured within this block as part of this study appear to be unchanging within the level of precision of the GPS measurements made to date. The locations of the Ramu-Markham fault and other smaller out-of-sequence thrust faults north of Lae have yet to be identified or monitored with any certainty.

4.2.5 Bismarck Sea Seismic Lineation (BSSL)

The rotation of the SBIS has resulted in the formation of oceanic rifts in the Manus Basin over the last 3.5 Ma (Taylor, 1979), centred along the BSSL (Denham, 1969). Spreading segments of the BSSL are connected by a number of left-lateral transform faults, the most easterly of the transform segments being

the seismically active Weitin Fault, through Southern New Ireland, which marks the boundary between the South Bismarck and Pacific Plates (Mori, 1989). The location of the BSSL has been well defined by both seafloor bathymetry in the Manus Basin and earthquake locations (Taylor, 1979). A Manus microplate has been proposed (Martinez and Taylor, 1996) as a submerged continental fragment south of the BSSL. Near the New Guinea coast, the BSSL is largely an east/west left-lateral strike-slip boundary (110 mm/yr) onto which it projects as a series of anastomosing faults in the Toricelli Mountains (Cooper and Taylor, 1987). Spreading rates increase to 130-140 mm/yr near New Ireland (Taylor, 1979; Tregoning *et al.*, 1998) with associated strike-slip along the Weitin Fault estimated at 130 mm/yr (Tregoning *et al.,* 1998). The Wide Bay Fault Zone in East New Britain appears to accommodate some of the relative strike-slip motion between South Bismarck and Pacific Plates and is wrenching the Gazelle Peninsula NW relative to the rest of New Britain (Madsen and Lindley, 1994). The Sapom fault in Southern New Ireland may accommodate some of the convergence between the SBIS/Pac (Mori, 1989). The Gazelle Peninsula and Southern New Ireland are among the most seismically active regions on the Earth. In November 2000, a sequence of several Mw 6.0 to Mw 8.0 earthquakes ruptured the Weitin fault resulting in co-seismic displacements of 5.7 m for stations located near the fault. Distribution of co-seismic slip was observable at the 0.1 m level as far as away as the western Gazelle Peninsula, 100 km from the epicentre (Tregoning, *pers. corr,* 2001).

Geodetic observations at a single site at Bogia (BOGI), combined with seismic data from an active left-lateral strike slip zone northwest of Madang and the western segment of the BSSL, suggest that the Adelbert Block may be independent of the South Bismarck Plate (Wallace, 2002). Additional geodetic measurements between the Adelbert Block and NGH are required to verify or discount this hypothesis.

4.2.6 New Britain Trench (NBT)

The rapid clockwise rotation of the South Bismarck Plate has also resulted in subduction of the Solomon Sea plate (SSP) beneath New Britain along the deep NBT. Convergence across the trench increases from 80 mm/yr at the 149°E

embayment to *c.* 130 mm/yr at the 70° bend in the trench at 153°E (Tregoning *et al.* 1998) (Figure 4.6). Magmatism as a result of this subduction has given rise to the formation of the volcanic Bismarck Arc comprising a string of active volcanoes (Rabaul, Ulawun, Pago and Karkar) along the north coast of New Britain and the Finisterre Terrane (Johnson, 1979). The NBT trends southeast, east of 153°E. The SSP subducts north-northeasterly beneath the Solomon Islands along this section.

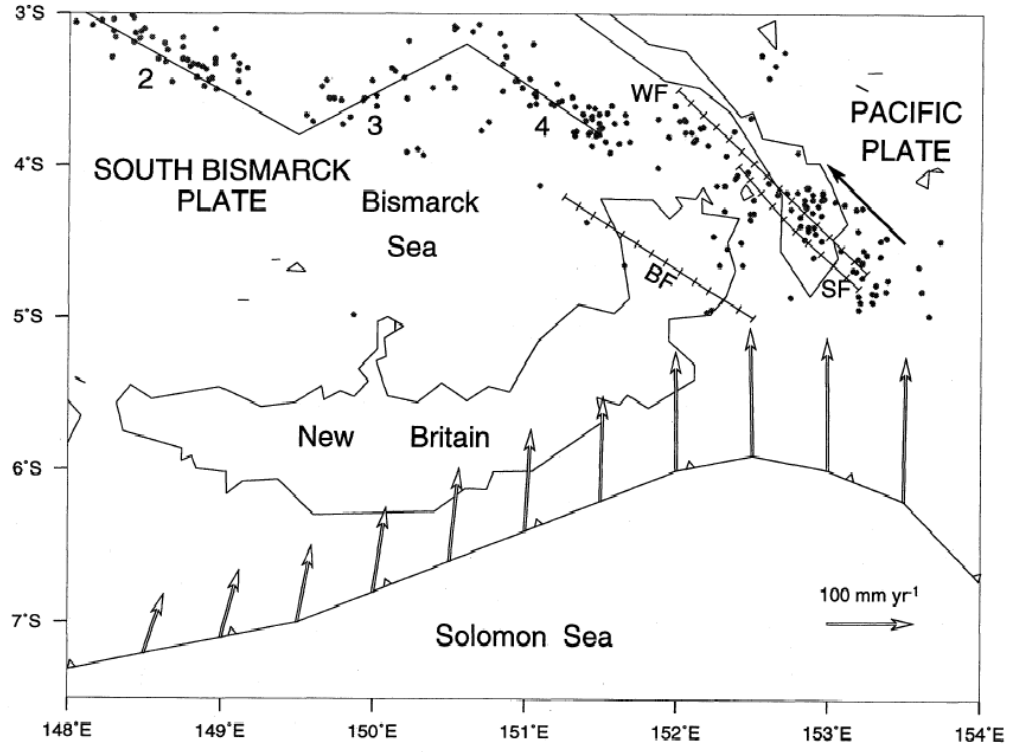

Figure 4.6 Predicted relative motion between the Solomon Sea Plate and the South Bismarck Plate along the New Britain Trench (from Tregoning *et al.*, 1998) **WF –** Weitin Fault, **SF –** Sapom Fault, **BF –** Baining Fault

4.2.7 Trobriand Trough

The Trobriand Trough separates the Solomon Sea and Woodlark Plates east of the easterly migrating triple junction at *c.* 149° E. It is believed that the Solomon Sea plate extends west underneath the active NGH / SBIS collision along the RMFZ (Cooper and Taylor, 1987; Pegler *et al.*, 1995) and represents relict subduction along a former western extension of the Trobriand trough, now closed by the Finisterre Arc / NGH collision along the RMFZ. The Solomon Sea plate is subducting very slowly along the Trobriand Trough, or has recently

become inactive (Davies *et al.*, 1987) as a likely result of gravitational pull of the subducting Solomon Sea slab along the New Britain trench. Volcanism evident at Mt. Lamington and Mt. Victory along the Papuan Peninsula, is possibly a relic of this subduction (Davies *et al.*, 1987), but could also be related to rifting of the Woodlark Plate away from the Australian Plate (Lus *et al.*, 1998), or a complex interaction of both these processes. The absence of any land surface on the Solomon Sea Plate makes any geodetic measurement of the convergence that may be occurring across the Trobriand Trough possible only using sea-floor geodetic techniques.

4.2.8 Woodlark Basin Spreading Centre (WBSC)

The opening of the Woodlark Basin Spreading Centre (WBSC) from 6 Ma (Weissel *et al.*, 1982; Taylor *et al.*, 1999) has resulted in anti-clockwise rotation of the Woodlark Plate (WP) (Weissel *et al.*, 1982) and the northern part of EPCT, away from the Australian Plate at a rate of 1.8°/Ma (Tregoning *et al.*, 1998). Rifting is also beginning towards the eastern extremity of the Papuan Peninsula as the WBSC propagates west as indicated by active metamorphic core complexes and extensional basins (Baldwin *et al.*, 1993). Observed spreading rates across the WBSC increase from *c.* 13 mm/yr at the eastern tip of the Papuan Peninsula to *c.* 26 mm/yr between Misima and Woodlark Island (Tregoning *et al.*, 1998) (Figure 4.7). These spreading rates are half those predicted from paleomagnetic observations indicating changes in the tectonic setting in the basin as recently as 80,000 years BP (Goodliffe *et al.*, 1997).

4.2.9 Owen-Stanley Fault Zone (OSFZ)

The OSFZ is the likely boundary zone between the Woodlark Plate to the northeast and the Australian Plate to the west and southwest. Extension resulting from the propagation of the WBSC changes to left-lateral strike slip along the OSFZ west of 147°E, with 7-9mm/yr predicted between 9.5°S and 8.5°S (Wallace, 2002). The Gira fault in the Garaina region shows evidence of recently active left-lateral strike slip displacement (Davies *et al.*, 1984). North of 8°S, convergent motion is predicted at 10-15 mm/yr normal to the OSFZ (Wallace, 2002). The

sparsity of geodetic observations across the OSFZ makes the distribution of transpressional deformation across this region difficult to quantify at this time. The Aure Trough has been recently active (Dow, 1977) and may accommodate some of this east-west convergence.

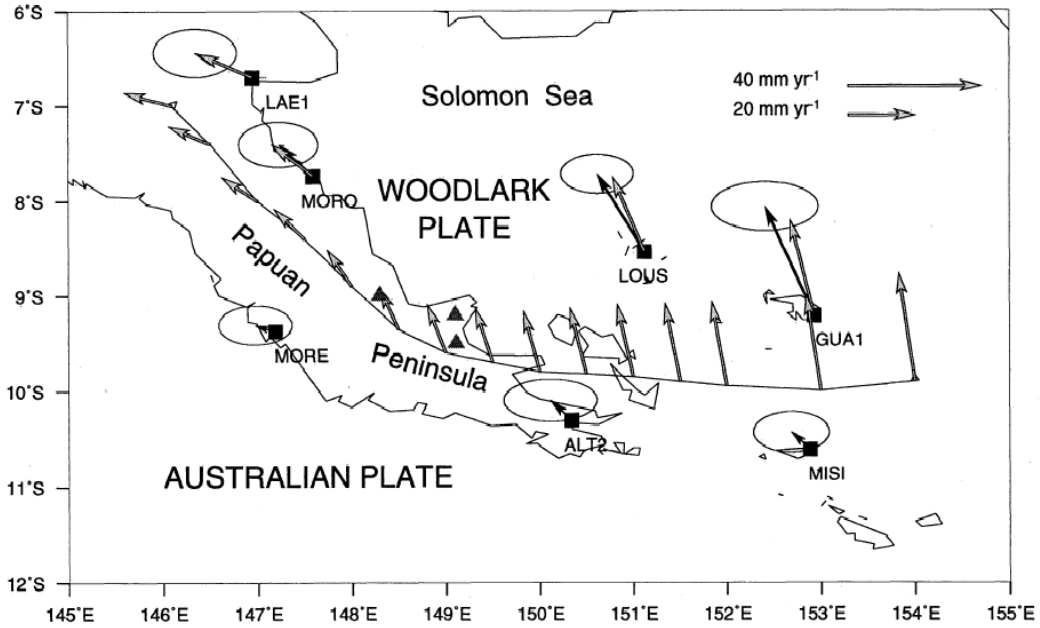

Figure 4.7 Predicted relative motion between the Australian and Woodlark Plates. The motion is extensional to the east of the Papuan Peninsula along the Woodlark Basin Spreading Centre, and left-lateral strike slip trending to convergent along the Owen Stanley Fault Zone. GPS vectors relative to the Australian Plate are shown (from Tregoning *et al.*, 1998)

4.2.10 Manus Trench

A North Bismarck Plate was proposed by Johnson and Molnar (1972) and its existence has been verified by geodetic observations (Tregoning, 2002). Sites north of the BSSL exhibit *c.*10 mm/yr northward motion relative to the rigid Pacific Plate indicating that the Pacific Plate is subducting obliquely along the Kilinailau Trench at a rate of *c.* 10 mm/yr and the Pacific/Caroline Plate to the west may be subducting along the Manus Trench at a rate of *c.* 9 mm/yr.

The NGH is colliding obliquely with the North Bismarck Plate along the NGT. Evidence suggests that the left-lateral strike slip faults are active close to the trench (Cooper and Taylor, 1987).

4.3 Estimation of Euler Poles for tectonic plates in Papua New Guinea

A combination of geodetic measurements (site velocities), transform fault orientations, earthquake slip vectors estimated from the Harvard Centroid Moment Tensor (CMT) catalogue, Quaternary fault slip rates, and spreading rates estimated from geomagnetic reversals have been used to invert for Euler vectors using a least squares inversion method (Minster *et. al.* 1974). Table 4.3 lists the most recent estimates of Euler vectors of the major tectonic plates and microplates in PNG. Coordinates of polygons which define these tectonic units are defined in Appendix B.

Displacement of sites from predicted rigid plate velocities in deforming zones will assist in the estimation of strain dislocation models using other geological methods. Non-linear inversion techniques such as simulated annealing have been used by other researchers (McCaffrey, 2002; Wallace, 2002) to estimate fault locking parameters.

Plate	source	Lat. pole (°)	Long. pole (°)	Rate (°/ Myr)	σ Rate (°/ Myr)	σ maj pole (°)	σ min pole (°)	Az. (°)
Australian	Beavan *et al.* 2002	32.76	37.54	0.621	0.002	0.4	0.13	109
Pacific	Beavan *et al.*, 2002	-63.75	110.86	0.677	0.002	0.61	0.15	85
N Bismarck	Tregoning 2002	-45.0	126.4	0.85	0.07	5.5	0.5	36
S Bismarck	Tregoning *et al.* 1999	6.75	147.98	8.11	0.16	0.1	0.06	4
Woodlark	Tregoning *et al.* 1998	-0.7	128.4	1.78	0.30	4.2	0.65	289
NGH	derived from Wallace *et al.*, 2004	0.80	132.97	2.21	0.22	2.13	0.12	300
Adelbert	derived from Wallace *et al.*, 2004	-6.65	148.64	-5.58	0.60	0.56	0.14	126

Table 4.3 ITRF Euler vectors for plates in PNG

Chapter 5

Analysis of geodetic datum distortion in PNG

5.1 Re-analysis of the GPS data archive in PNG

5.1.1 GPS Data collation

A major task of this study has been to collate a PNG GPS data archive from all known sources, in order to ascertain which data were useful for development of a geodetic datum and velocity field for PNG. Over 3,000 observation files of GPS data from 192 sites around PNG were assessed and analysed. These data were converted where necessary into a compressed Hatanaka RINEX (Receiver Independent Exchange) format and assembled into a directory structure for processing, and also archived onto CD. A database of site occupations was also created. Site and occupation-specific data were validated and entered into the database after cross-checking with any available field sheets and site logs.

5.1.2 Overview of the geodetic analysis

A regional network analysis strategy was chosen for re-analysis of the PNG GPS dataset. For each Universal Time (UT) day of observations, the PNG network data were processed with regional IGS sites to provide a connection between the PNG network and ITRF as well as to compute regional GPS orbits.

Much of the data in the PNG data archive was of sufficient duration (8 – 150 hrs) to be processed concurrently with data from the IGS network to provide ITRF coordinates of the sites with uncertainties of less than 20 mm. The IGS regional network comprised stable continuous GPS with well estimated ITRF coordinates and velocities and reliable 24hr data. Smaller period static GPS observations have also been gathered for computing local site ties and for local network analyses. These shorter period static observation data files were not processed in

the regional network and can be analysed separately to provide local tie information if required at a later date.

The processing and analysis was essentially a three-step process. Firstly, GPS RINEX carrier-phase data from a combination of PNG sites and 17 regional IGS GPS tracking stations were processed to derive loosely constrained network solutions, GPS satellite orbit parameters and Earth Orientation Parameters for each UT day. IGS precise GPS satellite ephemerides (in SP3 format) were used *a priori*, however regional orbits were estimated for each 24 hr period. The GAMIT software (King and Bock, 2000) developed by MIT and SCRIPPS was used to process the GPS data.

Secondly, these daily parameter estimates and their VCVs were then aligned, using a selection of ITRF stations to compute daily estimates of station coordinates with respect to the pre-stabilised ITRF, by computing a seven parameter conformal transformation for each day. The GLRED/GLORG components of the GLOBK suite (Herring, 2002) were used for this purpose.

Finally, weighted linear regression was used to compute ITRF Cartesian site velocities from the daily coordinate estimates and their VCV. I developed a program, LINREG to perform this regression using a standard algorithm (Wolf and Ghilani, 1997). Source code is listed in Appendix C.

A more detailed description of the GAMIT/GLOBK processing and analysis is described in literature (Feigl *et al.*, 1993; Morgan *et al.*, 1996; Tregoning *et al.*, 1998)

5.1.3 Estimation of daily ITRF2000 coordinates using GLRED/GLORG

GLRED is a Kalman filter program which aligns each loosely constrained daily network solution with a selection of ITRF stations included in each daily solution. For the purposes of this study, these ITRF station coordinates, their velocities and variances have been pre-defined by the ITRF2000 realisation (Altamimi *et al.*, 2002). Eight geodetically stable core IGS GPS tracking stations,

with well estimated ITRF2000 coordinates (formal uncertainty <3 mm) and site velocities (formal uncertainty <1 mm/yr)
(http://lareg.ensg.ign.fr/ITRF/ITRF2000/results/ITRF2000_GPS.SSC)
independently verified from other co-located space geodetic techniques, were adopted as fiducial sites in the daily network analysis (Figure 5.1). The other IGS sites included in the network analysis were left free for the purpose of independently verifying the quality of the analysis and to compare position and velocity estimation with ITRF estimates of these sites.

Each daily solution was aligned to ITRF using a seven parameter Helmert transformation, representing the best fit of the minimally constrained network to the ITRF for that day using the variances and covariances of the estimated parameters from the least-squares solution. Loose constraints were applied to all other parameters. The GLORG output ASCII file lists the daily realisation of the ITRF coordinates of the stations and their variances.

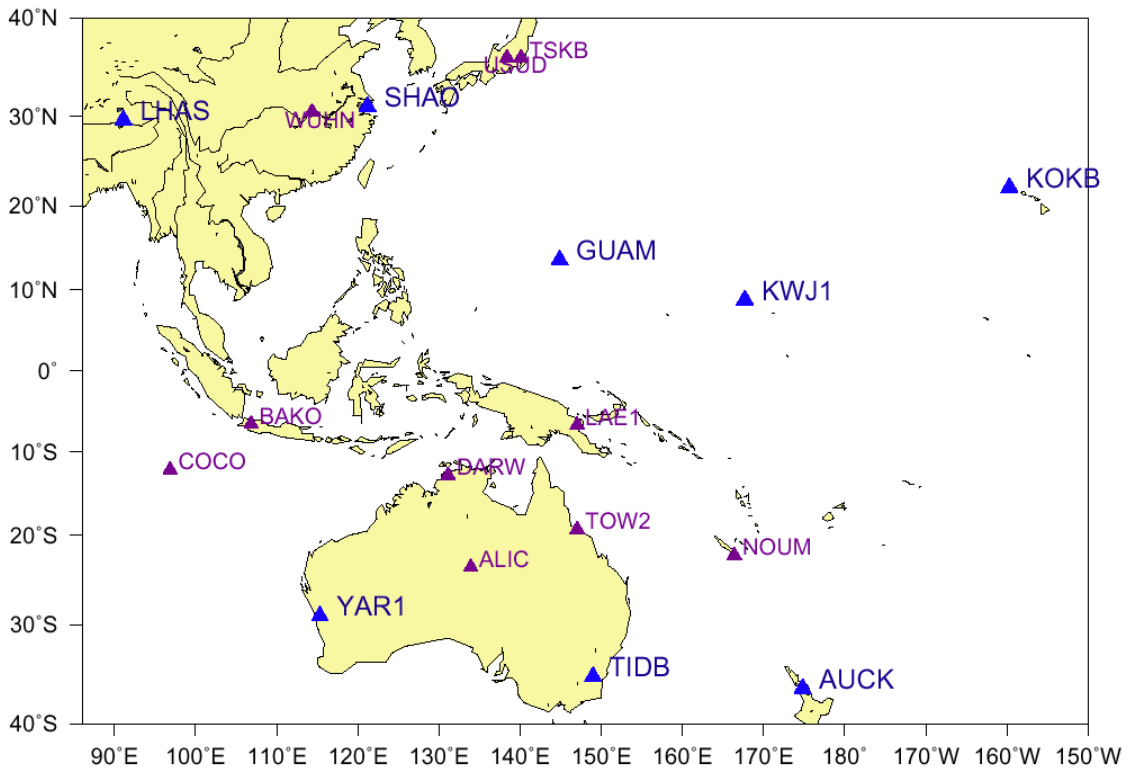

Figure 5.1 IGS sites used in this study for ITRF2000 realisation; Stations in blue are collocated ITRF sites used to align daily GAMIT network solutions; Stations in purple were used as validation sites.

5.1.4 Estimation of ITRF site velocities in PNG

Daily realisations of the PNG network site coordinates and their variances were then combined using a program LINREG in order to estimate their ITRF site velocities. This approach was preferred to a classical GLOBK forward solution which assumes linearity of each site's time series. Many of the PNG site time series are non-linear due to unmodelled co-seismic displacements and antenna setup errors, or have velocities estimated from sparse observations. These unmodelled offsets propagate errors into the estimation of site velocities if the site motion is assumed to be linear. The stability of the ITRF solution at the 2 mm level (Altamimi *et al.*, 2002) has enabled the coordinates of the PNG sites to be estimated independently for each day.

The independent estimates of the non-fiducial IGS station positions and velocities agreed within the levels of uncertainty specified for those sites, notwithstanding the smaller data set used in the analysis (Figures 5.2 and 5.3). This indicates that the analysis of the PNG network is accurate to the levels of uncertainty computed for the PNG sites.

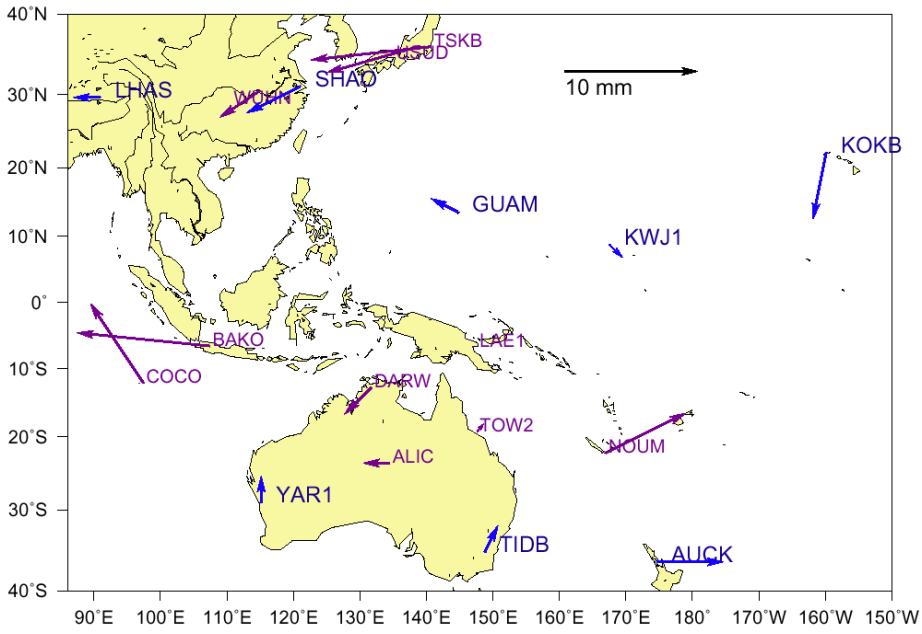

Figure 5.2 Goodness of fit of this analysis to the regional IGS network ITRF2000 at epoch 1997.0. Vectors indicate coordinate differences between this analysis and the tabulated ITRF2000 coordinates. Stations in blue were used to align daily GAMIT network solutions; Stations in purple were used as validation sites. The formal uncertainties of the fiducial ITRF2000 horizontal coordinates are ~4mm, in good agreement with this analysis.

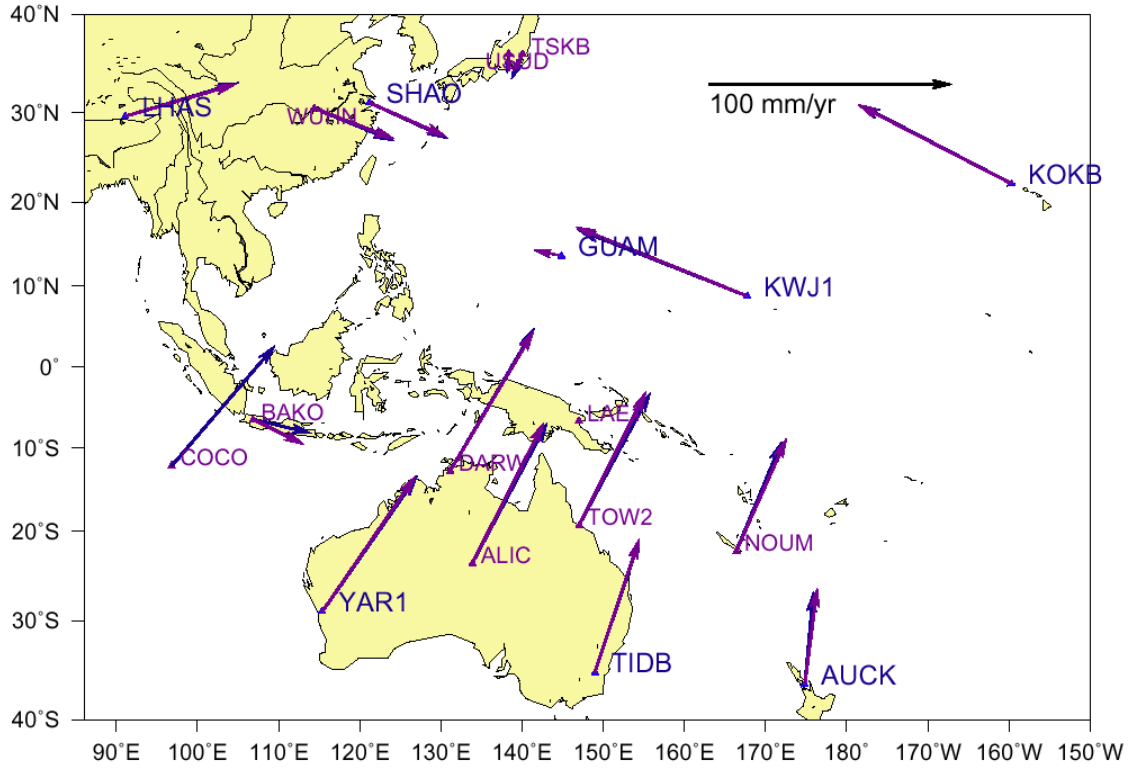

Figure 5.3 ITRF2000 velocity comparisons between IGS sites and analysis for this study. IERS ITRF2000 velocities are shown in blue. Velocities from this analysis are plotted in purple.

5.1.5 An analysis of site time series

The time series and error estimates were examined in order to detect outliers in the estimates. Where only two occupations have been made at a site and a velocity derived between the two epochs, this velocity estimation is critically dependent upon the absence of any of systematic biases and errors, particularly centering errors, unstable antenna setups and monument disturbance.

Figure 5.4 shows a typical time series from a stable IGS site. Figures 5.5 and 5.6 show sites where co-seismic displacement and antenna setup errors are evident. It can be difficult to distinguish between these two errors in the absence of redundant measurements, checks of independent site ties and rigorous checks of antenna setups and antenna phase centre modelling.

Another difficulty arises from time series analysis in seismically active regions. Unless the co-seismic offsets are directly measured or computed from a dislocation model for each large event, these propagate as errors in the velocity estimation.

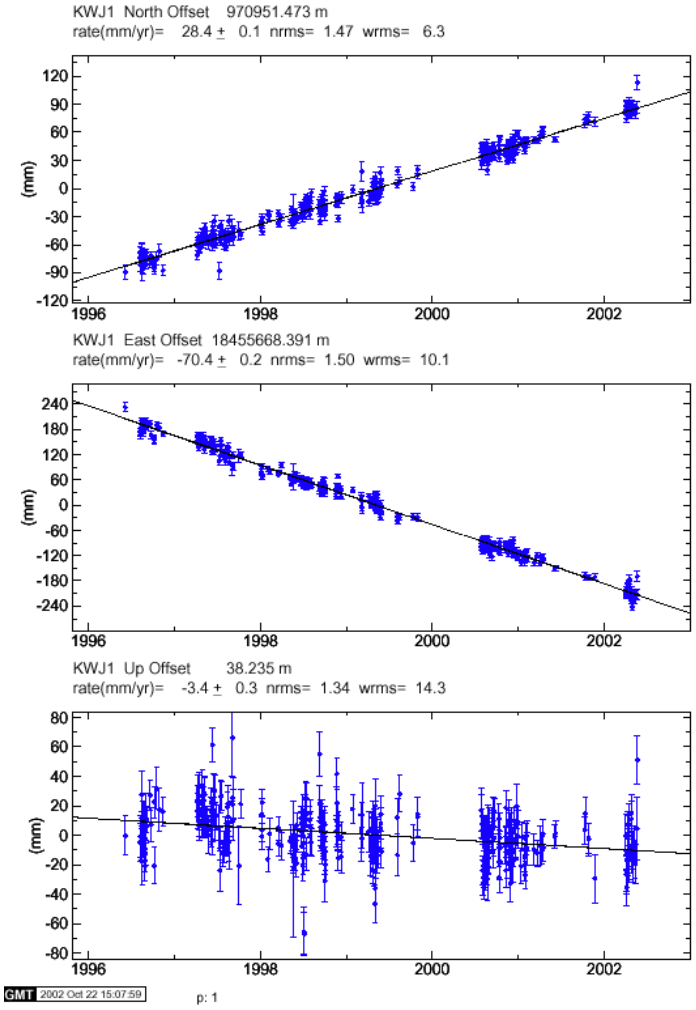

Figure 5.4 Typical IGS site time series from this analysis; KWJ1 Kwajalein, Pacific Plate. The larger variation in the UP time series may be due to unmodelled temporal vertical variations of the earth's crust. Only days where concurrent PNG site observations have been made were processed in this analysis.

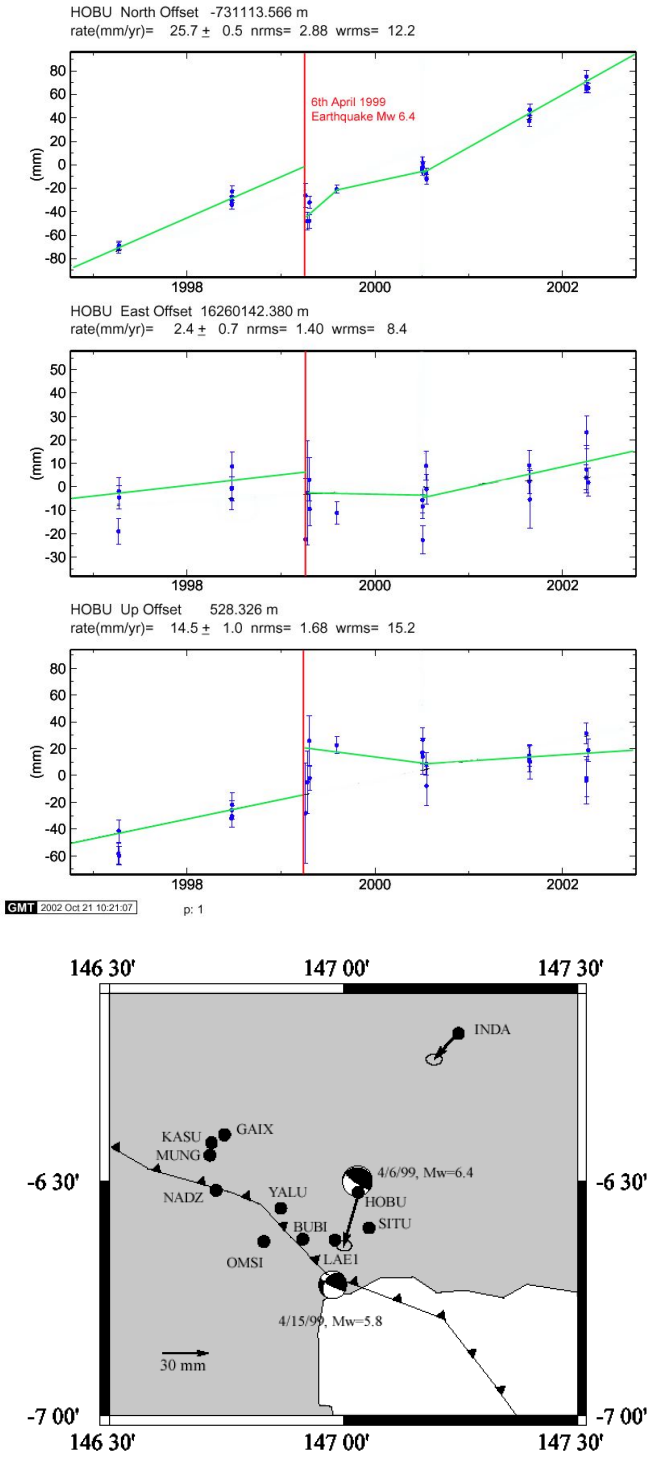

Figure 5.5 (above) Time series for HOBU, located in the Ramu-Markham Fault Zone (this study). Co-seismic deformation is evident after the 6th April 1999 Mw 6.4 earthquake. **(below)** Earthquake locations (from Wallace, 2002).

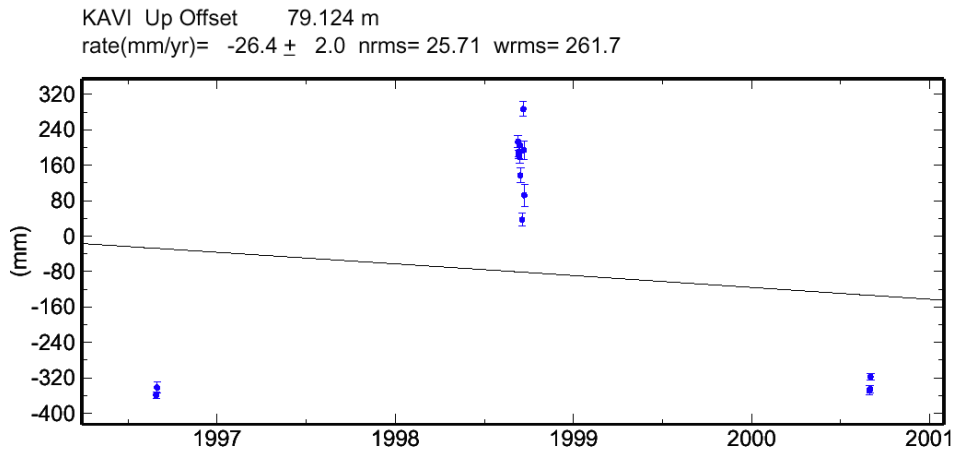

Figure 5.6 Typical vertical time series (KAVI) where the antenna height was assumed at 1.5 m (actual measurements unavailable) for multiple setups on different days during 1998. Antenna heights during 1997 and 2000 were measured, hence good agreement for those occupations.

5.1.6 Computing the ITRF2000 velocity field in PNG

The ITRF2000 coordinate solutions in the GLORG output file were summarised into a text file listing Cartesian coordinates, epochs, and formal uncertainties for further analysis. Estimates with uncertainties greater than 15mm were flagged as outliers and not used in subsequent analysis.

ITRF2000 Cartesian and ellipsoidal coordinates at specified epochs, velocities and their standard deviations were computed with LINREG. The ordinate standard errors are initially scaled by three to better reflect the spread of the solution repeatability. This scaling strategy was deemed appropriate for campaign style measurements where spectral noise is impossible to distinguish from antenna centering errors and other episodic systematic errors (Williams, 2003). With the exception of the permanent stations in PNG (MORE, LAE1 and RVO_) geodetic observations are made from tripod setups, and therefore not forced centered. Vertical velocites have not been used in the analysis, due to the sparsity of data, the high level of uncertainty resulting from antenna measurement offsets, and the small signal.

A detailed listing of the results of the PNG analysis from this study are included in Appendix A. Appendix A lists a selection of core PNG stations and their

ITRF2000 coordinates and their standard errors at epoch 2000.0. Tabulated Cartesian velocities are sourced directly from the linear regression analysis, however, the UP velocities, derived from this analysis, are not tabulated, due to the high uncertainty of these estimates.

5.2 An evaluation of online GPS processing services

Many geodetic agencies, such as the Jet Propulsion laboratory (JPL) and Geoscience Australia (GA), are now providing online processing of GPS RINEX data for users who require coordinates and geoidal heights in either a specified geodetic datum or in ITRF. The service provided by GA is discussed here.

The National Mapping Division of GA (formerly AUSLIG) has developed a particularly user-friendly, free service called AUSPOS (http://www.ga.gov.au/nmd/geodesy/sgc/wwwgps) for processing of global GPS data. Users submit via file transfer protocol (ftp) or direct upload, dual-frequency GPS RINEX files of at least one hour duration to the processing server at GA. Both ITRF2000 and GDA94 coordinates are computed and listed in a report sent back to the user by email. Geoidal heights are computed using AUSGEOID98 for the Australian Continent and EGM96 for the rest of the world. AUSPOS has a quick turn-around time with results usually sent within an hour of submission of the RINEX data. The AUSPOS program incorporates the MicroCosm GPS processing software suite. Reference station data from the nearest three IGS stations are used to constrain the solution into ITRF. IGS-SSC (Sets of Station) cumulative solutions and IGS Final (or next best available at the time of processing) precise orbits are used for the analysis.

The typical estimated uncertainties of 3D position estimations using AUSPOS are; (http://www.ga.gov.au/nmd/geodesy/sgc/wwwgps/wwwfaq.htm)

- 2 hours at 30 second epoch; $\sigma_{\phi,\lambda}$ 20mm, σ_h 50mm
- 6 hours at 30 second epoch; $\sigma_{\phi,\lambda}$ 15mm, σ_h 30mm
- 24 hours at 30 second epoch; $\sigma_{\phi,\lambda}$ 10mm, σ_h 20mm

One of the main limitations of AUSPOS for application in PNG is the lack of a suitable transformation model to convert dynamic ITRF coordinates to PNG94 coordinates, which are referred to ITRF92 epoch 1994.0. While this is also the same realisation as used for GDA94, tectonic distortion between 1994.0 and the epoch of the submitted data is not modelled and can result in metre errors for sites in PNG that are not located on the rigid Australian Plate. This demonstrates the need for a dynamic datum in PNG.

A selection of PNG GPS observations from 2002 were processed with AUSPOS in parallel with the GAMIT analysis. The comparison was made in order to evaluate the performance of AUSPOS in the PNG environment. ITRF2000 horizontal coordinates computed by AUSPOS were found to be in good agreement with those derived from this study (Figure 5.7), however, the repeatability of daily solutions indicated that the positional uncertainties of the positions estimated by AUSPOS are too small. AUSPOS specifications do not appear to indicate that a noise model, or scaling strategy is used for coordinate error estimations. AUSPOS could be improved in the future (a PNGPOS?) to include a velocity model to provide coordinates in the PNG datum, (J. Dawson, *pers. comm*. 2002). The velocity model and algorithm presented in this study could be adapted for this purpose.

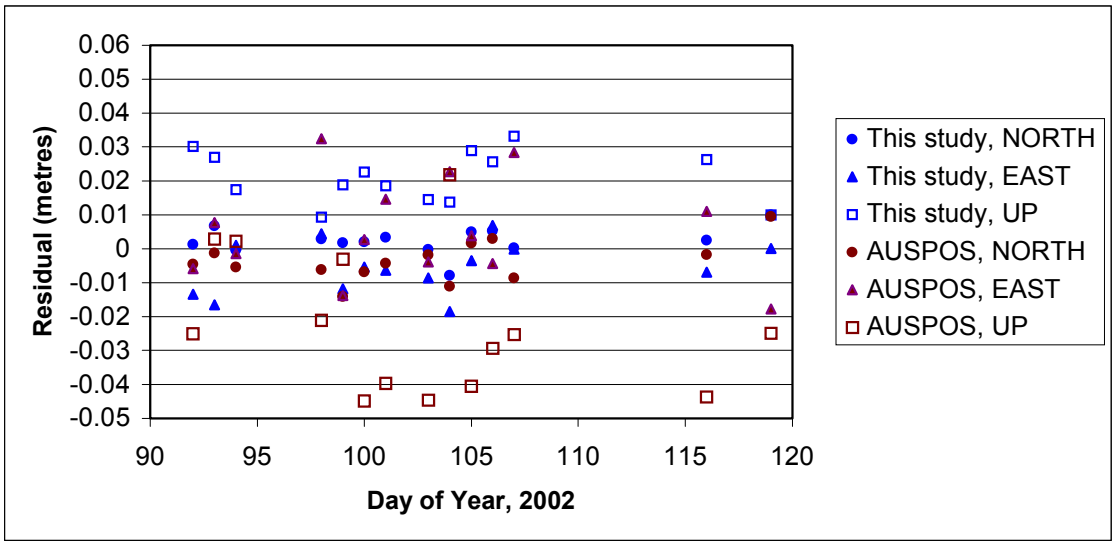

Figure 5.7 Detrended comparison of daily (24 hour obs.) coordinate residuals of site LAE1 between days of year 92 and 118, 2002. Blue symbols show residuals of coordinate estimates related to a common mean using results from this analsyis. Brown symbols are the AUSPOS residuals related to a common mean.

5.3 An evaluation of the PNG94 datum

Epoch 1994.0 coordinates were derived using velocities computed from the NNR NUVEL-1A tectonic model (DeMets *et al.*, 1990; Argus and Gordon, 1991; DeMets *et al.*, 1994) from campaign GPS observations in the realisation of the PNG94 fiducial network (Morgan *et al.*, 1996). The NNR NUVEL-1A tectonic model is very generalised near complex global scale boundary zones such as found in the New Guinea region and can result in gross differences between predicted and observed velocities. PNG94 Datum stations in the Bismarck Sea and New Ireland were assumed to be on, or near the Australian Plate, even though velocities at these sites are closer to Pacific Plate motion (Tregoning *et al.*, 1998). Fortunately, observations were made close enough to epoch 1994.0 that the velocity error has not propagated noticeably into the coordinate solution for the datum realisation. A plot of the raw coordinate differences between ITRF2000 Epoch 1994.0 and ITRF92 Epoch 1994.0 is shown in Figure 5.8. ITRF92 and ITRF2000 are not coincident due to improvements in the ITRF definition between 1992 and 2000, and so the residual vector plots also include differences in the two reference frames as well as other errors. Importantly, the analysis shows that the accuracy of the realisation of the PNG94 datum lies within the 0.1 m positional uncertainty stated by Morgan *et al.* (1996) and Allman (1996).

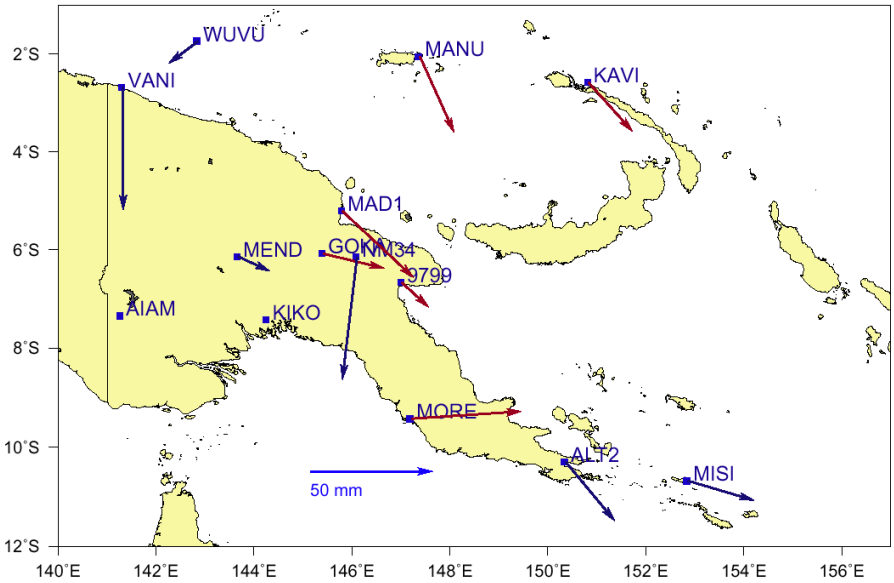

Figure 5.8 Difference between PNG94 (ITRF92 epoch 1994.0), (Morgan *et al.*, 1996) and ITRF2000 epoch 1994.0. Maroon displacement vectors are from this analysis. Blue vectors are displacements derived from other analyses (Tregoning *et al.*, 1998; Wallace, 2002).

The majority of second and third order geodetic stations in PNG were not reobserved as part of realisation of PNG94. The only additional GPS measurements made were to connect tide gauges to the fiducial network and to reobserve the St. George's Channel crustal monitoring network as a response to the Rabaul eruptions in 1994. A strategy was implemented by the geodetic specialist group supporting the Australian Contribution to the Land Mobilisation Project (ACLMP) whereby earlier GPS, Transit Doppler and terrestrial measurements were input into the geodetic network analysis package, NEWGAN, and subsequently adjusted and transformed to PNG94. Tectonic distortion of the constraining network over the intervening twenty years was unaccounted for and the lack of precision inherent with the pre-1990 space geodetic and terrestrial observations was propagated into the adjustment. There exist positional uncertainties of up to 5 metres in the coordinates of geodetic stations included in the PNG94 primary dataset resulting from a combination of tectonic distortion and inaccuracies in the earlier positioning techniques.

5.3.1 Effect of tectonic motion on a static datum in Papua New Guinea

The effects of tectonic deformation on both national and local networks in PNG are analysed and described in detail. Figure 5.9 shows the distortion of the current PNG datum, PNG94, with respect to ITRF2000 over a ten year period between 1994 and 2004.

Figure 5.10 shows the predicted relative displacement vectors of the PNG network in the ten years between 1994 and 2004 using MORE as the GPS base station. This gives a better indication of the magnitude of the datum distortion in practical terms. By 2014 many stations in the PNG network will have moved by up to three metres relative to other stations in the network since the 1994.0 realisation.

Figure 5.11 shows a comparison of the datum displacement with the precision of a typical repeat static GPS baseline measurement made from the LAE1 GPS site using a broadcast ephemeris. Where the displacement vector exceeds that of the

precision circle, the effect of tectonic distortion on PNG94 will be noticeable by surveyors using proprietary GPS positioning equipment and baseline processing software. The effect will be even more apparent with users of AUSPOS. A comparison of the magnitudes of the displacement vectors and precision circles with the positioning accuracy standards in Chapter 2 shows that the distortion is significant, and exceeds acceptable limits for many high precision positioning applications. The distortion is very evident for surveys between the PNG mainland, the Huon Peninsula, New Britain and New Ireland.

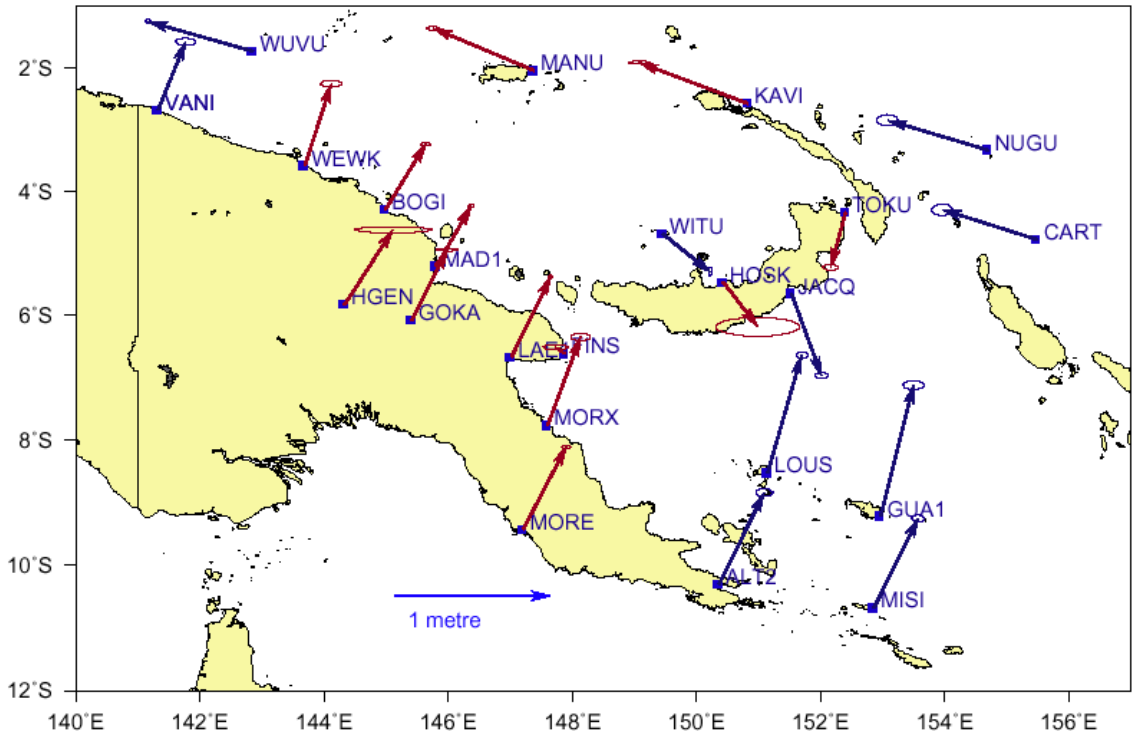

Figure 5.9 Plot of the distortion of the PNG Geodetic Datum 1994 (PNG94) with respect to ITRF2000 between epochs 1994.0 and 2004.0. Maroon vectors are from this study. Blue vectors derived from other previous analyses (Tregoning *et al.*, 1998; Wallace, 2002).

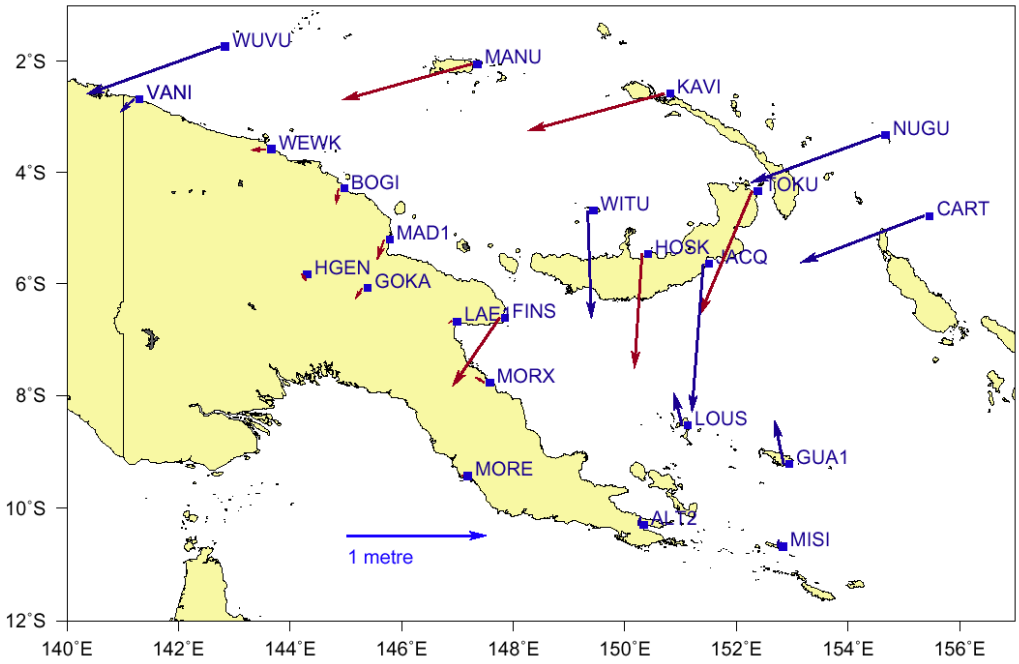

Figure 5.10 Diagram showing predicted displacement vectors between MORE and PNG94 between 1994 and 2004 (excluding co-seismic displacement). Maroon vectors from this study, blue vectors from previous analysis (Tregoning, 1998; 1999).

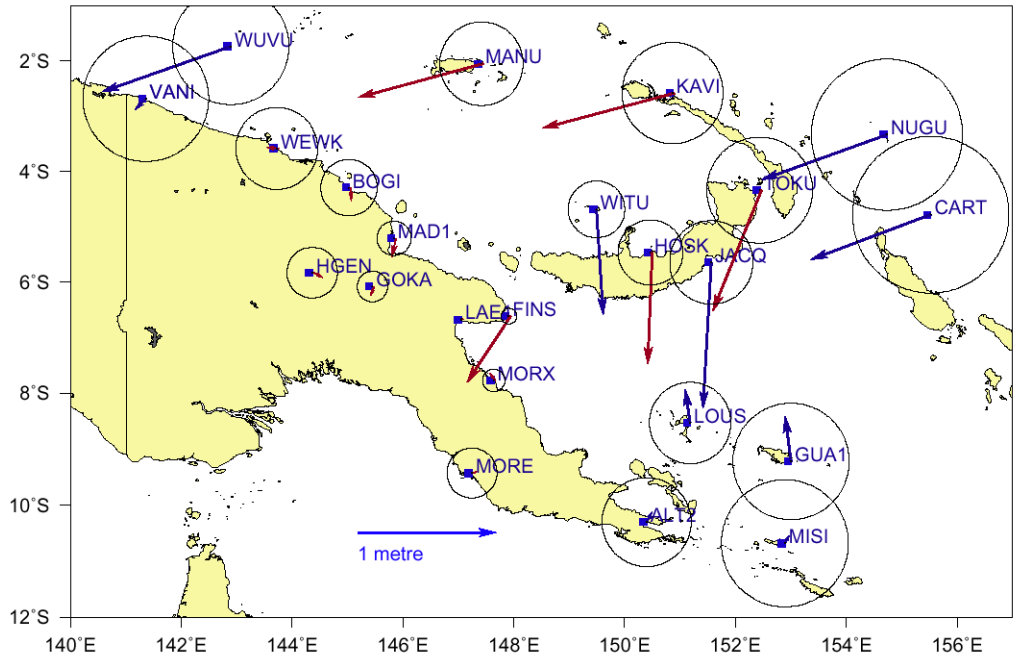

Figure 5.11 Diagram showing displacement vectors between LAE1 and PNG94 between 1994 and 2004; error circles show precision of baseline measurement from LAE1 using typical specifications for a dual frequency GPS receiver and broadcast ephemeris for combined 24hr observations (5mm + 0.5ppm) (Leica SR500 series Technical Specifications).

5.3.2 Localised case-study

Specific local areas subject to significant localised deformation include; Rabaul and the Gazelle Peninsula, Southern New Ireland, Lae and the Markham Valley and Wewak.

Lae and the Gazelle Peninsula are two zones of particular economic importance in PNG, with large populations and extensive spatial infrastructures and cadastres. These locations provide ideal case studies for examining the effects of tectonic distortion on a local datum. An analysis of localised distortion was conducted as part of this study in the Lae area, which lies within the RMFZ. The purpose of this case study was to ascertain the effect of tectonic deformation on a typical urban geodetic network in PNG.

Velocities at LAE1, HOBU, and SITU indicate a rapid transition from the NGH Plate to South Bismarck Plate velocities over 5-10 km, with baseline shortening of 25 mm/yr between SITU and HOBU. This implies that the out-of-sequence thrust faults between SITU and HOBU are still undergoing convergence.

In April 2002, the monitoring network was densified around Lae in the zones where the greatest changes in baseline length have been evident. The transect of sites between POSI, SITU and HOBU was extended and another transect was established between BUBI and HOBU to determine whether the Atzera anticline is undergoing deformation relative to the Lae area. A site on the southern side of the Markham River at Markham Point (MARK) was established to determine whether shortening is occurring across the Markham Valley to BUBI, west of Lae.

In order to derive accurate estimates of baseline changes and site velocities, three epochs of measurements at each of these new sites are required over a period of at least three years. Reobservation of the extended network has not been possible within the duration of this study; however, enough measurements have been made during earlier campaigns to show that the deformation is significant and exceeds relative positioning tolerances over short time periods. The extended network should form a basis for future deformation studies and earthquake hazard monitoring in the future.

Vertical deformation rates, derived from spasmodic GPS measurements, are unreliable over short observation histories, particularly if different receiver and antenna configurations are used during the observation history and the actual signal is small in magnitude. A first order precise geometric levelling run between the Lae tide gauge and LAE1 was undertaken by final year surveying students at Unitech in May 2002 as part of this study. If time and resources permit, it will be advantageous to extend the levelling network between sites in the monitoring network in order to monitor vertical deformation to a precision of a few millimetres. This work will also result in a higher resolution geoid model for the Lae area.

Figure 5.12 shows the effect of tectonic deformation on the Lae area geodetic datum. The magnitude of the deformation clearly exceeds many of the positioning tolerances described in Chapter 2.

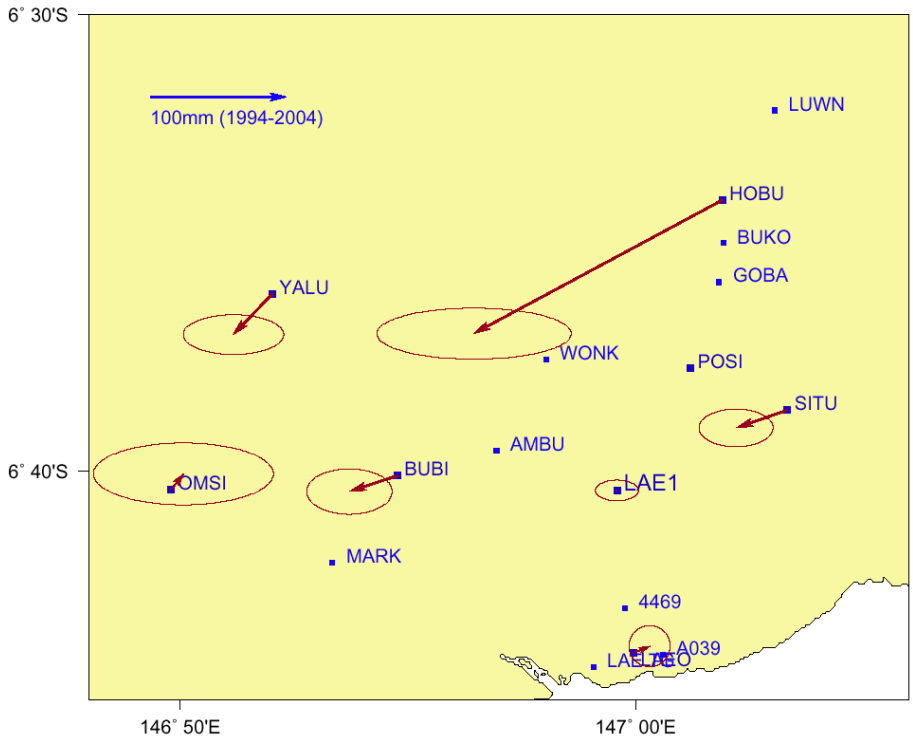

Figure 5.12 Estimated displacement of sites from 1994.0 to 2004.0 in the vicinity of Lae, with respect to LAE1. Sites without displacement vectors are either new sites, or existing sites where insufficient data are available to estimate a velocity. The deformation is significant between Lae and Hobu. Additional measurements are required at other sites in the Lae network to better show the rate of change of deformation.

Figure 5.13 shows the same network, with error circles derived for a simulated single-frequency GPS survey. The distortion again exceeds many tolerances for relative positioning.

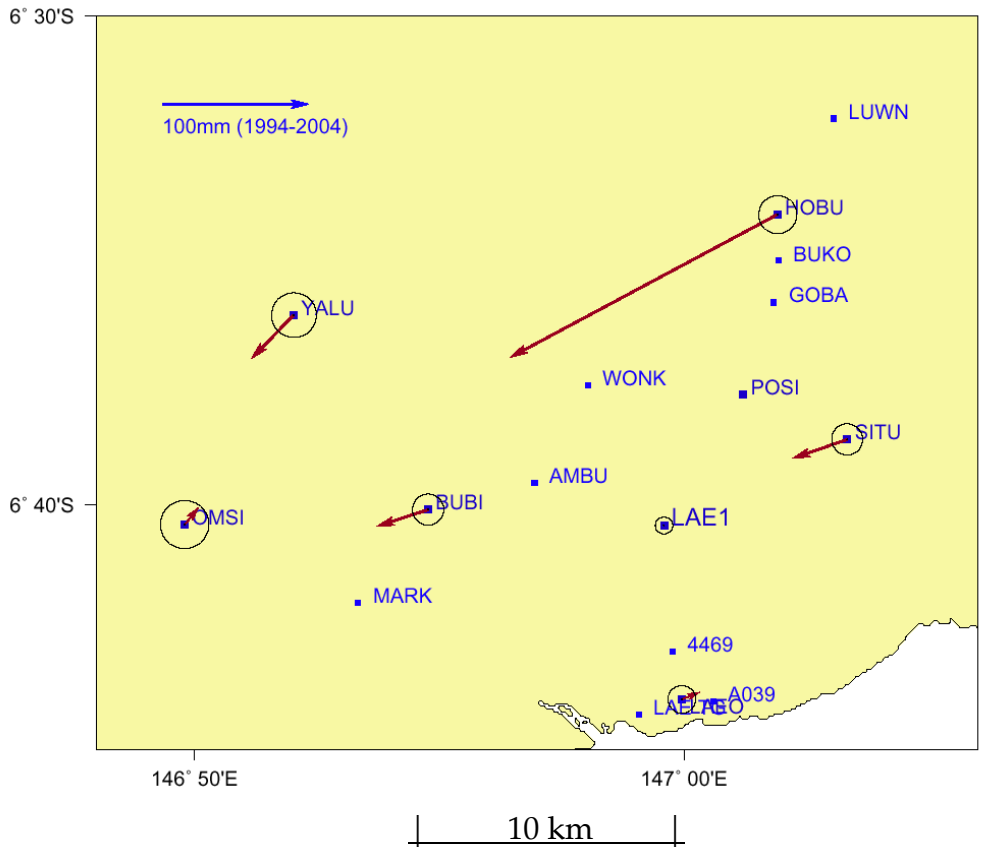

Figure 5.13 Diagram showing displacement vectors between LAE1 and the Lae network between 1994 and 2004; error circles show precision of baseline measurement from LAE1 using specifications for a typical single-frequency GPS receiver and broadcast ephemeris in static mode (5mm + 1ppm).

The Gazelle Peninsula and Southern New Ireland region is also subject to significant internal deformation (Figure 5.14), and *c.* 12 m of relative co-seismic displacement was measured across the Weitin Fault after the November 2000 earthquake sequence (P. Tregoning, *pers. comm.*, 2001). The region is one of the most seismically and volcanically active areas on the Earth. The Gazelle region supports a high population and is of major economic importance to PNG with production of copra, cocoa and other light industry. The intensive land use in the

region requires a good cadastral system, spatial data infrastructure and datum for positioning tasks to support land development. Figure 5.15 shows the rapidity of the internal deformation occurring in the Gazelle Peninsula during the inter-seismic period.

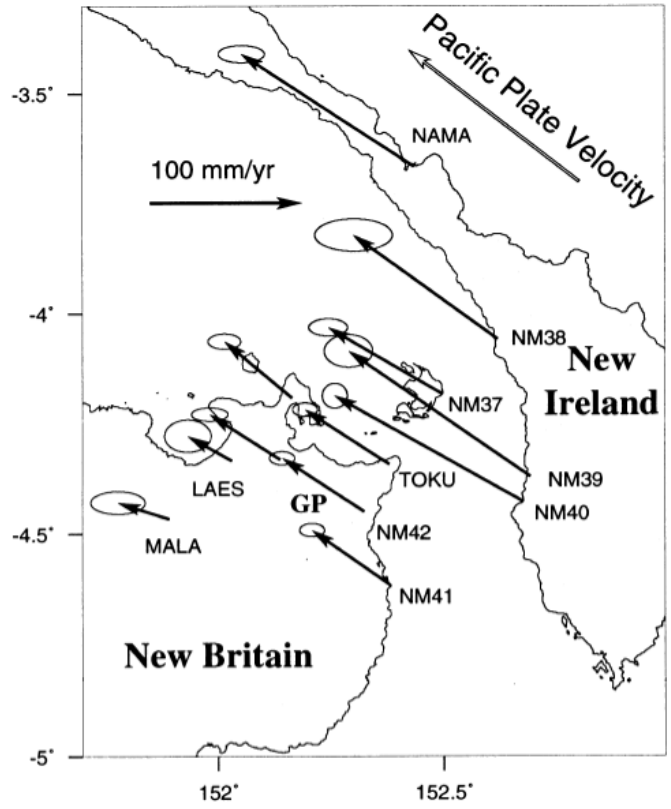

Figure 5.14 Velocities (and 95% error ellipses) relative to the South Bismarck Plate prior to the November 2000 earthquake sequence. The motion of the rigid Pacific Plate is plotted in the top right corner. GP: Gazelle Peninsula. (from Tregoning *et al.,* 2000)

5.4 An adjustment strategy for realisation of a dynamic datum

The majority of existing geodetic network adjustment packages do not accommodate time variation of coordinates in their mathematical model. Constraining the coordinates of stations assumed to be static, but which in reality are dynamic, in a relative reference frame will eventually cause the network adjustment to fail as the baseline measurements between constrained stations change with time. High precision baseline measurements become adjusted to fit

an increasingly distorted network and this becomes evident as the χ^2 statistic increases with time.

An algorithm to better enable dynamic datum network adjustments from geodetic baseline observations has been developed as a major part of this study, to facilitate geodetic datum development in tectonically active developing countries such as PNG. A similar algorithm and program, QOCA (Quasi-Observation Combination Analysis) is also under development, specifically to analyze crustal deformation (Dong *et al.*,1998; http://gipsy.jpl.nasa.gov/qoca). A Reverse Polish Lisp (RPL) program 4DADJ (Appendix D) was developed to test the algorithm using typical GPS baseline results made at different epochs across plate boundaries in PNG as computed with GAMIT. The program was tested on a Hewlett Packard HP48 calculator. A standard weighted least squares and propagation of variances algorithm is adopted (Wolf and Ghilani, 1997);

$$\mathbf{X} = (\mathbf{A}^T\mathbf{W}\mathbf{A})^{-1}\mathbf{A}^T\mathbf{W}\mathbf{L}$$

where,

X is the matrix of parameters (adjusted Cartesian coordinates of the stations),
A is the coefficient matrix,
W is the weight matrix (inverse of the VCV of the baseline quasi-observations),
L is the observation matrix.

In a conventional static datum network adjustment, the quasi-observations are simply the baseline results and VCV computed from the GPS processing software. In a semi-dynamic datum adjustment, the baseline results are pre-adjusted to account for deformation of stations at baseline nodes between the epoch of measurement and the epoch of adjustment.

The primary aim of 4DADJ is to enable computation of coordinates at a specified epoch in a dynamic reference frame from a weighted least squares adjustment of a network of baseline measurements made at different epochs. The algorithm allows for time variation of site coordinates. The time variation may be linear (i.e. site velocity), non-linear (post-seismic relaxation) or episodic (co-seismic displacement or monument disturbance). Coordinates can be computed at a specified epoch using the following equation (also Dong *et al.*, 1998);

$$\begin{bmatrix} X_{t_e} \\ Y_{t_e} \\ Z_{t_e} \end{bmatrix} = \begin{bmatrix} X_{t_0} \\ Y_{t_0} \\ Z_{t_0} \end{bmatrix} + (t_e - t_0) \begin{bmatrix} \frac{\partial X}{\partial t} \\ \frac{\partial Y}{\partial t} \\ \frac{\partial Z}{\partial t} \end{bmatrix} + \begin{bmatrix} \sum \Delta X_{Coseis_{(t_e - t_0)}} \\ \sum \Delta Y_{Coseis_{(t_e - t_0)}} \\ \sum \Delta Z_{Coseis_{(t_e - t_0)}} \end{bmatrix} + \begin{bmatrix} \sum \Delta X_{Postseis_{(t_e - t_0)}} \\ \sum \Delta Y_{Postseis_{(t_e - t_0)}} \\ \sum \Delta Z_{Postseis_{(t_e - t_0)}} \end{bmatrix}$$

where,

t_e is the specified epoch,

t_0 is the reference epoch,

$[X_{te}, Y_{te}, Z_{te}]$ are the Cartesian coordinates at the specified epoch,

$[X_{t0}, Y_{t0}, Z_{t0}]$ are the Cartesian coordinates at the reference epoch

$[\partial X/\partial t, \partial Y/\partial t, \partial Z/\partial t]$ is the Cartesian site velocity,

$[\Sigma\Delta X_{Coseis(te-t0)}, \Sigma\Delta Y_{Coseis(te-t0)}, \Sigma\Delta Z_{Coseis(te-t0)}]$ is the sum of co-seismic displacements between the reference epoch and specified epochs, and

$[\Sigma\Delta X_{Postseis(te-t0)}, \Sigma\Delta Y_{Postseis(te-t0)}, \Sigma\Delta Z_{Postseis(te-t0)}]$ is the sum of post-seismic displacements between the reference epoch and specified epochs.

Co-seismic and post-seismic data are estimated from analysis of site time series, independent of 4DADJ. 4DADJ could be modified to include VCV information for these parameters.

The program applies corrections to the baseline measurements, derived from the tectonic model to form quasi-observations at the time of the adjustment epoch before performing the adjustment.

4DADJ operates on the following input files;

SDAT Datum file

(station_name, position_constraint_flag, velocity_constraint_flag, X, Y, Z, σX, σY, σZ, ∂X/∂t, ∂Y/∂t, ∂Z/∂t, σ (∂X/∂t), σ (∂Y/∂t), σ (∂Z/∂t), epoch)

BDAT Baseline result file

(station_name_from, station_name_to, ΔX, ΔY, ΔZ, $\sigma^2\Delta X$, σΔXσΔY, σΔXσΔZ, $\sigma^2\Delta Y$, σΔYσΔZ, $\sigma^2\Delta Z$, epoch)

EDAT Co-seismic offset (Earthquake) file (estimated from time series analysis)
(station_name, ΔX, ΔY, ΔZ, epoch)

PDAT Plate file (Tregoning *et al.*, 1998; Wallace *et al.*, 2004)
(plate_name, ϕ_{pole}, λ_{pole}, ω, a, b, az, polygon_vertices)
polygon vertices { $[\phi_1,\lambda_1]$ $[\phi_2,\lambda_2]$ $[\phi_3,\lambda_3]$ …….$[\phi_n,\lambda_n]$ }
LDAT Deforming zone strain file (Tregoning *et al.*, 1998; Wallace *et al.*, 2004)
(zone_name, locking_ parameter_list, polygon_vertices)
polygon vertices { $[\phi_1,\lambda_1]$ $[\phi_2,\lambda_2]$ $[\phi_3,\lambda_3]$ …….$[\phi_n,\lambda_n]$ }

RDAT Post-seismic relaxation file (estimated from time series analysis)
(station_name, X_{start}, Y_{start}, Z_{start}, X_{end}, Y_{end}, Z_{end}, epoch start, epoch end, { $[X_1, Y_1, Z_1]$ $[X_2, Y_2, Z_2]$ ….$[X_{n-1}, Y_{n-1}, Z_{n-1}]$ })

4DADJ creates an ASCII output file which lists adjusted coordinates, velocities, their VCV and the reference variance of the adjustment (Wolf and Ghilani, 1997). Ancillary programs of 4DADJ compute baseline changes and plate velocities at specified locations. The velocity model used by 4DADJ has been derived independently, from GLOBK analysis.

To show how 4DADJ removes the effects of tectonic distortion from network adjustments, an ensemble of simulated GPS baseline results from a typical PNG national network observed in 2006, was analysed (Appendix E). The network was initially adjusted in static mode with minimum constraint (PNG94 coordinates of MORE fixed) and the differences between adjusted and tabulated PNG94 coordinates plotted (Figure 5.15). A second over-constrained solution was then computed. Constraints were applied with two stations on different plates, MORE and KAVI, held fixed. This is the methodology still being used for PNG94 network adjustments. The reference variance increases rapidly as the interval between the reference epoch and the adjustment epoch increases (Figure 5.16). The same data were then run by 4DADJ in dynamic mode with a reference epoch of 1994.0 and the adjustment results compared. (Figure 5.17). The equivalent analysis was repeated for a reference epoch of 2000.0 (Figure 5.18). It is clear that a dynamic approach to network adjustments in PNG produces a more consistent estimation of station coordinates, and should be incorporated into future network adjustment for datum development and densification in PNG.

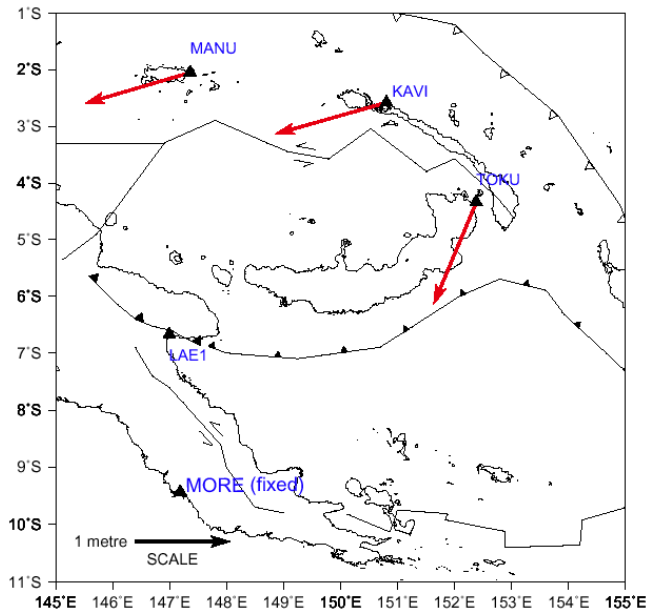

Figure 5.15 Plot showing the coordinate differences between tabulated PNG94 and the output of a minimally constrained adjustment of the simulated 2006 network, with MORE fixed. The error ellipses for the network are too small to be shown at the same scale (< 15mm). The reference variance for the adjustment is 0.48. KAVI and MANU lie on the North Bismarck Plate, which is moving rapidly westward relative to the Australian Plate. Note the small magnitude of the displacement of LAE1, which has a similar velocity to MORE, in the adjustment.

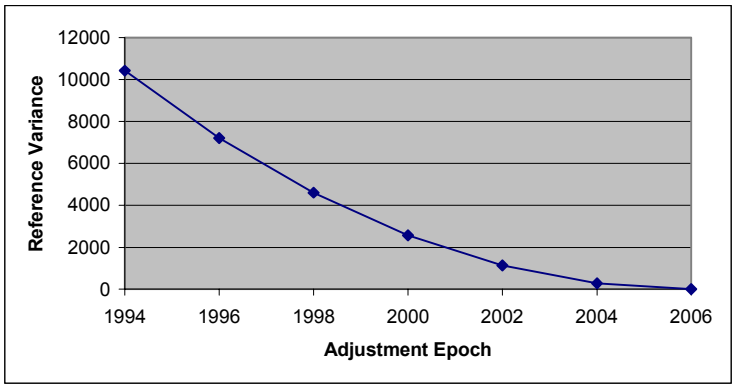

Figure 5.16 Plot showing how the reference variance of a static network adjustment decreases as the interval between the reference and measurement epochs decreases with time. The measurement epoch is 2006. The reference variance for the same network, adjusted using a tectonic model decreases from 54 to 2 over the same period.

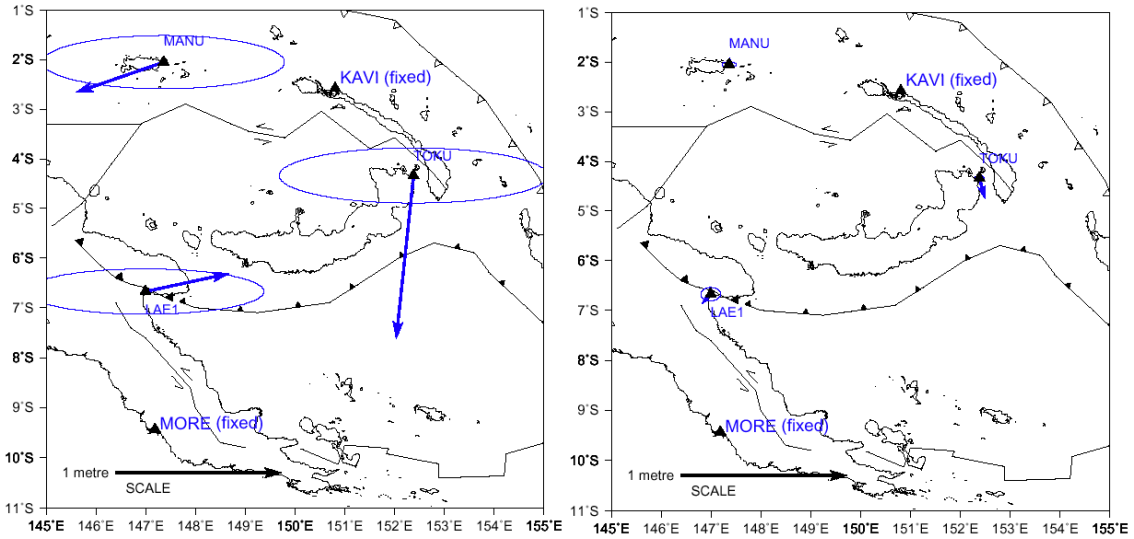

Figure 5.17 A plot comparing the coordinate differences (residuals) between a constrained static adjustment (MORE and KAVI fixed) **(left)** and a dynamic adjustment at reference epoch 1994 **(right)**, using simulated 2006 baseline results. Tectonic distortion is indicated in the magnitude of both the residual vectors and the error ellipses of the positional uncertainties. Including a model of plate motion, strain and co-seismic offsets largely removes the effects of distortion and reduces the magnitude of distortion and formal uncertainties by 90%.

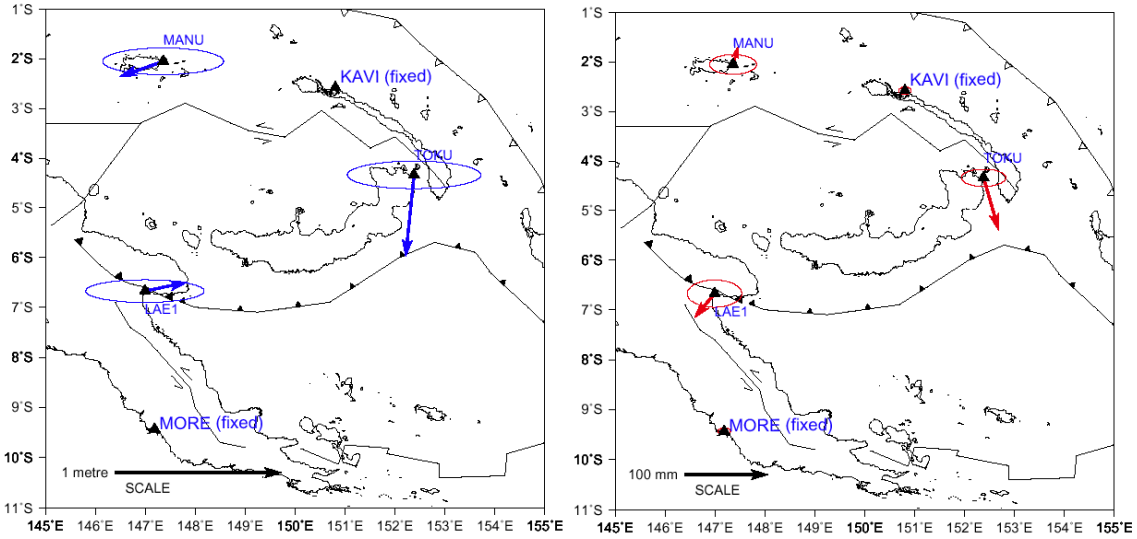

Figure 5.18 The same network as the shown in the previous figure, adjusted at reference epoch 2000.0 (i.e. six years closer to the epoch of measurement). The dynamic adjustment (right) shows a significant improvement in the estimation of station coordinates from a static adjustment (left). (Note the change in scale between the two plots). A comparison between figures 5.17 (left) and 5.18 (left) shows how the magnitude of the residuals decreases as the epoch of measurement and the reference epoch decreases with time in a tectonically active environment.

4DADJ can also be run in multiple baseline mode with LINREG in order to estimate velocities of network sites.

Although 4DADJ mitigates against the effects of modelled and measured tectonic deformation, unmodelled and unmeasured effects cannot be accounted for. Forward and reverse computations for an epoch which lies outside the period of data availability are based upon the assumption of time series linearity for that site. For example, coordinates of a site located in a seismically active location are required at epoch 1994.0. No geodetic time series is available for this site prior to 1998, and the time series between 1998 and the present day indicates two episodes of co-seismic displacement. A large earthquake occurred in the vicinity of the site in 1995, and the co-seismic offset was not measured. Because this offset is unknown, the exact coordinates of the site at epoch 1994.0 will be in error. This is a theoretical problem if no survey related development has occurred in the area before the period of co-seismic displacement.

Chapter 6

Conclusions and Recommendations

Tectonic distortion of geodetic datums is now impairing the application of existing positioning technology for positioning tasks in the 21st Century. Where the distortion exceeds positioning specifications for land surveys, the distortion should be modelled during the survey analysis and network adjustment to mitigate the effects of this distortion.

This study has shown that PNG94 in its existing form is rapidly being distorted as a result of tectonic deformation. Not only has the distortion been shown to be evident in the national network, but also in smaller networks located in deforming zones such as those in the Gazelle and Lae areas. The distortion exceeds the positional accuracy requirements for many survey applications, especially where space geodetic methods, such as GPS, are used to measure longer baselines with high relative precision. The rapidity of distortion in PNG resulting from tectonic deformation has degraded PNG94 to the extent that it is now only suitable for small-scale mapping (1:50,000 or smaller) and navigation purposes. Tectonic distortion also exacerbates the inaccuracies inherited by PNG94 during its realisation. Localised control surveys adopting PNG94 coordinates for their origin are offset by as much as 5 metres from absolute PNG94. The mismatch between relative PNG94 and absolute PNG94 coordinates in these instances is the potential source of major confusion and positioning error with the increasing use of GPS technology in PNG. 4DADJ enables linear, piecewise and non-linear time variation of geodetic coordinates to be accommodated in network adjustments, removing the first order affects of tectonic deformation.

6.1 Implementation Options for a dynamic datum in PNG

6.1.1 Retaining PNG94 in its present form

The easiest option is to retain the existing datum without any development or modification in the foreseeable future. The only advantage of this option is that no additional input and cost is required. The disadvantages are numerous. PNG94 is internally homogeneous at the 5 m level for horizontal coordinates. This accuracy is sufficiently suitable for navigational purposes and marginally suitable for low resolution GIS, but little else. As a result of tectonic deformation, geodetic surveys will become increasingly restricted to localised areas. Nationwide surveys will produce PNG94 coordinates of stations, only relative to the reference station at the epoch of measurement and will differ from locally realised PNG94 due to tectonic distortion. Integration of surveys will not be feasible without complex re-adjustment. Errors will increase over time due to tectonic distortion. Survey integration is the biggest issue, especially if network metadata (i.e. the network constraints) are not included in the tabulation of PNG94 coordinates. As rural development projects start to interconnect, large discrepancies in geodetic data of up to ~5 metres will become evident. Automated cadastral mapping and management of location based services will be adversely affected by a heterogeneous datum and tectonic deformation. The use of a multiple reference station network spanning plate boundaries and deforming zones in PNG will not be feasible unless relative motion between the reference stations is accommodated somehow.

6.1.2 Retaining PNG94 with dynamic computations

Fiducial PNG94 stations are consistent at *c.* 50mm level at epoch 1994.0. Lower order PNG94 stations however, inherit the lack of precision of earlier geodetic measurements. A dynamic network adjustment will only be effective if the network is constrained by these core stations. Densification of PNG94 subsequent to its realisation has been made on the assumption of a static datum, and derived coordinates incorporate the distortion of the datum between 1994.0 and the date of the survey. Introduction of a dynamic adjustment process to

regress coordinates back to epoch 1994.0 would produce coordinates inconsistent with those computed using existing practices.

6.1.3 Re-adjust PNG94 to a static PNG2004 (ITRF2000, epoch 1994.0)

The change in coordinates resulting from a change in reference frame from ITRF92 to ITRF2000 does not exceed *c.* 50mm in PNG as described previously (5.3.1). This relatively small magnitude of change is swamped by the tectonic deformation which in turn is swamped by the errors that were accepted in the adjustment of PNG94. The disadvantages highlighted with the option of retention of PNG94 still apply, with the added cost of implementation and confusion of datum change. A combination of distortion modelling based upon models of tectonic deformation, and transformation parameters between ITRF92 and ITRF2000 at epoch 1994.0, would need to be applied to PNG94 data.

6.1.4 Implement a new static PNG2004 (ITRF2004, epoch 2004)

A fresh realisation of the PNG datum will bring the datum into synchronisation with ITRF, however without any proposal to update the datum the same issues with retaining PNG94, or a re-adjusted PNG94 (PNG2004), apply. There is a sufficiently wide and dense network of stations observed by GPS, for an update to be feasible.

6.1.5 Implement a semi-static datum

Every several years a newer re-observation, adjustment, or forward computation could update the coordinates including the intervening tectonic displacement. The time interval between updates would be dependent upon how quickly the tectonic signal exceeds the accuracy requirements (2.6). This option is impractical for hardcopy representations of geographic data, such as large-scale topographic maps and coordinate listings, which would need to be updated every time the datum is updated. This is especially true in a developing country like PNG where reprographic services are limited and the cost involved is high.

6.1.6 Implement a semi-dynamic datum with dynamic computations

Using a dynamic computational reference frame and velocity field, that also makes allowance for co-seismic offsets, enables tectonic displacements of the datum and GIS to be accommodated while still maintaining the benefits of a static datum. This has been the conclusion of datum development researchers in New Zealand (Grant, 1998; Grant *et al.*, 1999). The complexities of geodetic distortions are handled by a smaller number of geodetic specialists rather than by a much larger number of surveyors and end users of the spatial data.

It was considered that a semi-dynamic datum was more suitable, presenting less risk to the New Zealand Government and the various stakeholders in spatial information in the country. A semi-dynamic approach allows for a "static" spatial dataset at a given reference epoch, however any geodetic computations are done in a dynamic computational reference frame. The coordinates of stations are "frozen" at epoch 2000.0 but, for computation purposes, the station velocities derived by interpolation from a curvilinear velocity model are used to compute the quasi-coordinates at the epoch of measurement in a dynamic computational reference frame. The resulting adjusted coordinates are then regressed back to epoch 2000.0 using the same velocity model. This has resulted in a datum that is both dynamically stable and statistically rigorous. Because coordinates are always referred to epoch 2000.0, the complication of adding velocity or epoch metadata in geographical databases is removed. Users and managers of spatial data are spared the potential confusion arising from a dynamic dataset. This strategy does not, however, make allowances for co-seismic or other non-linear deformation of the geodetic network resulting from earthquakes. Earth scientists and geophysical hazard managers would continue to use a truly dynamic ITRF in order to monitor earth deformation.

6.1.7 Implement a dynamic datum (ITRF)

A fully dynamic datum would require a considerable expansion of spatial metadata in a spatial dataset to include epoch information, site velocities and other time dependent information. This option is really only suitable for geodynamics studies and many spatial databases do not support dynamic

coordinates, or epoch-dependent data. A dynamic datum does not support paper based or other hardcopy geographic data products.

6.1.8 Co-seismic displacement strategies

Geodetic monuments located near plate boundaries in PNG are susceptible to episodic co-seismic displacement resulting from larger earthquakes. Co-seismic displacement from great earthquakes is regularly in the order of metres in magnitude. This, and associated non-linear post-seismic relaxation, should be included in a dynamic datum model. The offset can be measured directly with either CGPS, campaign style measurements, InSAR for localised deformation, or can be inferred from slip dislocation models. A rubber-sheeting transformation, or finite element model (FEM) can be applied to allow interpolation of co-seismic offsets in areas located between monitoring stations. Integration of a geodetic model with other geophysical models is an important area for future research in datum development.

6.2 Geodetic infrastructure considerations and recommendations

The main practical considerations for datum development in PNG include;

- The cost to the PNG Government of implementation
- The accessibility of the technology and knowledge required to drive the datum
- Changes to the geodetic infrastructure (physical marks, data analysis, information transfer)

6.2.1 Cost

PNG is a developing country still heavily dependent upon international aid. The priority areas of the national budget are health, education and other essential services. Datum development has a fairly low priority in terms of the immediate

needs of the nation, however, in the long term, it is something that needs to be addressed if the land-based economy is to develop towards first world levels. As a result of the extensive crustal motion surveys undertaken since the 1990s, there exists a substantial physical infrastructure of monitoring stations, whose positions and velocities have been well estimated. This infrastructure could form the basis of an updated datum resulting in a substantial reduction in the cost of implementation.

6.2.2 Technology and Software

NMB and UNITECH are both well equipped with dual-frequency GPS receivers to develop the geodetic infrastructure in PNG and provide training for surveyors and geodesists. At present, GPS data analysis within PNG is limited by the use of proprietary software useful only for localised surveys. There is no facility in PNG to enable high precision estimation of longer baselines, or allow for dynamic coordinates in network adjustments. It would be advantageous in the long-term for software such as GAMIT/GLOBK, Bernese, or GIPSY/OASIS to be installed at NMB and Unitech, to enable primary network analysis to occur in PNG. A Graphical User Interface (GUI) would be advantageous for users of this software, not fully conversant with geodetic computing. The algorithms developed in this study could be used or integrated with existing packages to allow for dynamic computations. Other software programs are available that perform dynamic computations for specific epochs, for example;

- QOCA, developed by Danan Dong, Space Geodesy and Geodynamics Systems Group, NASA, (http://gipsy.jpl.nasa.gov/qoca/index.html)
- PNGVEL, developed by Paul Tregoning at RSES,
- HTDP (Horizontal Time-Dependent Positioning), developed by the US NGS (Snay, 1999) to model geodetic distortion of the North American Datum (NAD83) along the Pacific margin,

The limitation with PNGVEL and HTDP is that they do not perform least-squares network adjustments, or generate VCV of station coordinates and velocities. There is a requirement for a platform independent web-based program, to perform geodetic computations and dynamic network adjustments

for this purpose. The same routines would need to be incorporated into online positioning services such as a PNGPOS and MRS/VRS, should they ever be adopted within PNG.

6.2.3 Educational issues

Continued development and maintenance of geodetic datums in PNG can only be successful if resident geodesists have a direct role in the process, especially in the management of the geodetic infrastructure. Many geodetic and surveying consultants operating in PNG fail to appreciate the impact of earth deformation on the PNG datum when they extend control into areas of new development, or perform wide area network adjustments. A "part to the whole" mentality persists where local realisations of the PNG datum are inconsistent. The use of satellite positioning technology for high accuracy positioning requires a high level of expertise in geodesy, especially in a dynamic environment such as is found in PNG. The successful application of a geodetic datum in PNG is dependent upon the training, expertise and certification of geodesists, surveyors and geographic data managers who operate in the country.

The PNG University of Technology (UNITECH) in Lae is the only accredited tertiary institution providing professional education and qualifications for land surveyors and Geographical Information Systems operators in PNG. The nationalisation of geodetic surveying in PNG is severely hampered by the lack of suitably qualified geodesists and teaching staff required to train geodetic surveyors, and the lack of opportunities for Continuing Professional Development (CPD) for existing surveyors to further develop their skills. There is a cogent requirement for the education of geodetic surveyors at both undergraduate and post-graduate level.

Any future datum development requires the full participation of PNG geodetic staff (Rosa, 1999) in order for the geodetic infrastructure to be sustained into the future. Continued support from regional geodetic organisations is essential in the early stages of this development. Three key components to the geodetic infrastructure in PNG need to be reviewed;

- The physical infrastructure,
- accessibility of the datum to various users, and,
- data processing and data transfer.

6.2.4 Physical Infrastructure of a proposed PNG geodetic network

Existing first and second order geodetic monumentation in PNG has largely been inherited from the terrestrial survey era when intervisibility and the geometry of photogrammetric ground control were the principal considerations in the siting of geodetic stations. As a consequence, many of these stations are located on remote summits of mountain ranges and are only accessible by foot or helicopter, at great cost and time. Extension of control from many of these higher order stations is now impracticable due to the high cost of access to the site and the loss of the marks over time. Many of these stations have been disturbed and destroyed during the last thirty years and the life expectancy of the remaining stations is in question, due to their lack of accessibility, maintenance and disturbance by natural or anthropogenic processes.

As mentioned previously, space based geodetic positioning techniques are well suited to the PNG environment and better use could be made of airports and other more readily accessible locations to expand the geodetic network. A zero order fiducial geodetic network for PNG should comprise a nationwide network of stable primary geodetic stations located at each major provincial airport, preferably low-set concrete pillars with threaded bolts, together with an extensive local reference and recovery mark network. Ideally, these stations would be continuous tracking sites, however issues of security, power, data storage and real-time transmission by radio or internet mitigate against this option in PNG at the present time. These stable sites would also form the fundamental control network for geodynamic monitoring. The existing PNG fiducial network that defines the PNG94 datum consists mostly of standard brass plaques set in concrete. The only forced-centred stations in the current PNG94 fiducial network are at NMB Port Moresby (steel tower) and the Wankkun pillar (NM/J/34) in the Markham Valley. The brass plaque stations are really only suitable as second order stations due to their lack of facility for forced-centering.

The fiducial network could be extended by construction of low-set pillars at the following airports and bases; Jacksons (Port Moresby), Nadzab, Goroka, Gurney (Alotau), Madang, Vanimo, Kavieng, Tokua, Hoskins, Kagamuga (Mt. Hagen), Buka and Wewak. A CGPS pillar has already been constructed at the Lombrum Naval Base on Manus as part of the South Pacific Sea Level and Climate Monitoring Project (SPSLCMP).

A second order network of pillars, or well-constructed, stable ground marks could be established at the following airports; Mendi (to replace old mark now destroyed), Popondetta, Tabubil (use existing mark), Wau (use existing mark), Kainantu, Kerema, Londolovit (Lihir), Daru, Wapenamanda and Misima (use existing mark).

A suitable auxiliary first order network of accessible sites, though not necessarily as stable as the fiducial sites, could be located close to, or on the roofs of Lands Department or other government buildings, where security, power, data storage and transmission are more feasible in the PNG environment. These stations could form the basis of a VRS or MRS network to provide control for local and provincial geodetic surveys. Ideally, major provincial centres should have 3-4 widely spaced primary stations at secure, stable locations, to provide some redundancy in local survey networks. Any two can be operated as reference stations, the remainder being used as checks, for reinstatement and local network densification when required. The location and spacing of these primary stations should be such that positioning accuracy specifications be met for development within a specified radius of the station using a broadcast ephemeris.

Existing stations are located at; Unitech (Sandover Building), NMB Tower Port Moresby, RVO Office roof and Manus Tide Gauge, Lombrum

Additional stations could be established at; OTML Office Roof, Lihir Mine Office, Porgera Mine Office, Morobe Gold Office – Wau, Kimbe - Niugini Surveys Office, Kenabot/Kokopo Lands Office, Wewak Lands Office.

Other suitable locations for VRS or CGPS include; District / Provincial Government Offices, Lands Department / Provincial Surveyor Offices, Research Institutes, Weather station compounds, Schools

Each gazetted town, or development area should have a network of second order stations located at airstrips, or within stable, clear, secure and accessible locations to enable them to be used as reference stations for lower order surveys. Densification of recovery networks is essential in rapidly deforming zones, due to the loss of integrity of the local deformation field resulting from the loss of primary monuments

6.2.5 Accessibility of data from a proposed PNG network

Geodetic data can include station metadata (coordinates, velocities, station summaries etc.), or geodetic observations from the network such as GPS carrier-phase and pseudorange data. In order to maximise the utility of the datum to support positioning activities and development, there needs to be a system in place to enable contributors, managers and users of the data to be able to access the datum.

The NMB should be the sole central holding office for geodetic metadata in order to avoid inconsistency. Datum information and station summaries should be available either online (preferred) at no cost, or by fax CD/DVD to users on a user-pays or *quid-pro quo* basis. The advances in information technology and internet should be taken advantage of to steer away from the need for paper based records and data delivery. The lack of plotting facilities and difficulties with document delivery in many regional centres in PNG preclude this in any case.

Observation data, such as GPS carrier-phase data from CGPS or VRS, should be made available to users by the NMB via ftp, internet at no cost, or by delivery of CD on a *quid-pro quo* basis as with the geodetic metadata. Delivery of phase or pseudorange data could also be made available in real-time via HF, mobile net, satellite, or internet. The NMB would be responsible for archiving and management of any of this data.

Data processing and network adjustment should be carried out by NMB to ensure consistency and maintenance of a high standard of accuracy, with the use

of the software described previously. An online processing service similar to AUSPOS could be setup, i.e., an PNGPOS. Alternatively, AUSPOS could be configured to allow data to be processed in a defined PNG dynamic datum. Accredited surveyors in other institutions or private practice could be sub-contracted to provide NMB with these services on a *quid-pro quo* basis.

6.3 Directions for future research and development

A more rigorous approach to geodetic analysis and interpretation of the geophysical phenomena which result in non-linear geodetic time series would greatly benefit from the development of dynamic datums, especially at the fiducial level, i.e., ITRF. Integration of InSAR, photogrammetry and RTK controlled by a dynamic MRS would enable ground deformation to be modelled at a much higher resolution than is available at present. While this is primarily of interest to geophysicists, the applications for real-time hazard monitoring and deformation of the land based economic infrastructure would be of benefit in areas where deformation is significant. The realisation of a non-linear dynamic reference frame could accommodate discrete deformations at the zero order level and should be applied to network adjustment where dynamic networks are densified.

4DADJ could be modified to run with LINREG to estimate a site velocity where multiple measurements are made at different epochs to stations in the network. Site coordinates for datum stations can be either constrained or estimated. Site velocities could be fixed, assumed from a plate model or estimated. Co-seismic and post-seismic deformation, where measured, could be accounted for in the network adjustment. Interpolation of the post-seismic input data would be performed by a logarithmic fit of observations at a site during the post-seismic relaxation period. A simplified fault locking model would be used to estimate a strain correction to be applied to stations located near active boundary zones.

References

Abbott, L., Silver, E., and Galewsky, J., Structual evolution of a modern arc-continent collision in Papua New Guinea, *Tectonics*, 13, 1007-1034, 1994.

Abbott, L., Silver, E., Anderson, R., Smith, R., Ingles, J., Kling, S., Haig, D., Small, E., Galewsky, J., and Sliter, W., Measurement of tectonic surface uplift in a young collisional mountain belt, *Natur*e, 385, 501–507, 1997.

Abers, G. and McCaffrey, R., Active deformation in the New Guinea fold-and-thrust belt: seismological evidence for strike-slip faulting and basement-involved thrusting, *Journal of Geophysical Research*, 93, 13,332–13,354, 1988.

Abers, G and McCaffrey, R., Active arc-continent collision: Earthquakes, gravity anomalies, and fault kinematics in the Huon-Finisterre collision zone, Papua New Guinea, *Tectonics*, 13, 227-245, 1994.

Allman, J., *Geodetic Datum & Geodetic Adjustment for Papua New Guinea (PNG94)*, ACLMP report, 1996.

Altamimi, Z., Sillard, P., and Boucher, C., ITRF2000: A new release of the International Terrestrial Reference Frame for earth science applications, *Journal of Geophysical Research*, 107, B10, 2214, doi:10.1029/2001JB000561, 2002.

Anhert, F., The role of the equilibrium concept in the interpretation of landforms of fluvial erosion and deposition, in Macar, P., ed., *L'evolution des versants*; Liege, Belgium, Universite de Liege, p. 22-41, 1967.

Angus-Leppan, P., Allman J., and Sloane, B., Crustal Movement from Satellite Observations in the Australian Region, *Tectonophysics*, 97, 87-93, 1983.

Argus, D., and Gordon, R., No-Net-Rotation model of current plate velocities incorporating plate model NUVEL-1, *Geophysical Research Letters*, 18, 2039-2042, 1991.

Baldwin, S., Lister, G., Hill, E., Foster, D., and McDougall, I., Exhumation of high pressure metamorphic rocks during crustal extension in the D'Entrecasteaux Islands, Papua New Guinea, *Tectonics*, 12, 611-628, 1993.

Beavan, J., and Haines, J., Contemporary horizontal velocity and strain rate fields of the Pacific-Australian plate boundary zone through New Zealand, *Journal of Geophysical Research*, 106, 741-770, 2001.

Beavan, J., Tregoning, P., Bevis, M., Kato, T., Meertens, C., Motion and rigidity of the Pacific Plate and implications for plate boundary deformation, *Journal of Geophysical Research*, 107, B10, 2261, doi:10.1029/2001JB000282, 2002.

Blick, G., Crook, C., Grant, D., and Beavan, J., Implementation of a Semi-Dynamic Datum for New Zealand, *IAG Proceedings* (in press), 2003.

Bomford, G., *Geodesy*, 4th Ed., Clarendon Press, Oxford, 1980.

Braun, J., Heimsath, A., and Chappell, J., Sediment transport mechanisms on soil-mantled hillslopes, *Geology*, 29, 683-686, 2001.

Buleka, J., Prior, D., and Van der Spek, A., *COASTPLAN geology and natural hazards of Lae City and surroundings, Papua New Guinea*. CCOP COASTPLAN Case Study Report No. 3, Geological Survey Division, Department of Mineral Resources, Papua New Guinea and Committee for Coordinating Geoscience Programmes in East and Southeast Asia, 1999.

Chappell, J., Ota, Y. and Berryman, K., Late Quarternary Co-seismic Uplift History of Huon Peninsula, Papua New Guinea, *Quarternary Science Reviews*, 15, 7-22, 1996.

Coleman, P., Australia and the Melanesian Arcs: A review of the tectonic settings, *Journal of Australian Geology and Geophysics*, AGSO, 17, 113-125, 1997.

Cooke, R., Cooke-Ravian Volume of Volcanological Papers, *Geological Survey Of Papua New Guinea Memoir 10*, 115-123, 1981.

Cooper, P. and Taylor, B., Seismotectonics of New Guinea; A model for arc reversal following arc-continent collision, *Tectonics*, 6, 53-67, 1987.

Crook, K., Quaternary uplift rates at a plate boundary, Lae urban area, Papua New Guinea, *Tectonophysics*, 163, 105-118, 1989.

Crowhurst, P., Hill, K., Foster, D., and Bennett, A., Thermochronology and geochemical constraints on the tectonic evolution of northern Papua New Guinea, In; *Tectonic Evolution of Southeastern Asia* (Eds. Hall, R. and Blundell, D.,) 525-537, Geological Society of London Special Publication, 1996.

Curley, R., Practical Procedures for Implementing GPS and PNG94 in the year 2000, *Proceedings from Association of Surveyors of Papua New Guinea, 34th Annual Survey Congress, Port Moresby, 8-10th July* 1999.

Curtis, J., Plate tectonics in the Papua New Guinea-Solomon Islands region, *Journal of the Geological Society of Australia,* 20, 21-35, 1973.

Davies, H., Symonds, P., and Ripper, I., Structure and evolution of the southern Solomon Sea region, *BMR Journal of Australian Geology and Geophysics*, 9, 49-68, 1984.

Davies, H., Lock, J., Tiffin, D., Honza, E., Okuda, Y., Murakami, F., and Kisimoto, K., Convergent tectonics in the Huon Peninsula region, Papua New Guinea, *Geo-Marine Letters*, 7, 143-152, 1987.

Davies, H., *The 1994 Eruption of Rabaul Volcano - A Case Study in Disaster Management*, University of Papua New Guinea, Port Moresby, 1995.

Davies, H., Sissano tsunami: A reconstruction of the events of July 17, 1998, based upon interviews with survivors. *1998 Fall Meeting American Geophysical Union, Supplement to EOS*, Transactions AGU 79(45) p.F572, 1998.

Dawson, J., Govind, R., and Manning, J., The AUSPOS Online GPS Processing System, *Proceedings from The Australian Surveyors Congress, Brisbane*, 25-28 September 2001.

DeMets, C., Gordon, R., Argus D. and Stein, S., Current Plate Motions, *Geophysical Journal International*, 101, 1990.

DeMets, C., Gordon, R., Argus, D., and Stein, S., Effect of recent revisions to the geomagnetic reversal timescale on estimates of current plate motion, *Geophysical Research Letters*, 21, 2191-2194, 1994.

Denham, D., Distribution of earthquakes in the New Guinea-Solomon Islands region, *Journal of Geophysical Research*, 74, 4290-4299, 1969.

Done, P., Development-related survey work in Papua New Guinea, *Survey Review*, 27, 212, 1984.

Dong, D., Herring, T., and King, R., Estimating regional deformation from a combination of space and terrestrial geodetic data, *Journal of Geodesy*, 72, 200-214, 1998

Dong, D., Fang, P., Bock, Y., Cheng, M., and Miyazaki, S., Anatomy of apparent seasonal variations from GPS-derived site position time series, *Journal of Geophysical Research*, 107, B4, ETG 9-1 - ETG 9-16, 2002

Dow, D., A geological synthesis of Papua New Guinea, *Bureau of Mineral Resources Bulletin* 201, 1-41, 1977.

Feigl, K., Agnew, D., Bock, Y., Dong, D., Donnellan, A., Hager, B., Herring, T., Jackson, D., Jordan, T., King, R., Larsen, S., Larson, K., Murray, M., Shen, Z., and Webb, F., Space Geodetic Measurement of Crustal Deformation in Central and Southern California, 1984-1992, *Journal of Geophysical Research*, 98, 21,677-21,712, 1993.

Goodliffe, A., Taylor, B., Martinez, F., Hey, R., Maeda, K., Ohno, K., Synchronous reorientation of the Woodlark basin spreading center, *Earth and Planetary Science Letters*, 146, 233-242, 1997.

Grant, D., and Pearse, M., Proposal for a Dynamic National Geodetic Datum for New Zealand, *Proceedings from IUGG XXI General Assembly*, Boulder, Colorado, July 2-14, 1995.

Grant, D., *A Proposal for Geodetic Datum Development*, OSG TR2.1, Land Information New Zealand (LINZ), 1998.

Grant, D., Blick, G., Pearse, M., Beavan, R., and Morgan, P., The development and implementation of New Zealand Geodetic Datum 2000, *Proceedings from IUGG XXII General Assembly*, Birmingham, UK, July 18-30, 1999.

Hamilton, W., Tectonics of the Indonesian region, *United States Geological Survey Professional Paper, 1078*, 1-345, 1979.

Herring, T., *GLOBK, Global Kalman filter VLBI and GPS analysis program Version 10.0*, Massachusetts Institute of Technology, 2002

Hill, K., and Raza, A., Arc-continent collision in Papua Guinea (*sic*.): Constraints from fission track thermochronology, *Tectonics*, 18, 950-966, 1999.

Hofmann-Wellenhof, B., Lichtenegger, H. and Collins, J., *Global Positioning System, Theory and Practice*, 5th Edition, Springer-Verlag, 2001.

Honza, E., Davies, H., Keene, J. and Tiffin, D., Plate Boundaries and Evolution of the Solomon Sea Region, *Geo-Marine Letters*, 7, 161-168, 1987.

Intergovernmental Committee on Surveying and Mapping (ICSM), *The Australasian Geodetic Infrastructure: 10 Years and Beyond, Discussion Paper,* version 2.2.1, 2000.

Intergovernmental Committee on Surveying and Mapping (ICSM), Standards and Practices for Control Surveys (SP1), Version 1.5, 2002.

Jaques, A., and Robinson, G., The continent/island-arc collision in northern Papua New Guinea, *BMR Journal of Australian Geology & Geophysics*, 2, 289-303, 1977.

Jenkins, D., Detachment tectonics in western Papua New Guinea, *Geological Society of America Bulletin*, 85, 533-548, 1974.

Johnson, R., Geotectonics and volcanism in Papua New Guinea: a review of the late Cainozoic, *BMR Journal of Australian Geology & Geophysics*, 4, 181-207, 1979.

Johnson, T., and Molnar, P., Focal Mechanisms and Plate Tectonics of the Southwest Pacific, *Journal of Geophysical Research*, 77, 5000-5032, 1972.

Johnson, H., and Agnew, D., *Correlated noise in geodetic time series, June 1, 1997-May 31, 1999,* final technical report to USGS, IGPP & UCSD, 2000.

Kearsley, W., and Ahmad, Z., *Report on the Geoid Computation for Papua New Guinea*, Australian Component of the Land Management Project for Papua New Guinea, 1996.

King, R., and Bock, Y., *Documentation for the GAMIT GPS anaylsis software, Release 10.0,* Massachusetts Institute of Technology, Scripps Institution of Oceanography, Cambridge, 2000.

Kroenke L., *Cenozoic Development of the Southwest Pacific*. UN ESCAP, CCOP/SOPAC Technical Bulletin, 6., 1984.

Kulig, C., McCaffrey, R., Abers, G., and Letz, H., Shallow seismicity of arc-continent collision near Lae, Papua New Guinea, *Tectonophysics*, 227, 81-93, 1993.

Langbein, J., and Johnson, H., Correlated errors in geodetic time series: Implications for time-dependent deformation, *Journal of Geophysical Research*, 102, B1, 591-603, 1997.

Lee, L., *First-Order Geodetic Triangulation of New Zealand 1909-49 and 1973-74. Technical Series No.1,* Dept. Lands and Survey, New Zealand, 1978.

Lus, W., McDougall, I., and Davies, H., Emplacement age of the Papuan Ultramafic Belt Ophiolite: constraints from K-Ar and $^{40}Ar/^{39}Ar$ geochronology from hornblende granulites at the base of the ophiolite near the Musa-Kumusi divide. *In Geological Society of Australia Abstracts No. 49,* 1998.

Ma, C., Arias, E., Eubanks, T, Fey, A., Gontier, A.-M., Jacobs, C., Sovers, O., Archinal, B., and Charlot, P., The International Celestial Reference Frame as realized by Very Long Baseline Interferometry, *The Astronomical Journal, 116*, 516-546, 1998.

McCaffrey, R., Crustal block rotations and plate coupling, in *Plate Boundary Zones*, S. Stein and J. Freymueller, editors, AGU Geodynamics Series 30, 101-122, 2002.

McClusky, S., Mobbs, K., Stolz, A., Barsby, D., Loratung, W., Lambeck, K., and Morgan, P., The Papua New Guinea satellite crustal motion surveys, *The Australian Surveyor*, 39, 194–214, 1994.

Madsen J., and Lindley, I., Large-scale structures on Gazelle Pensinsula, New Britain: Implications for the evolution of the New Britain Arc, *Australian Journal of Earth Sciences*, 41, 561-569, 1994.

Manning, J., and Steed, J., *Positional Accuracy, a Spatial Data Foundation, International Symposium on Spatial Data Infrastructure (SDI)*, University of Melbourne, 19-20 November 2001.

Mao, A., Harrison, C., and Dixon, T., Noise in GPS coordinate time series, *Journal of Geophysical Research,* 104, 2797-2816, 1999.

Martinez, F., and Taylor, B., Backarc Spreading, Rifting, and Microplate Rotation, Between Transform Faults in the Manus Basin, *Marine Geophysical Researches*, 18, 203-224, 1996.

Milsom, J., Woodlark Basin, A minor center of seafloor spreading in Melanesia, *Journal of Geophysical. Research*, 75, 7335-7339, 1970.

Minster, J., Jordan, T., Molnar, P., and Haines, E., Numerical Modelling of Instantaneous Plate Tectonics, *Geophysical Journal of the Royal Astronomical Society*, 36, 541-576, 1974.

Mobbs, K., *Tectonic interpretation of the Papua New Guinea region from repeat satellite measurements*, Unisurv Report S-48, University if New South Wales, 1997.

Morgan, P., Simulation studies for crustal motion monitoring by Doppler in Papua New Guinea, *Australian Journal of Geodesy, Photogrammetry and Surveying*, 35, 1562, 1981.

Morgan P., Bock, Y., Coleman, R., Feng, P., Garrard, D., Johnston, G., Luton, G., McDowall, B., Pearse, M., Rizos, C., and Tiesler, R., *A Zero Order GPS Network for the Australian Region*, University of Canberra, 1996 (also printed as University of New South Wales, School of Geomatic Engineering, Unisurv S-46, 1996)

Morgan P., and Pearse, M., *A First-Order Network for New Zealand*, Unisurv S-56, University of New South Wales, 1999.

Mori, J., The New Ireland Earthquake of July 3, 1985 and associated seismicity near the Pacific-Solomon Sea-Bismarck Sea triple junction, *Phys. Earth Planet. Int.*, 55, 144-153, 1989

Müller, R., Gaina, C., and Clarke, S., Seafloor spreading around Australia, In: J. Veevers (ed), *Billion-year earth history of Australia and neighbours in Gondwanaland – BYEHA*. p. 18-28, 2000.

Okada, Y., Surface Deformation due to Shear and Tensile Faults in a Half-space, *Bulletin of the Seismological Society of America*, 75, 4, 1135-1154, 1985.

Papua New Guinea, *Survey Directions*, Surveyor General's Department, Department of Lands, Independent State of Papua New Guinea, 1990.

Pearse, M., Realisation of the New Zealand Geodetic Datum 2000, *OSG Technical Report 5*, Land Information New Zealand, 2000.

Pegler, G., Das, S. and Woodhouse, J., A seismological study of the eastern New Guinea and the western Solomon Sea regions and its tectonic implications, *Geophysical Journal International*, 122, 961-981, 1995.

Pigram, C., and Panggabean, H., Rifting of the northern margin of the Australian continent and the origin of some microcontinents in eastern Indonesia, *Tectonophysics*, 107, 331-353, 1984.

Pigram, C. and Davies, H., Terranes and the accretion history of the New Guinea orogen, *BMR Journal of Australian Geology & Geophysics*, 10, 193-211, 1987.

Ripper, I., and McCue, K., The seismic zone of the Papuan fold belt, *Journal of Australian Geology and Geophysics*, 8, 147-156, 1983.

Rosa, R., *Status Report on geodetic Activities of Papua New Guinea, Proceedings from PCGIAP Working Group 1* – Second Workshop on Regional Geodetic Network, Ho Chi Minh City, 12th-13th July 1999.

Sella, G., Dixon, T., and Mao, A., REVEL: A model for recent plate velocities from space geodesy, *Journal of Geophysical Research*, 107(B4), 2081, 2002.

Silver, E., Abbott, L., Kirchoff-Stein, K., Reed, D. and Bernstein-Taylor, B., Collision Propagation in Papua New Guinea and the Solomon Sea, *Tectonics*, 10, 863-874, 1991.

Sloane, B., and Steed, J., *Crustal Movement survey, Markham Valley – Papua New Guinea, Technical Report 23,* Department of Natural Resources, Division of National Mapping, Australia, 1976a.

Sloane, B., and Steed, J., *Crustal Movement survey, St. Georges Channel – Papua New Guinea, Technical Report 24,* Department of Natural Resources, Division of National Mapping, Australia, 1976b.

Snay, R., Using HTDP Software to Transform Spatial Coordinates Across Time and Between Reference Frames, *Surveying and Land Information Systems*, 59,1,15-25, 1999.

Stevens, C., McCaffrey, R., Silver, E., Sombo, Z., English, P., and Van der Keive, J., Mid-crustal detachment and ramp faulting in the Markham Valley, Papua New Guinea, *Geology*, 26, 847–850, 1998.

Stolz, A., *Monitoring crustal motion in Papua New Guinea using the Global Positioning System*, Association of Surveyors, Papua New Guinea, 24th Survey Congress, Port Moresby, 26th-28th June 1989.

Sun, W., Okubo, S., and Vanicek, P., Global displacement caused by dislocation in a realistic earth model, *Journal of Geophysical Research*, 101, 8561-8577, 1996.

Taylor, B., Bismarck Sea: Evolution of a back-arc basin, *Geology*, 7, 171-174, 1979.

Taylor, B., Goodliffe, A., Martinez, F., and Hey, R., Continental rifting and initial sea-floor spreading in the Woodlark Basin. *Nature,* 374:534-537, 1995.

Taylor, B., Goodliffe, A., and Martinez, F., How continents break up: Insights from Papua New Guinea, *Journal of Geophysical Research*, 104, 7497-7512, 1999.

Torge, W., *Geodesy*, Third Edition. W. de Gruyter, Berlin, New York, 2001.

Tregoning, P., Lambeck, K., Stolz, A., Morgan, P., McClusky, S., van der Beek, P., McQueen, H., Jackson, R., Little, R., Laing, A., and Murphy, B., Estimation of current plate motions in Papua New Guinea from Global Positioning System observations, *Journal of Geophysical Research*, 103, 12,181–12,203, 1998.

Tregoning, P., and Jackson, R., The Need for Dynamic Datums, *Geomatics Research Australasia*, 71, 87-102, 1999.

Tregoning, P., and McQueen, H., *PNGVEL Tectonic Motion Program*, ANU, 1999.

Tregoning, P., Jackson, R., McQueen, H., Lambeck, K., Stevens, C., Little, R., Curley, R. and Rosa, R., Motion of the South Bismarck Plate, Papua New Guinea, *Geophysical Research Letters*, 26, 3517–3520, 1999.

Tregoning, P., McQueen, H., Lambeck, K., Jackson, R., Little. R, Saunders, S. and Rosa, R., Present-day crustal motion in Papua New Guinea, *Earth Planets Space*, 52, 727-730, 2000.

Tregoning, P., H. McQueen, Resolving slip-vector azimuths and plate motion along the southern boundary of the South Bismarck Plate, Papua New Guinea, *Australian Journal of Earth Sciences*, **48**, 745-750, 2001.

Tregoning, P., Plate kinematics in the western Pacific derived from geodetic observations, *Journal of Geophysical Research*, 107, B1, 10.1029/2001JB000406, 2002.

Tregoning, P., Is the Australian Plate Deforming? A space geodetic perspective, Joint Special Publication *Geological Society of Australia and Geological Society of America Monograph*, in press, 2003.

Turcotte, D. and Schubert, G., *Geodynamics*, 2nd Edition, Cambridge University Press, 2001.

United States Air Force (USAF), *Geodesy for the Layman*, National Imagery and Mapping Agency, United States of America, 1959. (also http://earth-info.nima.mil/GandG/geolay/toc.htm)

Veeh, H., and Chappell, J., Astronomical theory of climate change: support from New Guinea. *Science*, 167, 862–865, 1970.

Veevers J. Change of tectono-stratigraphic regime in the Australian plate during the 99 Ma (mid-Cretaceous) and 43 Ma (mid-Eocene) swerves of the Pacific. *Geology* 28, 47-50, 2000

Wallace, L., Tectonics and arc-continent collision in Papua New Guinea: Insights from geodetic, geophysical and geologic data. 244 pp., *PhD Thesis*, University of California, Santa Cruz, 2002.

Wallace, L., Stevens, C., Silver, E., McCaffrey, R., Stanaway, R., Loratung, W., Hasiata, S., Curley, R., Rosa, R., and Taugaloidi, J., GPS constraints on active tectonics and arc-continent collision in Papua New Guinea: implications for mechanics of microplate rotations in a plate boundary zone, *Journal of Geophysical Research*, in press, 2004.

Weiler,P. and Coe, R., Rotations in the actively colliding Finisterre Arc Terrane: paleomagnetic constraints on Plio-Pleistocene evolution of the South Bismarck microplate, northeastern Papua New Guinea, *Tectonophysics*, 316, 297-325, 2000

Weissel, J., and Watts, A., Tectonic evolution of the Coral Sea Basin, *Journal of Geophysical Research*, 84, 4572-4582, 1979.

Weissel, J., Taylor B., and Karner, G., The opening of the Woodlark Basin, subduction of the Woodlark spreading system and the evolution of northern Melanesia since mid-Pliocene time, *Tectonophysics,* 87:253-277, 1982.

Wessel, P. and Kroenke, L., Ontong Java Plateau and Late Neogene changes in Pacific plate motion, *Journal of Geophysical Research*, 105, 28255-28277, 2000.

Williams, S., The effect of coloured noise on the uncertainties of rates estimated from geodetic time series, *Journal of Geodesy*, 76, 483-494, 2003.

Williamson, P., Swift, M., O'Brien, G., and Falvey, D., Two-stage Cretaceous rifting of the Otway Basin margin of south-eastern Australia: implications for rifting of the Australian margin, *Geology*, 18, 75-78, 1990.

Wolf, P., and Ghilani, C., *Adjustment Computations*, Wiley, 1997.

Young, G. and Laurie, J., (eds) *An Australian Phanerozoic Timescale*. Oxford University Press, 279 pp., 1996 .

Zhang, J., Bock, Y., Johnson, H., Fang, P., Genrich, J., Williams, S., Wdowinski, S., and Behr, J., Southern California Permanent GPS Geodetic Array: Error analysis of daily position estimates and site velocities, *Journal of Geophysical Research*, 102, 18,035-18,055, 1997.

Appendix A
PNG ITRF2000 station coordinates and velocities

SITE ID	Number	X	Y	Z	σX	σY	σZ
9799	PSM 9799	-5313156.720	3450683.372	-736065.421	0.014	0.009	0.005
AIAM	PSM 9550	-4934886.677	3958248.497	-810300.776	0.008	0.004	0.005
ALT2	PSM 9538	-5453535.923	3105804.692	-1134062.348	0.018	0.016	0.013
AMAN	PSM 15286	-4962464.998	3987772.410	-396576.755	0.009	0.012	0.014
BOGI	BOGIA	-5208105.356	3651103.323	-474523.915	0.002	0.001	0.001
BUK1	PSM 4871	-5739291.205	2716749.722	-599127.878	0.011	0.008	0.009
BULO	BULOLO	-5285205.544	3481561.160	-794946.129	0.003	0.001	0.001
FINS	PSM 19471	-5364735.008	3371177.691	-729909.248	0.008	0.005	0.002
GOKA	PSM 9833	-5221573.552	3603226.422	-671386.767	0.005	0.004	0.001
HGEN	PSM 3419	-5154756.711	3703166.606	-643969.027	0.004	0.005	0.003
HOSK	PSM 9795	-5521270.312	3135397.013	-603596.614	0.004	0.004	0.007
KAVI	PSM 9513	-5562412.688	3107930.321	-285346.000	0.009	0.013	0.006
KERE	PSM 31703	-5223111.736	3553360.188	-877169.298	0.007	0.009	0.006
KIKO	PSM 5583	-5133225.893	3695553.549	-818611.999	0.006	0.006	0.006
KIUN	PSM 9465	-4948011.402	3967206.134	-676258.418	0.008	0.009	0.007
LAE1	PSM 31107	-5312857.081	3451108.025	-736322.751	0.002	0.001	0.001
MAD1	GS 15495	-5252527.447	3571989.551	-575482.494	0.003	0.002	0.001
MANU	PSM 9522	-5367596.150	3437943.634	-226704.782	0.007	0.005	0.002
MEND	PSM 3507	-5109574.970	3759378.735	-678236.196	0.022	0.020	0.012
MISI	PSM 9520	-5576759.466	2862000.948	-1175220.670	0.011	0.009	0.014
MORE	PSM 15832	-5288519.345	3409952.719	-1038573.992	0.004	0.002	0.002
MORX	MOROBE	-5334985.688	3388420.626	-856749.669	0.004	0.003	0.002
NADZ	ST 31024	-5297991.384	3476466.738	-724197.657	0.006	0.005	0.002
NING	AA 426	-4942681.153	3982281.923	-625676.664	0.009	0.006	0.004
NM34	NM/J/34	-5262950.564	3539058.507	-678565.061	0.008	0.007	0.005
POPN	PSM 9371	-5359876.799	3318934.538	-965986.257	0.015	0.014	0.008
RVO_	RVO	-5625350.005	2970460.107	-463019.178	0.008	0.007	0.012
TABU	PSM 9466	-4951875.859	3978535.259	-580618.756	0.012	0.010	0.005
TOKU	GS 9822	-5635232.639	2948609.446	-479565.061	0.009	0.005	0.008
VANI	PSM 63/1	-4972629.979	3983208.072	-296766.930	0.005	0.003	0.005
WEWK	PSM 15497	-5128211.419	3771635.303	-396055.590	0.003	0.004	0.002
WUVU	PSM 15456	-5080554.712	3851303.909	-191868.890	0.007	0.010	0.012

Table A.1 ITRF2000 Cartesian Coordinates at Epoch 2000.0 from this analysis (metres)

SITE ID	Number	VX	VY	VZ	σVX	σVY	σVZ
9799	PSM 9799	-0.0173	-0.0192	0.0518	0.0008	0.0006	0.0005
AIAM	PSM 9550	-0.0289	-0.0243	0.0575	0.0012	0.0008	0.0007
ALT2	PSM 9538	-0.0241	-0.0216	0.0566	0.0014	0.0010	0.0039
AMAN	PSM 15286	-0.0201	-0.0201	0.0495	0.0010	0.0011	0.0013
BOGI	BOGIA	-0.0108	-0.0241	0.0427	0.0017	0.0014	0.0009
BUK1	PSM 4871	0.0228	0.0548	0.0305	0.0009	0.0017	0.0011
BULO	BULOLO	-0.0191	-0.0169	0.0592	0.0019	0.0008	0.0008
FINS	PSM 19471	0.0004	0.0069	0.0037	0.0053	0.0031	0.0013
GOKA	PSM 9833	-0.0325	-0.0056	0.0433	0.0040	0.0029	0.0007
HGEN	PSM 3419	-0.0242	-0.0194	0.0479	0.0008	0.0010	0.0008
HOSK	PSM 9795	-0.0085	-0.0202	-0.0271	0.0012	0.0014	0.0040
KAVI	PSM 9513	0.0317	0.0592	0.0271	0.0022	0.0038	0.0020
KERE	PSM 31703	-0.0229	-0.0209	0.0516	0.0019	0.0023	0.0020
KIKO	PSM 5583	-0.0237	-0.0210	0.0534	0.0020	0.0023	0.0020
KIUN	PSM 9465	-0.0281	-0.0256	0.0554	0.0015	0.0017	0.0007
LAE1	PSM 31107	-0.0173	-0.0192	0.0518	0.0008	0.0006	0.0005
MAD1	GS 15495	-0.0130	-0.0188	0.0391	0.0012	0.0008	0.0006
MANU	PSM 9522	0.0417	0.0508	0.0276	0.0024	0.0019	0.0008
MEND	PSM 3507	-0.0210	-0.0201	0.0467	0.0033	0.0038	0.0040
MISI	PSM 9520	-0.0226	-0.0218	0.0544	0.0016	0.0018	0.0034
MORE	PSM 15832	-0.0100	-0.0265	0.0549	0.0020	0.0011	0.0008
MORX	MOROBE	-0.0183	-0.0137	0.0563	0.0037	0.0026	0.0019
NADZ	ST 31024	-0.0219	-0.0148	0.0548	0.0043	0.0034	0.0012
NING	AA 426	-0.0258	-0.0235	0.0539	0.0011	0.0010	0.0025
NM34	NM/J/34	-0.0187	-0.0188	0.0467	0.0017	0.0016	0.0018
POPN	PSM 9371	-0.0195	-0.0159	0.0535	0.0030	0.0030	0.0060
RVO_	RVO	0.0046	-0.0098	-0.0512	0.0032	0.0028	0.0077
TABU	PSM 9466	-0.0266	-0.0248	0.0563	0.0022	0.0021	0.0050
TOKU	GS 9822	0.0194	0.0009	-0.0343	0.0029	0.0023	0.0014
VANI	PSM 63/1	-0.0098	-0.0088	0.0448	0.0019	0.0023	0.0005
WEWK	PSM 15497	-0.0176	-0.0083	0.0522	0.0026	0.0038	0.0015
WUVU	PSM 15456	0.0404	0.0542	0.0191	0.0016	0.0021	0.0010

Table A.2 ITRF2000 Cartesian Coordinate velocities from this analysis (m/yr)

SITE ID	Number	Latitude	Longitude	Ht	σLat (m)	σLong (m)	σHt (m)
9799	PSM 9799	-6°40'16.96051"	146°59'52.38039"	130.296	0.004	0.015	0.007
AIAM	PSM 9550	-7°20'51.80924"	141°16'01.45427"	95.515	0.004	0.008	0.008
ALT2	PSM 9538	-10°18'37.49814"	150°20'18.09726"	94.869	0.011	0.023	0.010
AMAN	PSM 15286	-3°35'18.77145"	141°12'54.33638"	477.320	0.014	0.015	0.007
BOGI	BOGIA	-4°17'43.22167"	144°58'04.47852"	76.492	0.001	0.002	0.008
BUK1	PSM 4871	-5°25'34.36523"	154°40'08.42577"	73.247	0.008	0.012	0.007
BULO	BULOLO	-7°12'25.02367"	146°37'32.23155"	802.059	0.001	0.002	0.009
FINS	PSM 19471	-6°36'55.42008"	147°51'17.68560"	74.253	0.002	0.008	0.009
GOKA	PSM 9833	-6°04'53.06284"	145°23'30.45147"	1664.588	0.001	0.006	0.009
HGEN	PSM 3419	-5°49'55.74967"	144°18'23.80062"	1710.166	0.003	0.006	0.007
HOSK	PSM 9795	-5°28'00.41257"	150°24'31.66565"	101.354	0.007	0.005	0.008
KAVI	PSM 9513	-2°34'53.06067"	150°48'22.52305"	78.806	0.006	0.016	0.011
KERE	PSM 31703	-7°57'28.00896"	145°46'19.07848"	97.573	0.006	0.011	0.008
KIKO	PSM 5583	-7°25'24.64257"	144°14'55.77376"	88.925	0.006	0.008	0.006
KIUN	PSM 9465	-6°07'37.96966"	141°16'41.27693"	103.266	0.007	0.012	0.007
LAE1	PSM 31107	-6°40'25.35597"	146°59'35.47182"	140.357	0.001	0.002	0.003
MAD1	GS 15495	-5°12'41.28152"	145°46'56.19840"	73.250	0.001	0.003	0.006
MANU	PSM 9522	-2°03'02.28907"	147°21'37.62357"	129.715	0.002	0.008	0.008
MEND	PSM 3507	-6°08'36.72524"	143°39'22.17141"	1815.076	0.011	0.029	0.007
MISI	PSM 9520	-10°41'19.89416"	152°49'58.94544"	87.461	0.013	0.013	0.008
MORE	PSM 15832	-9°26'02.75921"	147°11'12.20709"	116.654	0.002	0.004	0.005
MORX	MOROBE	-7°46'16.83073"	147°34'44.61398"	141.250	0.002	0.005	0.006
NADZ	ST 31024	-6°33'47.97704"	146°43'39.65887"	148.856	0.002	0.007	0.007
NING	AA 426	-5°40'02.39111"	141°08'30.70308"	168.091	0.004	0.010	0.008
NM34	NM/J/34	-6°08'52.06469"	146°04'52.44729"	509.976	0.005	0.010	0.011
POPN	PSM 9371	-8°46'09.63936"	148°14'00.40129"	187.534	0.007	0.020	0.007
RVO_	RVO	-4°11'27.20155"	152°09'49.51208"	266.208	0.012	0.010	0.009
TABU	PSM 9466	-5°15'27.39439"	141°13'12.75969"	672.233	0.005	0.015	0.010
TOKU	GS 9822	-4°20'27.79014"	152°22'45.81956"	81.964	0.008	0.009	0.006
VANI	PSM 63/1	-2°41'05.27313"	141°18'15.65875"	80.589	0.005	0.005	0.005
WEWK	PSM 15497	-3°35'02.57446"	143°40'00.15138"	83.942	0.002	0.005	0.007
WUVU	PSM 15456	-1°44'07.59138"	142°50'10.06493"	79.032	0.012	0.012	0.008

Table A.3 ITRF2000 Ellipsoidal Coordinates at Epoch 2000.0 from this analysis

SITE ID	Number	VN	VE	σVN	σVE
9799	PSM 9799	0.0519	0.0255	0.0005	0.0009
AIAM	PSM 9550	0.0580	0.0370	0.0006	0.0014
ALT2	PSM 9538	0.0575	0.0307	0.0037	0.0015
AMAN	PSM 15286	0.0496	0.0283	0.0013	0.0015
BOGI	BOGIA	0.0422	0.0259	0.0009	0.0021
BUK1	PSM 4871	0.0306	-0.0593	0.0011	0.0019
BULO	BULOLO	0.0596	0.0246	0.0006	0.0017
FINS	PSM 19471	0.0041	-0.0061	0.0010	0.0054
GOKA	PSM 9833	0.0455	0.0231	0.0005	0.0047
HGEN	PSM 3419	0.0484	0.0299	0.0008	0.0013
HOSK	PSM 9795	-0.0272	0.0218	0.0039	0.0018
KAVI	PSM 9513	0.0271	-0.0671	0.0020	0.0044
KERE	PSM 31703	0.0521	0.0301	0.0019	0.0030
KIKO	PSM 5583	0.0538	0.0309	0.0019	0.0030
KIUN	PSM 9465	0.0557	0.0375	0.0007	0.0023
LAE1	PSM 31107	0.0519	0.0255	0.0005	0.0009
MAD1	GS 15495	0.0390	0.0229	0.0005	0.0013
MANU	PSM 9522	0.0273	-0.0653	0.0008	0.0029
MEND	PSM 3507	0.0470	0.0286	0.0039	0.0050
MISI	PSM 9520	0.0553	0.0297	0.0033	0.0023
MORE	PSM 15832	0.0532	0.0277	0.0006	0.0020
MORX	MOROBE	0.0569	0.0214	0.0016	0.0042
NADZ	ST 31024	0.0556	0.0244	0.0010	0.0052
NING	AA 426	0.0542	0.0345	0.0025	0.0015
NM34	NM/J/34	0.0470	0.0260	0.0017	0.0023
POPN	PSM 9371	0.0541	0.0238	0.0058	0.0041
RVO_	RVO	-0.0517	0.0066	0.0076	0.0040
TABU	PSM 9466	0.0565	0.0360	0.0049	0.0030
TOKU	GS 9822	-0.0355	-0.0098	0.0013	0.0034
VANI	PSM 63/1	0.0448	0.0130	0.0005	0.0030
WEWK	PSM 15497	0.0527	0.0171	0.0015	0.0046
WUVU	PSM 15456	0.0191	-0.0676	0.0010	0.0026

Table A.4 ITRF2000 Horizontal site velocities from this analysis (m/yr)

SITE ID	Number	X	Y	Z	σX	σY	σZ
4472	PSM 14472	-5311609.717	3451573.163	-742534.181	0.016	0.038	0.017
BUBI	ST 31021	-5308046.978	3458567.729	-735726.891	0.003	0.003	0.002
HOBU	ST 31028	-5316641.808	3448467.748	-724722.078	0.007	0.006	0.003
LAE1	PSM 31107	-5312857.081	3451108.025	-736322.751	0.002	0.001	0.001
NADZ	ST 31024	-5297991.384	3476466.738	-724197.657	0.006	0.005	0.002
OMSI	ST 31025	-5302978.811	3466197.473	-736283.187	0.001	0.016	0.004
POSI	POSIE	-5315041.299	3448980.884	-731432.588	0.027	0.019	0.006
SITU	ST 31029	-5316947.957	3445548.683	-733099.926	0.004	0.002	0.002
YALU	ST 31027	-5306004.034	3463261.438	-728440.463	0.005	0.003	0.002

Table A.5 Lae Network ITRF2000 Cartesian Coordinates at Epoch 2000.0 from this analysis (m)

SITE ID	Number	VX	VY	VZ	σVX	σVY	σVZ
4472	PSM 14472	-5311609.717	3451573.163	-742534.181	0.016	0.038	0.017
BUBI	ST 31021	-0.0156	-0.0160	0.0506	0.0018	0.0018	0.0014
HOBU	ST 31028	-0.0076	-0.0041	0.0420	0.0043	0.0042	0.0017
LAE1	PSM 31107	-0.0173	-0.0192	0.0518	0.0008	0.0006	0.0005
NADZ	ST 31024	-0.0219	-0.0148	0.0548	0.0043	0.0034	0.0012
OMSI	ST 31025	-0.0168	-0.0206	0.0531	0.0003	0.0064	0.0015
POSI	POSIE	0.0086	-0.0357	0.0509	0.0147	0.0104	0.0036
SITU	ST 31029	-0.0144	-0.0166	0.0506	0.0020	0.0012	0.0012
YALU	ST 31027	-0.0152	-0.0173	0.0489	0.0027	0.0018	0.0013

Table A.6 Lae Network ITRF2000 Cartesian Coordinate velocities from this analysis (m/yr)

SITE ID	Number	Latitude	Longitude	Ht	σLat (m)	σLong (m)	σHt (m)
4472	PSM 14472	-6°43'49.18156"	146°59'0.64513"	78.104	0.018	0.041	0.005
BUBI	ST 31021	-6°40'05.95446"	146°54'46.49045"	106.920	0.002	0.004	0.001
HOBU	ST 31028	-6°34'03.73861"	147°01'54.64553"	528.335	0.003	0.009	0.003
LAE1	PSM 31107	-6°40'25.35597"	146°59'35.47182"	140.357	0.001	0.002	0.001
NADZ	ST 31024	-6°33'47.97704"	146°43'39.65887"	148.856	0.002	0.007	0.002
OMSI	ST 31025	-6°40'24.22242"	146°49'48.28210"	97.523	0.005	0.014	0.007
POSI	POSIE	-6°37'44.70316"	147°01'12.27735"	243.063	0.005	0.031	0.013
SITU	ST 31029	-6°38'39.62144"	147°03'19.79871"	169.888	0.002	0.004	0.002
YALU	ST 31027	-6°36'07.14532"	146°52'02.16649"	111.991	0.002	0.005	0.003

Table A.7 Lae Network ITRF2000 Ellipsoidal Coordinates at Epoch 2000.0 from this analysis

SITE ID	Number	VN	VE	σVN	σVE
4472	PSM 14472	0.0519	0.0330	0.0104	0.0243
BUBI	ST 31021	0.0507	0.0220	0.0013	0.0025
HOBU	ST 31028	0.0421	0.0073	0.0015	0.0060
LAE1	PSM 31107	0.0519	0.0255	0.0005	0.0009
NADZ	ST 31024	0.0556	0.0243	0.0010	0.0052
OMSI	ST 31025	0.0531	0.0264	0.0019	0.0055
POSI	POSIE	0.0475	0.0251	0.0028	0.0169
SITU	ST 31029	0.0506	0.0218	0.0011	0.0021
YALU	ST 31027	0.0489	0.0227	0.0011	0.0030

Table A.8 Lae Network ITRF2000 Horizontal site velocities from this analysis (m/yr)

Appendix B
Bounding coordinates of Tectonic Blocks in PNG

@ Papua New Guinea Plate File in 4DADJ
@ List is in the following order
@ 1 Plate number
@ 2 Plate Name
@ 3 Absolute Euler Pole Latitude decimal degrees
@ 4 Absolute Euler Pole Longitude decimal degrees
@ 5 Absolute Euler Pole rotation degs/Ma
@ 6 Pole semi-major axis standard error ellipse decimal degrees
@ 7 Pole semi-minor axis standard error ellipse decimal degrees
@ 8 Pole semi-major axis azimuth degrees
@ 9 Pole rotation sigma dec.degs/Ma
@ 10 vertices of plate polygon { lat1 long1 lat2 long2 .... latn-1 longn-1 }

{{ 1 "AUS" 32.76 37.54 0.621 0.40 0.13 109 0.002
{ -12 140.5 -4.7 140.5 -5.7 142 -6.3 142.7 -6.8 143.6 -7 144.6 -7.3 145 -8 145.4
-10.4 147.7 -9.8 149 -9.82 150.12 -10.13 150.86 -9.75 151 -9.8 151.68 -9.82 151.88
-9.92 151.84 -10.12 152.88 -10.4 152.88 -10.36 154.2 -9.92 154.24 -9.28 156.48 -7.7 155.4
-10 160 -12 160 }}
{{ 2 "NGH" 3.94 127.59 1.54 2.7 3.5 138.6 0.22
{ -4.7 140.5 -3.2 140.5 -4.1 144.1 -5.35 145.13 -5.71 145.65 -6.138 146.086 -6.415 146.425
-6.53 146.72 -6.598 147.026 -6.83 147.47 -6.9 146.4 -7.4 146.7 -7.6 147 -8.6 147.9 -9 148
-9.7 148.5 -9.8 149 -10.4 147.7 -8 145.4 -7.3 145 -7 144.6 -6.8 143.6 -6.3 142.7 -5.7 142 }}
{{ 3 "SPK" 3.94 127.59 1.54 2.7 3.5 138.6 0.22
{ -3.2 140.5 -2.4 140.5 -2.5 142 -2.8 142.6 -3 143.55 -3.3 143.92 -4.1 144.1 }}
{{ 4 "ADL" 6.73 328.54 5.73 1.04 0.76 83 0.61
{ -4.1 144.1 -3.3 143.92 -3.3 146.9 -4.9 145.72 -5.35 145.13 }}
{{ 5 "SBIS" -6.75 147.98 8.11 0.1 0.06 4 0.16
{ -5.35 145.13 -4.9 145.72 -3.3 146.9 -2.9 147.8 -3.45 149.07 -3.58 149.8 -5 151.8 -5.7 152.8
-6 152.1 -6.9 150.7 -7.1 149.25 -7 148 -6.83 147.47 -6.598 147.026 -6.53 146.72 -6.415 146.425
-6.138 146.086 -5.71 145.65 }}
{{ 6 "WDL" -3.98 136.5 2.67 1.16 0.80 129 0.16
{ -6.83 147.47 -7 148 -7.1 149.25 -6.9 150.7 -6 152.1 -5.7 152.8 -5.9 153.6 -6.3 153.9 -7.7 155.4
-9.28 156.48 -9.92 154.24 -10.36 154.2 -10.4 152.88 -10.12 152.88 -9.92 151.84 -9.82 151.88
-9.8 151.68 -9.75 151 -10.13 150.86 -9.82 150.12 -9.8 149 -9.7 148.5 -9 148 -8.6 147.9 -7.6
147 -7.4 146.7 -6.9 146.4 }}
{{ 7 "GAZ" -6.75 147.98 8.11 0.1 0.06 4 0.16
{ -3.58 149.8 -3.05 150.53 -3.8 151.5 -3.58 152 -4.2 152.672 -4.419 152.883
-4.622 153.033 -5.8 153.7 -6.3 153.9 -5.9 153.6 -5.7 152.8 -5 151.8 }}
{{ 8 "NBIS" -45 126.4 0.85 5.5 0.5 36 0.07
{ -2.5 142 -1.3 142 -0.8 143.4 -0.3 146.5 -0.3 149 -0.7 149.5 -1.2 152 -1.7 152.5 -2.8 153.8
-4.4 154.9 -5.1 155.2 -6.3 156.5 -8 160 -10 160 -7.7 155.4 -6.3 153.9 -5.8 153.7 -4.622 153.033
-4.419 152.883 -4.2 152.672 -3.58 152 -3.8 151.5 -3.05 150.53 -3.58 149.8
-3.45 149.07 -2.9 147.8 -3.3 146.9 -3.3 143.92 -3 143.55 -2.8 142.6 }}
{{ 9 "PAC" -63.75 110.86 0.677 0.61 0.15 85 0.002
{ -2.4 140.5 0 140.5 0 160 -8 160 -6.3 156.5 -5.1 155.2 -4.4 154.9 -2.8 153.8 -1.7 152.5
-1.2 152 -0.7 149.5 -0.3 149 -0.3 146.5 -0.8 143.4 -1.3 142 -2.5 142 }}
}

Appendix C
LINREG: RPL Source code

```
%%HP: T(3)A(D)F(.);
\<<
@ Program to compute geodetic datum
@ from timeseries XYZ

@ Text file of data series in same directory
@ epoch X Y Z sigmaX sigmaY sigmaZ in sets of 7 in file
@

@ control global variables
@ WEIGHT ( factor to multiply standard error
@ by default to 3 for GPS absolute coords )
@ EPOCH ( list of epochs to compute )

CLEAR

"File to process ?"
"" INPUT  DUP DUP ".OUT" +
\-> site outfil
\<<

OBJ\->

@ calculate number of records
DEPTH 7 /

@ calculate number of epochs to compute
EPOCH SIZE


@ create empty local variable list
{} {} {} {} {} {} {} {} {} {} {} {} {}
"
" 0
\-> n es wZ wY wX lZ lY lX am xZ xY xX vZ vY vX txt
a
\<<
@ Build observation lists
1 n FOR c
"Building
Observation lists
" c STD + "/" + n +
CLLCD 1 DISP

WEIGHT * SQ INV wZ + 'wZ' STO
WEIGHT * SQ INV wY + 'wY' STO
WEIGHT * SQ INV wX + 'wX' STO
lZ + 'lZ' STO
lY + 'lY' STO
lX + 'lX' STO

am 1 SWAP + + 'am' STO
NEXT


@ Build observation matrices
"Building Z
Observation matrix"
CLLCD 1 DISP
lZ OBJ\-> DROP n 1 2 \->LIST \->ARRY
'lZ' STO
"Building Y
Observation matrix"
CLLCD 1 DISP
lY OBJ\-> DROP n 1 2 \->LIST \->ARRY
'lY' STO
"Building X
Observation matrix"
CLLCD 1 DISP
lX OBJ\-> DROP n 1 2 \->LIST \->ARRY
'lX' STO
"Building Z
weight matrix"
CLLCD 1 DISP
wZ OBJ\-> DROP n 1 2 \->LIST \->ARRY n DIAG\->
'wZ' STO
"Building Y
weight matrix"
CLLCD 1 DISP
wY OBJ\-> DROP n 1 2 \->LIST \->ARRY n DIAG\->
'wY' STO
"Building X
weight matrix"
CLLCD 1 DISP

wX OBJ\-> DROP n 1 2 \->LIST \->ARRY n DIAG\->
'wX' STO


@ compute for each epoch
1 es FOR c

am

EPOCH c GET
\-> epo
\<<
"Computing Epoch
" epo 3 FIX +
CLLCD 1 DISP
epo 0
1 n 1 - START DUP2 NEXT
"Building epoch
matrix " epo +
CLLCD 1 DISP
n 2 * \->LIST
-
OBJ\-> DROP n 2 2 \->LIST \->ARRY

'a' STO

"Computing Z
epoch " epo +
CLLCD 1 DISP
```

```
@ compute parameters
a TRN wZ * a * INV
a TRN * wZ * lZ *
'xZ' STO

"Computing Y
epoch " epo +
CLLCD 1 DISP

@ compute parameters
a TRN wY * a * INV
a TRN * wY * lY *
'xY' STO

"Computing X
epoch " epo +
CLLCD 1 DISP

@ compute parameters
a TRN wX * a * INV
a TRN * wX * lX *
'xX' STO

"Building VCV Z
epoch " epo +
CLLCD 1 DISP

@ compute VCV Z
a xZ * lZ -
DUP TRN
wZ * SWAP *
n 2 - / OBJ\-> DROP
a TRN wZ * a * INV
*

xZ

OBJ\-> DROP
ROT OBJ\-> DROP
0.5 ^ SWAP DROP
SWAP DROP
SWAP 0.5 ^

"Building VCV Y
epoch " epo +
CLLCD 1 DISP

@ compute VCV Y
a xY * lY -
DUP TRN
wY * SWAP *
n 2 - / OBJ\-> DROP
a TRN wY * a * INV
*


xY

OBJ\-> DROP
ROT OBJ\-> DROP
0.5 ^ SWAP DROP
SWAP DROP
SWAP 0.5 ^

"Building VCV X
epoch " epo +
CLLCD 1 DISP

@ compute VCV X
a xX * lX -
DUP TRN
wX * SWAP *
n 2 - / OBJ\-> DROP
a TRN wX * a * INV
*

xX

OBJ\-> DROP
ROT OBJ\-> DROP
0.5 ^ SWAP DROP
SWAP DROP
SWAP 0.5 ^

\-> velz z sz svz vely y sy svy velx x sx svx
\<<
site " " + EPOCH c GET 3 FIX + " " +
3 FIX x + " " + y + " " + z + " " +
sx + " " + sy + " " + sz + " " +
4 FIX velx + " " + vely + " " + velz + " " +
svx + " " + svy + " " + svz + " " +
"
" + txt SWAP + 'txt' STO
\>>

\>>
NEXT
txt
"
" + 'txt' STO

txt 'OUTF' STO

 \>> \>> \>>
```

Appendix D
4DADJ: RPL Source code

GPSAN

```
%%HP:T(3)A(D)F(.);
\<<
@ Program to perform weighted least squares adjustment
@ of kinematic geocentric cartesian baseline network
@ using itrf cartesian coordinates and/or velocities for constraint stations
@ and eulerian kinematic model for free stations

@   Richard Stanaway
@   Research School of Earth Sciences,
@   The Australian National University
@   June 2003

@ BDAT is source baseline data ( from to DX DY DZ VarX CovXY CovXZ VarY CovYZ VarZ Epoch )
@ SDAT is source station data ( stn coordfix velfix X Y Z SX SY SZ VX VY VZ SVX SVY SVZ Epoch )

@ requires adjustment epoch in decimal years on level 1 of stack
@ if adjustment is for a static network adopt 0 for epoch

@ Set HP48 system flags
STD RECT -19 CF

@ create local variables

{ } { } { } { } { } { } { } 0 0 { } { } { } { } { } { } { } { } { } { } 0 { 0 0 0 0 0 0 }
{ } { } { } { } { } { } { } { } { } { } { } { } { } { } { } { } 0 0 TIME { } { } { } { } { } { } { }

\-> epoch bl bldat fr cn  flg f r w v from to slist clist acol a cols tmp tmp2
tmp3 tmp4 nm obs fid const vl vw sdev free rv x time sdlis fr1 fr2 cl2
vlist fvlist

\<<

@ bl is list of from/to baselines
@ fr is free stn (loose)
@ cn is connected stn
@ r is number of baseline observations
@ w is the weight matrix (in list format)
@ v is the baseline vector list (vectors embedded in list format)
@ from is the list of stations from the start of each baseline
@ to is the list of stations at the end of each of baseline
@ slist is the list of stations in the network
@ clist is the list of constraint stations in the network
@ acol is the list of unknown stations (un-constrained) in the network
@ a is the list of coefficients in the a matrix (by columns)
@ cols is the number of columns in the a matrix
@ tmp is a temp variable
@ nm is the normal matrix (in list format)
@ obs is the observation matrix (in list format)
@ fid is the list of constraint station coordinates
@ const is the constant matrix in list format
@ vl is residuals adjusted - observed of the baselines in list format
@ vw intermediate results v*w
@ sdev is list of the standard deviations of the coordinates
@ free is the list of free station coordinates
@ rv is the reference variance
@ x is the matrix of adjusted coordinates
```

```
CLEAR

@ remove baselines between constrained stations from
BDAT
@ to create bl (baseline summary) &
@ to bldat (baseline data)

@ extract observing station sequence
"Removing
unconnected
baselines"
CLLCD 1 DISP

BDAT
DEPTH 12 / 1 SWAP FOR c
10 DROPN 2 \->LIST 1 \->LIST bl + 'bl' STO
NEXT

@ create baseline list
BDAT
DEPTH 12 / 1 SWAP FOR c
10 \->LIST 1 \->LIST bldat + 'bldat' STO DROP2
NEXT

@ extract position constraint stn list from SDAT
SDAT DEPTH 16 / 1 SWAP FOR c
14 DROPN IF 1 == THEN cn + 'cn' STO ELSE DROP
END
NEXT

@ isolate constraint baselines
bl SIZE 1 SWAP FOR c
bl c GET DUP 1 GET cn SWAP POS
DUP IF 0 \=/ THEN DROP 1 END
SWAP 2 GET cn SWAP POS
DUP IF 0 \=/ THEN DROP 1 END
+ 'f' STO
IF f 2 == THEN
1 ELSE 0
END
flg SWAP + 'flg' STO
NEXT

@ remove constraint baselines
9 CF WHILE 9 FC? REPEAT
flg 1 POS 'f' STO
IF f 0 == THEN 9 SF ELSE
bl 1 f 1 - SUB bl f 1 + bl SIZE SUB + 'bl' STO
bldat 1 f 1 - SUB bldat f 1 + bldat SIZE SUB + 'bldat'
STO
flg 1 f 1 - SUB flg f 1 + flg SIZE SUB + 'flg' STO
END
END
9 CF

@ flag unconnected baselines first sweep
@ put accompanied stns in 'cn' file

bl SIZE 1 SWAP FOR c
bl c GET DUP 1 GET cn SWAP POS
DUP IF 0 \=/ THEN DROP 1 END
OVER 2 GET cn SWAP POS
DUP IF 0 \=/ THEN DROP 1 END
+ 'f' STO
IF f 0 == THEN flg c 1 PUT 'flg' STO DROP
ELSE

OBJ\-> DROP
cn
1 2 START
DUP 3 PICK POS 'f' STO
IF f 0 == THEN SWAP + ELSE SWAP DROP END
NEXT
'cn' STO
END
NEXT

@ isolate unconnected baselines reverse sweep by
changing flags

bl SIZE
\-> sz
\<<
sz 1 SWAP FOR c
bl sz c - 1 + GET DUP 1 GET cn SWAP POS
DUP IF 0 \=/ THEN DROP 1 END
OVER 2 GET cn SWAP POS
DUP IF 0 \=/ THEN DROP 1 END
+ 'f' STO
IF f 0 == THEN flg sz c - 1 + 1 PUT 'flg' STO DROP
ELSE
flg sz c - 1 + 0 PUT 'flg' STO
OBJ\-> DROP
cn
1 2 START
DUP 3 PICK POS 'f' STO
IF f 0 == THEN SWAP + ELSE SWAP DROP END
NEXT
'cn' STO
END
NEXT

@ remove unconnected baselines
9 CF WHILE 9 FC? REPEAT
flg 1 POS 'f' STO
IF f 0 == THEN 9 SF ELSE
bl 1 f 1 - SUB bl f 1 + bl SIZE SUB + 'bl' STO
bldat 1 f 1 - SUB bldat f 1 + bldat SIZE SUB + 'bldat'
STO
flg 1 f 1 - SUB flg f 1 + flg SIZE SUB + 'flg' STO
END
END
9 CF

\>>

@ compute number of observations
bl SIZE 'r' STO

1 r FOR c
@ build (to) list
bl r c - 1 + GET OBJ\-> DROP
to + 'to' STO

@ build (from) list
from + 'from' STO
NEXT

@ compile list of stations in network
"Compiling
```

```
network station list"
CLLCD 1 DISP

from to + SORT
OBJ\-> OVER slist + 'slist' STO
2 SWAP START
DUP2 IF \=/
THEN DROP DUP slist + 'slist' STO
ELSE DROP
END
NEXT DROP

@ find constraint stations and compile constraint list

CLEAR
SDAT DEPTH 16 / 1 SWAP
START
14 DROPN
IF 1 == THEN clist + 'clist' STO ELSE DROP END
NEXT

@ remove constraint stations not included in network

CLEAR
clist OBJ\-> 1 SWAP
START DUP
slist SWAP POS
IF 0 == THEN clist DUP
3 PICK POS OVER SIZE OVER 1 +
4 PICK SWAP ROT SUB ROT
1 4 ROLL 1 - SUB SWAP +
'clist' STO
END DROP
NEXT

@ create list of column headings (unknown stations) for
A matrix
slist 'acol' STO
clist OBJ\->
1 SWAP START
acol DUP ROT POS
OVER SIZE OVER 1 +
4 PICK SWAP ROT SUB ROT
1 4 ROLL 1 - SUB SWAP +
'acol' STO
NEXT

@ Program to convert SDAT to Indexed List format
CLEAR
{ } { }
\-> no data
\<<
SDAT DEPTH 16 / 1 SWAP FOR c
15 \->LIST 1 \->LIST data + 'data' STO
 no + 'no' STO
NEXT
no data 2 \->LIST 'sdlis' STO

@ Program to compute initial coordinates of free
stations

"Computing
approximate
coords of free stns"
CLLCD 1 DISP

clist 'cl2' STO
1 2 START
1 bl SIZE FOR c
@ HALT
bl c GET
DUP 1 GET cl2 SWAP POS 'f' STO
IF f 0 \=/ THEN 1 ELSE 0 END
OVER 2 GET cl2 SWAP POS 'f' STO
IF f 0 \=/ THEN 1 ELSE 0 END
2 \->LIST 'f' STO

IF f { 1 0 } SAME THEN
DUP 1 GET
sdlis 1 GET SWAP POS
sdlis 2 GET SWAP GET
3 5 SUB
bldat c GET 1 3 SUB
ADD 1 \->LIST
fr2 + 'fr2' STO
2 GET DUP
fr1 + 'fr1' STO
cl2 + 'cl2' STO
END

IF f { 0 1 } SAME THEN
DUP 2 GET
sdlis 1 GET SWAP POS
sdlis 2 GET SWAP GET
3 5 SUB
bldat c GET 1 3 SUB
NEG ADD 1 \->LIST
fr2 + 'fr2' STO
1 GET DUP
fr1 + 'fr1' STO
cl2 + 'cl2' STO
END

IF f { 1 1 } SAME THEN DROP END
IF f { 0 0 } SAME THEN DROP END

NEXT
NEXT

acol SIZE 'cols' STO

\>>

IF epoch 0 \=/ THEN
@ ------ 4 D adjust option (if epoch \=/ 0 ) ----

@ Program to compute quasi-baselines in kinematic
network
@ using either constrained velocities or velocities
estimated from plate model

@ find velocity constraint stations and compile velocity
constraint list
CLEAR
"Extracting velocity
constraints"
CLLCD 1 DISP

sdlis 1 GET SIZE 1 SWAP
FOR c
```

```
sdlis 2 GET c GET OBJ\-> DROP
13 DROPN SWAP DROP
IF 1 == THEN
sdlis 1 GET c GET
vlist + 'vlist' STO END
NEXT

@ remove constraint stations not included in network

CLEAR
vlist OBJ\-> 1 SWAP
START DUP
slist SWAP POS
IF 0 == THEN vlist DUP
3 PICK POS OVER SIZE OVER 1 +
4 PICK SWAP ROT SUB ROT
1 4 ROLL 1 - SUB SWAP +
'vlist' STO
END DROP
NEXT

@ create list of unconstrained velocity stations

slist 'fvlist' STO
vlist OBJ\->
1 SWAP START
fvlist DUP ROT POS
OVER SIZE OVER 1 +
4 PICK SWAP ROT SUB ROT
1 4 ROLL 1 - SUB SWAP +
'fvlist' STO
NEXT

@ find free velocity stations
CLEAR
1 fvlist SIZE FOR c
fvlist c GET
DUP acol SWAP POS
IF 0 == THEN @ cds from SDAT & FVEL to find
velocity
sdlis 1 GET OVER POS sdlis 2 GET SWAP GET 3 5 SUB
OBJ\-> DROP
"Computing velocity
of Stn " 5 PICK STD +
" from model

Finding plate ...." +
CLLCD 1 DISP
SFVEL

 DROP2 +
@ Replace entry in sdlis
sdlis 1 GET ROT POS sdlis 2 GET OVER GET
9 4 ROLL REPL sdlis DUP 2 GET ROT 4 ROLL SWAP
PUT
2 SWAP PUT 'sdlis' STO

ELSE @"cds from FREE & FVEL to find velocity"
fr1 OVER POS fr2 SWAP GET DUP OBJ\-> DROP
"Computing velocity
of Stn " 6 PICK STD +
" from model

Finding plate ...." +
CLLCD 1 DISP
SFVEL DROP2 + { 0 0 0 } SWAP + +
fr1 ROT POS fr2 SWAP ROT PUT 'fr2' STO
END
NEXT

@ find fixed velocity stations

1 vlist SIZE FOR c
vlist c GET
DUP acol SWAP POS
IF 0 == THEN STD @ "cds from SDAT & SDAT to find
velocity"
ELSE @"cds from FREE & SDAT to find velocity"
fr1 OVER POS fr2 SWAP GET
sdlis 1 GET 3 PICK POS sdlis 2 GET SWAP GET 9 14
SUB { 0 0 0 } SWAP + +
fr2 fr1 4 ROLL POS ROT PUT 'fr2' STO

END
NEXT

DROP2 @ ??? why is this so ?

@ adjust baselines to epoch
1 bl SIZE FOR c
bl c GET bldat c GET
DUP 10 GET { } { }
\-> mepoch frm too
\<<
@ compute baseline from data at specified epoch
@ start station data
OVER 1 GET fr1 SWAP POS 'f' STO
IF f 0 == THEN OVER 1 GET sdlis 1 GET SWAP POS
sdlis 2 GET SWAP GET  3 15 SUB
ELSE
OVER 1 GET fr1 SWAP POS fr2 SWAP GET mepoch +
END
@ end station data
3 PICK 2 GET fr1 SWAP POS 'f' STO
IF f 0 == THEN ROT 2 GET sdlis 1 GET SWAP POS
sdlis 2 GET SWAP GET  3 15 SUB
ELSE
ROT 2 GET fr1 SWAP POS fr2 SWAP GET mepoch +
END
'too' STO 'frm' STO

@ compute from data at adjustment epoch
epoch frm
CDTIM

@ compute to data at adjustment epoch
epoch too
CDTIM

@ compute difference at adjustment epoch
SWAP DUP2 NEG ADD 1 3 SUB
@ compute baseline error at adjustment epoch
SWAP SQ  ROT SQ ADD \v/ 4 6 SUB +

@ compute from data at measurement epoch
mepoch frm
CDTIM

@ compute to data at measurement epoch
```

```
mepoch too
CDTIM

@ compute difference at measurement epoch
SWAP DUP2 NEG ADD 1 3 SUB
@ compute baseline error at measurement epoch
SWAP SQ  ROT SQ ADD \v/ 4 6 SUB +

@ compute difference (adjustment - measured epoch)
and apply to bldat
DUP2
NEG ADD 1 3 SUB
SWAP SQ ROT SQ ADD 4 6 SUB
OBJ\-> DROP 0 SWAP 0 4 ROLLD 0 4 ROLLD 6 \-
>LIST + 0 +
SWAP 10 epoch PUT
SWAP ADD

bldat SWAP c SWAP PUT 'bldat' STO

\>>
NEXT


@ ----- end 4 D adjust -----
END

@ Main adjustment program

@ for each baseline observation
1 r FOR c
bldat r c - 1 + GET OBJ\-> DROP2
"Building
VCV & Weight Matrix
... Observation " c +
CLLCD 1 DISP

@ build VCV
@ order VCV elements
4 PICK 3 ROLLD
OVER 4 ROLLD
7 PICK 6 ROLLD
@ build VCV matrix
{ 3 3 } \->ARRY
@ Invert VCV (Ref Var =1) to obtain Weight
INV
@ convert to list format
ARRY\-> DROP
6 ROLL DROP
ROT DROP
SWAP DROP
6 \->LIST 1 \->LIST

@ add to weight sub-matrix list
w + 'w' STO

@ build baseline vector observation list
\->V3 v + 'v' STO

NEXT

@ build list of column coefficients in A matrix
"Building
Coefficient (A)
matrix "
CLLCD 1 DISP

1 r START
0
NEXT
r \->LIST
1 cols 1 - START
DUP
NEXT
cols \->LIST 'a' STO

@ build coefficient list
a OBJ\-> DROP

1 r FOR c

from c GET
acol SWAP POS
DUP IF 0 == THEN
DROP ELSE
DUP cols SWAP - 2 +
ROLL c -1 PUT
SWAP cols SWAP - 1 +
ROLLD
END

to c GET
acol SWAP POS
DUP IF 0 == THEN
DROP ELSE
DUP cols SWAP - 2 +
ROLL c 1 PUT
SWAP cols SWAP - 1 +
ROLLD
END

NEXT

cols \->LIST 'a' STO

@ Build Normal Matrix

w OBJ\-> DROP
1 cols FOR acr
1 cols FOR c
"Computing Normal
Sub-matrix elements
" acr 1 - cols * c + + "/" + cols SQ +
CLLCD 1 DISP
a c GET ABS
a acr GET ABS ADD
 1 r FOR nr
 DUP nr GET DUP IF 2 == THEN DUP /
 r nr - 3 + PICK *
 tmp ADD 'tmp' STO ELSE DROP END
 NEXT DROP tmp IF acr c \=/ THEN -1 * END 1 \-
>LIST nm SWAP + 'nm' STO
 { 0 0 0 0 0 0 } 'tmp' STO

NEXT
NEXT CLEAR

{ } 'tmp' STO
@ Invert Normal matrix
1 cols FOR c
```

```
@ main rows
@ select row of submatrices

cols 3 * c 3 * - 1 + DUP 2 +
"Building Normal
Matrix
Rows " ROT + " to " + SWAP +
CLLCD 1 DISP

nm
cols SQ c cols * - 1 +
DUP 3 + SUB

@ build last row
1 cols FOR c2
DUP cols c2 - 1 + GET
OBJ\-> DROP
ROT DROP 4 ROLL DROP 4 ROLL DROP
3 \->LIST tmp + 'tmp' STO
NEXT

@ build second row
1 cols FOR c2
DUP cols c2 - 1 + GET
OBJ\-> DROP
DROP ROT DROP 4 ROLL DROP
3 \->LIST tmp + 'tmp' STO
NEXT

@ build first row
1 cols FOR c2
DUP cols c2 - 1 + GET
OBJ\-> DROP
3 DROPN
3 \->LIST tmp + 'tmp' STO
NEXT

DROP

NEXT

"Forming Normal
Matrix "
CLLCD 1 DISP
tmp OBJ\->
\v/
DUP
2 \->LIST
\->ARRY
"Inverting
Matrix"
CLLCD 1 DISP
 INV
'tmp' STO

@ Extract control coordinates
"Extracting
Constraint
Coordinates "
CLLCD 1 DISP

sdlis 1 GET SIZE
\-> sz
\<<
1 sz FOR c
sdlis 1 GET sz c - 1 + GET
sdlis 2 GET sz c - 1 + GET OBJ\-> DROP
10 DROPN 3 \->LIST
SWAP DROP SWAP DROP
clist 3 PICK POS
DUP IF 0 == THEN 3 DROPN
ELSE DROP + 1 \->LIST fid + 'fid' STO END
NEXT
\>>

@ Build Observation list
1 r FOR c
"Adding Observation
" c + "/" + r +
CLLCD 1 DISP
bl r c - 1 + GET OBJ\-> DROP
bldat r c - 1 + GET OBJ\-> 8 DROPN
3 \->LIST
clist 4 PICK POS
DUP IF 0 \=/ THEN DUP / END
clist 4 PICK POS
DUP IF 0 \=/ THEN DUP / END
2 \->LIST

DUP IF { 1 0 } SAME THEN DROP
SWAP DROP SWAP 0
\-> nu pt
\<<
fid OBJ\-> 1 SWAP
START
DUP 1 GET
IF nu == THEN TAIL 'pt' STO ELSE DROP END
NEXT pt ADD
@1 \->LIST
obs + 'obs' STO

\>>
ELSE @ 0 1 or 0 0 case

DUP IF { 0 1 } SAME THEN DROP

ROT DROP SWAP 0
\-> nu pt
\<<
fid OBJ\-> 1 SWAP
START
DUP 1 GET
IF nu == THEN TAIL NEG 'pt' STO ELSE DROP END
NEXT pt ADD
@1 \->LIST
obs + 'obs' STO
\>>

ELSE @ 0 0 case
DROP

SWAP DROP SWAP DROP
@1 \->LIST
obs + 'obs' STO
END
END
NEXT

@ convert to column matrix
obs OBJ\-> 1 2 \->LIST
```

```
\->ARRY 'obs' STO


@ create A(t)W matrix elements
a w
1 cols FOR c2
"Building AWL
Matrix " c2 + "/" + cols +
CLLCD 1 DISP

OVER c2 GET
{ } 'tmp3' STO
1 r FOR c
DUP c GET
3 PICK c GET
IF OVER 0 == THEN
DROP ELSE
* END
1 \->LIST
tmp3 SWAP + 'tmp3' STO

NEXT
DROP tmp3 1 \->LIST tmp2 SWAP + 'tmp2' STO
NEXT
DROP2

@ Multiply A(tran)W by L

tmp2

@ Main iterations
1 cols FOR c2 @ OUTER LOOP
DUP c2 GET

@ iterations for each column
@ sub-iteration row 1
"Multiplying L matrix
" c2 3 * 2 - + "/" + cols 3 * +
CLLCD 1 DISP

{ } 'tmp4' STO
1 r FOR c
DUP c GET
DUP IF 0 == THEN DROP { 0 0 0 }
ELSE
1 3 SUB END
tmp4 SWAP + 'tmp4' STO
NEXT tmp4 OBJ\-> 1 SWAP 2 \->LIST \->ARRY
obs * OBJ\-> DROP
const SWAP +

'const' STO

@sub-iteration row 2
"Multiplying L matrix
" c2 3 * 1 - + "/" + cols 3 * +
CLLCD 1 DISP

{ } 'tmp4' STO
1 r FOR c
DUP c GET
DUP IF 0 == THEN DROP { 0 0 0 }
ELSE
DUP 2 2 SUB SWAP 4 5 SUB + END
tmp4 SWAP + 'tmp4' STO
NEXT tmp4 OBJ\-> 1 SWAP 2 \->LIST \->ARRY
obs * OBJ\-> DROP
const SWAP +
'const' STO

@sub-iteration row 3
"Multiplying L matrix
" c2 3 * + "/" + cols 3 * +
CLLCD 1 DISP

{ } 'tmp4' STO
1 r FOR c
DUP c GET
DUP IF 0 == THEN DROP { 0 0 0 }
ELSE
DUP 3 3 SUB SWAP 5 6 SUB + END
tmp4 SWAP + 'tmp4' STO
NEXT tmp4 OBJ\-> 1 SWAP 2 \->LIST \->ARRY
obs * OBJ\-> DROP
const SWAP +
'const' STO
DROP
NEXT   @ OUTER LOOP
DROP

@ Multiply
@(A(Tran)WA)-1  * (ATWL)
tmp
const OBJ\-> 1 2 \->LIST
\->ARRY *
'x' STO

a OBJ\-> DROP
{ }
\-> ax
\<<

1 r FOR c

{ } { }
\-> acr acr2
\<<

1 cols FOR c2
cols c2 - 1 + PICK
c GET
acr SWAP + 'acr' STO
NEXT

acr

1 3 FOR c4

1 cols FOR c3
DUP c3 GET

"Computing Residual
(Computed-Observed)
" c 3 * 3 c4 - - + "/" + r 3 * +
CLLCD 1 DISP

CASE
c4 1 == THEN 0 0 END
c4 2 == THEN 0 SWAP 0 END
c4 3 == THEN 0 0 ROT END
```

```
END
3 \->LIST acr2 SWAP + 'acr2' STO
NEXT
acr2 OBJ\-> 1 SWAP 2 \->LIST \->ARRY
x * OBJ\-> DROP
ax SWAP + 'ax' STO
{ } 'acr2' STO
NEXT

DROP

\>>
NEXT

cols DROPN

ax
OBJ\-> 1 2 \->LIST \->ARRY obs -
'v' STO

@ Compute v*W

"Computing
Reference variance"
CLLCD 1 DISP

v OBJ\-> DROP r 3 *
\->LIST 'vl' STO 1 r
  FOR c w c GET
OBJ\-> DROP 4 PICK 3
ROLLD OVER 4 ROLLD
7 PICK 6 ROLLD { 3
3 } \->ARRY vl c 3 *
DUP 2 - 3 PICK SWAP
GET OVER 1 - 4 PICK
SWAP GET ROT 4 ROLL
SWAP GET { 1 3 }
\->ARRY SWAP * OBJ\->
DROP 3 \->LIST vw
SWAP + 'vw' STO
  NEXT

@ compute reference variance
vw OBJ\-> DROP
1 r 3 *
2 \->LIST \->ARRY v *
r 3 * cols 3 * -
DUP IF 0 \=/ THEN
/
OBJ\-> DROP
ELSE DROP2 1 END @ no redundancy (no loop
closure)
'rv' STO

@ Computing Standard deviations

"Computing
Standard Deviation
of Parameters"
CLLCD 1 DISP

tmp rv * \->DIAG
OBJ\-> OBJ\-> DROP
\->LIST \v/
'sdev' STO

@ convert x to list
{ } \-> xlist
\<<
x OBJ\-> OBJ\-> DROP2 3 / 1 SWAP FOR c
3 \->LIST 1 \->LIST xlist + 'xlist' STO
NEXT
xlist 'x' STO
\>>

@ convert sdev to list
{ } \-> sdevlist
\<<
sdev OBJ\-> 3 / 1 SWAP FOR c
3 \->LIST 1 \->LIST sdevlist + 'sdevlist' STO
NEXT
sdevlist 'sdev' STO
\>>

TIME time HMS- HMS\-> 3600 * 'time' STO

@ Output results
"Appending results
to AOUT"
CLLCD 1 DISP

IF epoch 0 == THEN "3D" ELSE "4D" END
" Adjustment results    Reference Variance " + rv 2 FIX +
"
" +

1 cols FOR c
acol c GET STD + " " +
x c GET OBJ\-> DROP
4 ROLL 4 ROLL 3 FIX + " " + ROT + " " + SWAP + " " +
sdev c GET OBJ\-> DROP
4 ROLL 4 ROLL 3 FIX + " " + ROT + " " + SWAP + " " +
IF epoch 0 \=/ THEN
acol c GET fr1 SWAP POS fr2 SWAP GET 7 12 SUB
OBJ\-> DROP
7 ROLL 7 ROLL 4 FIX + " " + 6 ROLL + " " + 5 ROLL + "
" +
4 ROLL + " " + ROT + " " + SWAP + " " + epoch 3 FIX + "
" +
ELSE "
" +
END
NEXT
AOUT SWAP +
'AOUT' STO

\>> \>>

TEMP
UPDIR
\>>
```

SUBROUTINES

CARTEUL

```
%%HP: T(3)A(D)F(.);
\<<
@ Program to compute Cartesian Velocities
@ from cartesian Plate model
@ X,Y,Z of point on levels 6,5,4
@ omega x,y,z of plate in rad/Ma on levels 3,2,1
@ output is VX, VY, VZ on levels 3,2,1 in mm/yr


@TEST DATA
@MORE
@-5288519 3409952 -1038574
@KAVI
@-5562412 3107930 -285346
@TOW2
@-5054582.754 3275504.442 -2091539.646
@ Aust plate
@0.00746 0.00530 0.00627
@ Pacific Plate
@-0.00001 0.00583 -0.01083
@ MORE vel -0.0100 -0.0265 0.0549
@ KAVI vel 0.0289 0.0642 0.0262
@ TOW2 vel -0.0301 -0.0130 0.0530


\-> x y z omx omy omz
\<<
@ compute vel X
omy z * omz y * - 1E6 /

@ compute vel Y
omz x * omx z * - 1E6 /

@ compute vel Z
omx y * omy x * - 1E6 /

\>> \>>
```

CDTIM

```
%%HP: T(3)A(D)F(.);
\<<
@ gets epoch and sdlis or fr2 extract
@ and generates list of coordinates & sdev at epoch

OBJ\-> DROP
\-> epoch x y z sx sy sz vx vy vz svx svy svz ep
\<<
@ compute coords of frm at adjustment epoch
epoch ep -
@ vectorise data
RECT x y z \->V3
vx vy vz \->V3
\-> t x0 dx
\<<
@ compute displacement
dx t *
@ compute new coords
x0 + V\-> 3 \->LIST
@ compute standard error of new coords
svx t * SQ sx SQ + \v/
svy t * SQ sy SQ + \v/
svz t * SQ sz SQ + \v/
3 \->LIST +

\>> \>>
\>>
```

CTG

```
%%HP: T(3)A(D)F(.);
\<<
@ Sub-program to convert Cartesian co-ordinates to GRS80 ellipsoidal coordinates
@ Requires X,Y,Z on stack
@ GRS80 ellipsoid parameters used
DEG

6378137
3.35281068118E-3
8.18191910428E-2


\-> x y z a f e
\<<

@ Compute P
x SQ y SQ + \v/

@ Compute R
DUP SQ z SQ + \v/

@ Compute u
a SWAP / e SQ * 1 f - + z * OVER / ATAN

\-> p u \<<

@ Compute latitude
z 1 f - * e SQ a * u SIN 3 ^ * +
1 f - p e SQ a * u COS 3 ^ * - * / ATAN

@ Compute ellipsoid height
DUP COS p *
OVER SIN z * +
OVER SIN SQ e SQ * 1 SWAP - \v/ a * -

@ Compute longitude
x y RECT \->V2 CYLIN V\-> RECT SWAP DROP


SWAP

@ latitude in decimal degrees returned on level 3
@ longitude in decimal degrees returned on level 2
@ ellipsoid height on level 1

\>> \>>  \>>
```

CV2GV

```
%%HP: T(3)A(D)F(.);
\<<
@ Convert Cartesian Velocity to GRS80 ellipsoidal velocity
@ X, Y, Z on levels 6,5,4
@ VX,VY,VZ mm/a point on levels 3,2,1
@ outputs Vlat, Vlong in deg/Ma and Vht in mm/a on levels 3,2,1
@ requires subroutines CTG and GTC

\-> x y z vx vy vz
\<<
DEG

@ compute xyz at 1 yr
x vx 1000 / +
y vy 1000 / +
z vz 1000 / +
CTG @ returns lat/long/ht at 1 yr

@ convert xyz at point 1 to lat/long/ht
x y z CTG  @ returns lat/long/ht

\-> lat2 lon2 ht2 lat1 lon1 ht1
\<<
lat2 lat1 - 1000000 *
lon2 lon1 - 1000000 *
ht2 ht1 - 1000 *

4 FIX
\>> \>> \>>
```

EULXYZ

```
%%HP: T(3)A(D)F(.);
\<<
@ Compute Cartesian Velocity from Cartesian plate model
@ X,Y,Z point on levels 6,5,4
@ omega x, omega y and omega z in rad/Ma of plate on levels 3,2,1
@ outputs VX, VY and VZ in mm/a on levels 3,2,1

\-> x y z wx wy wz
\<<
@ compute vx
wy z * wz y * - 1000 /

@ compute vy
wz x * wx z * - 1000 /

@ compute vz
wx y * wy x * - 1000 /
4 FIX


\>> \>>
```

FINDPOLY

```
%%HP: T(3)A(D)F(.);
\<<
@ FINDPOLY
@ searches PDAT polygon database to find
@ which polygon point is located within
@ returns polygon number in list format

@ latitude point on level 2
@ longitude of point on level 1
0 { } 0

\-> n0 e0 temp inl cnt
\<<

@ compute number of plates in file
 PDAT SIZE 1 SWAP FOR c
0 'cnt' STO
@ extract each plate at a time
PDAT c GET
DUP 1 GET 'temp' STO
10 GET

@ close the polygon
DUP 1 GET +
DUP 2 GET +

DUP SIZE 2 / 1 - 1 SWAP

@ check each line
FOR c2

c2 2 * 1 -
OVER OVER GET
3 PICK 3 PICK 1 + GET
4 PICK 4 PICK 2 + GET
5 PICK 5 ROLL 3 + GET
\-> n1 e1 n2 e2
\<<

e0 e2 >
e0 e1 > +
IF 1 == THEN
e0 e1 - e2 e1 - /
n2 n1 - * n1 + n0 >
IF 1 == THEN cnt 1 +
'cnt' STO
END
END

\>>
NEXT

IF cnt 2 / FP 0.5 == THEN
temp inl SWAP + 'inl' STO END

DROP

NEXT

inl

\>> \>>
```

G2MV

```
%%HP: T(3)A(D)F(.);
\<<
@ Program to compute VE & VN given GRS80 coordinates (in DMS)
@ and Euler pole in decimal degrees
@ Lat, Long in dec degrees on levels 5,4
@ Euler pole Lat, Long in decimal degs on lev 3,2
@ Rotation in deg/ma on levl 1
@ Outputs VE and VN in mm/yr on levels 2,1

\-> lat lon elat elon omega
\<<

@ convert coords to Cartesian
lat
lon
0 GTC

3 DUPN

@ convert Euler pole to Cartesian
elat elon omega SP2CAEUL



@ compute Cartesian velocity
EULXYZ


@ convert Cartesian velocity to ellipsoidal velocity
CV2GV

DROP

@ Convert Ellipsoidal velocity to e,n velocity
lat
lon

4 ROLL
4 ROLL

GV2MV

4 FIX


\>> \>>
```

GC2MV

```
%%HP: T(3)A(D)F(.);
\<<
@ Convert GRS80 ellipsoidal velocity to E,N velocity
@ E & N velocities computed on local ellipsoid (no ht scale factor)
@ lat, long in dec/degs on levels 4,3
@ Vlat, Vlong in deg/Ma on levels 2,1
@ returns VE and VN in mm/yr on levels 2,1

@ load GRS80 parameters
6378137
8.18191910428E-2
.998324298444
2.51460707284E-3
2.63904662023E-6
3.41804613675E-9

\-> lat lon vlat vlon a e A0 A2 A4 A6

\<<
@ compute lat,lon at 2
lat vlat 1000000 / + D\->R
lon vlon 1000000 / + D\->R
lat D\->R
lon D\->R

\-> lat2 lon2 lat lon
\<<
RAD

@ Compute meridian distance at lat0
a A0 lat * A2 lat 2 * SIN * -
A4 lat 4 * SIN * +
A6 lat 6 * SIN * - *

@ Compute meridian distance at lat2
a A0 lat2 * A2 lat2 2 * SIN * -
A4 lat2 4 * SIN * +
A6 lat2 6 * SIN * - *
SWAP
 - 1000 *

@ compute longitude difference (at lon2)
a 1 e SQ lat2 SIN SQ * - 0.5 ^ /
lat2 COS * lon2 lon - *
1000 *
SWAP
4 FIX
DEG

\>> \>> \>>
```

GTC

```
%%HP: T(3)A(D)F(.);
\<<
@ Sub-program to convert GRS80 Ellipsoidal co-ordinates to Cartesian
@ Requires latitude, longitude (in decimal degs) and ell.ht on stack
DEG


6378137
3.35281068118E-3
8.18191910428E-2

\-> lat lon h a f e
\<<

@ Compute v
a 1 e SQ lat SIN SQ * - \v/ /
\-> v
\<<

@ Compute X
v h + lat COS * DUP lon COS *

@ Compute Y
SWAP lon SIN *

@ Compute Z
1 e SQ - v * h + lat SIN *


@ X returned on level 3
@ Y returned on level 2
@ Z on level 1

\>> \>> \>>
```

GV2MV

```
%%HP: T(3)A(D)F(.);
\<<
@ Convert GRS80 ellipsoidal velocity to E,N velocity
@ E & N velocities computed on local ellipsoid (no ht scale factor)
@ lat, long in dec/degs on levels 4,3
@ Vlat, Vlong in deg/Ma on levels 2,1
@ returns VE and VN in mm/yr on levels 2,1

@ load GRS80 parameters
6378137
8.18191910428E-2
.998324298444
2.51460707284E-3
2.63904662023E-6
3.41804613675E-9

\-> lat lon vlat vlon a e A0 A2 A4 A6

\<<
@ compute lat,lon at 2
lat vlat 1000000 / + D\->R
lon vlon 1000000 / + D\->R

lat D\->R
lon D\->R

\-> lat2 lon2 lat lon
\<<
RAD

@ Compute meridian distance at lat0
a A0 lat * A2 lat 2 * SIN * -
A4 lat 4 * SIN * +
A6 lat 6 * SIN * - *

@ Compute meridian distance at lat2
a A0 lat2 * A2 lat2 2 * SIN * -
A4 lat2 4 * SIN * +
A6 lat2 6 * SIN * - *
SWAP
 -
1000 *

@ compute longitude difference (at lon2)
a 1 e SQ lat2 SIN SQ * - 0.5 ^ /
lat2 COS * lon2 lon - *

1000 *

SWAP


4 FIX
DEG

\>> \>> \>>
```

SFVEL

```
%%HP: T(3)A(D)F(.);
\<<
@ program to find Cartesian velocity and estimated standard error
@ X,Y,Z on levels 3,2,1
@ searches PDAT plate directory to find Plate
@ uses plate data to compute cartesian velocity
9 CF
0
\-> x y z c
\<<
@ convert xyz to ellipsoidal
x y z CTG DROP DUP2

@ Find Polygon
FINDPOLY
OBJ\-> DROP

@ Extract plate parameters
WHILE 9 FC? REPEAT
c 1 + 'c' STO

PDAT c GET DUP 1 GET
IF 3 PICK == THEN 9 SF ELSE DROP END

END 9 CF
SWAP DROP
3 9 SUB

OBJ\-> DROP
\-> lat lon latpol lonpol omeg a b az som
\<<

@ convert lat long reduced to ellipsoid surface to XYZ
lat lon 0 GTC

@ convert euler pole to cartesian
latpol lonpol omeg SP2CAEUL

@ compute Cartesian velocity
CARTEUL
3 \->LIST

@ compute velocity with pole error ellipse
DEG RECT a 0.68 * az CYLIN \->V2 RECT
b 0.68 * az 90 + CYLIN \->V2 RECT +
V\-> lonpol + SWAP latpol +
\-> clonpol clatpol
\<<
@ compute cartesian with pole error
lat lon 0 GTC
clatpol clonpol omeg
SP2CAEUL CARTEUL 3 \->LIST
OVER NEG ADD SQ

@ compute cartesian with rotation error
lat lon 0 GTC
latpol lonpol omeg som +
SP2CAEUL
CARTEUL
3 \->LIST
3 PICK NEG ADD SQ
ADD \v/

@ Compute standard error
@ compute NE velocity
lat lon latpol lonpol omeg
G2MV 2 \->LIST

@ compute NE velocity error
lat lon clatpol clonpol omeg
G2MV 2 \->LIST
OVER SWAP NEG ADD SQ

@ compute
lat lon latpol lonpol omeg som +
G2MV 2 \->LIST
3 PICK NEG ADD SQ
ADD \v/

4 FIX
\>> \>> \>> \>>
```

SP2CAEUL

```
%%HP: T(3)A(D)F(.);
\<<
@ Program to convert Spherical Euler pole to Cartesian
@ lat pole in deceimal degs on level 3
@ long pole in decimal degs on level 2
@ rotation rate in deg/Ma on level 1
@ outputs wx, wy, wz in rad/Ma on level 3,2,1

D\->R

\-> phi lamb omeg
\<<
@ compute omegax
DEG phi COS lamb COS * omeg *

@ compute omegay
phi COS lamb SIN * omeg *

@ compute omega z
phi SIN omeg *
\>> \>>
```

Appendix E
Simulated sample data and analysis summary

From	To	ΔX	ΔY	ΔZ	σ^2ΔX	σΔXΔY	σΔXΔZ	σ^2ΔY	σΔYΔZ	σ^2ΔZ
LAE1	MANU	-54738.741	-13163.958	509617.824	8.10E-05	-3.91E-05	4.88E-06	4.90E-05	-2.63E-06	4.00E-06
MANU	TOKU	-267636.608	-489334.497	-252860.652	6.40E-05	-2.85E-05	3.10E-06	3.60E-05	-9.84E-07	4.00E-06
KAVI	MANU	194816.617	330013.218	58641.230	3.60E-05	-1.72E-05	2.46E-06	2.50E-05	-7.30E-07	4.00E-06
KAVI	LAE1	249555.346	343177.183	-450976.596	4.90E-05	-2.06E-05	4.73E-06	2.50E-05	-2.30E-06	4.00E-06
LAE1	TOKU	-322375.349	-502498.455	256757.173	6.40E-05	-2.74E-05	5.89E-06	3.60E-05	-2.98E-06	4.00E-06
KAVI	MORE	273893.143	302021.828	-753227.824	3.60E-05	-1.70E-05	4.42E-06	2.50E-05	-2.58E-06	4.00E-06
LAE1	MORE	24337.797	-41155.356	-302251.223	4.90E-05	-2.10E-05	6.50E-06	2.50E-05	-3.49E-06	4.00E-06
MANU	MORE	79076.538	-27991.397	-811869.047	6.40E-05	-2.90E-05	4.32E-06	3.60E-05	-2.22E-06	4.00E-06
MORE	TOKU	-346713.147	-461343.100	559008.396	4.90E-05	-1.88E-05	5.59E-06	2.50E-05	-2.71E-06	4.00E-06

Table E.1 Simulated baseline results at measurement epoch 2006.0 for sample network analysis used in this study.

	Static Adjustment				Dynamic Adjustment			
Station	ΔE (metres)	ΔN (metres)	σΔE (metres)	σΔN (metres)	ΔE (metres)	ΔN (metres)	σΔE (metres)	σΔN (metres)
LAE1	0.505	0.109	-0.481	0.092	-0.053	-0.058	-0.040	0.027
TOKU	-0.105	-0.983	-0.544	0.112	0.035	-0.125	-0.018	0.011
MANU	-0.527	-0.182	-0.490	0.108	0.001	0.042	-0.029	0.012

Table E.2 Coordinate differences and standard errors between adjustment epoch of 1994.0 and measurement epoch using different adjustment strategies (Static and Dynamic). MORE and KAVI have been fixed at their epoch 1994.0 estimates.

	Static Adjustment				Dynamic Adjustment			
Station	ΔE (metres)	ΔN (metres)	σΔE (metres)	σΔN (metres)	ΔE (metres)	ΔN (metres)	σΔE (metres)	σΔN (metres)
LAE1	0.254	0.054	-0.239	0.046	-0.024	-0.029	-0.022	0.011
TOKU	-0.051	-0.491	-0.270	0.056	0.018	-0.063	-0.018	0.007
MANU	-0.261	-0.092	-0.244	0.054	0.006	0.021	-0.019	0.008

Table E.3 Coordinate differences and standard errors between adjustment epoch of 2000.0 and measurement epoch using different adjustment strategies (Static and Dynamic). MORE and KAVI have been fixed at their epoch 2000.0 estimates.